# The role of CaMKK2 in natural killer cell anti-tumor immunity

by

Patrick Kennedy Juras

Department of Pharmacology and Cancer Biology

Duke University

Date: _____

Approved:

_____
Donald McDonnell, supervisor

_____
Kris Wood

_____
Timothy Haystead

_____
Brent Hanks

Dissertation submitted in partial fulfillment of the requirements for the degree of Doctor of Philosophy in the Department of Pharmacology and Cancer Biology in the Graduate School of Duke University.

2022

ABSTRACT

# The role of CaMKK2 in natural killer cell anti-tumor immunity

by

Patrick Kennedy Juras

Department of Pharmacology and Cancer Biology

Duke University

Date: _____

Approved:

_____
Donald McDonnell, supervisor

_____
Kris Wood

_____
Timothy Haystead

_____
Brent Hanks

Dissertation submitted in partial fulfillment of the requirements for the degree of Doctor of Philosophy in the Department of Pharmacology and Cancer Biology in the Graduate School of Duke University.

2022

# Abstract

Calcium/calmodulin-dependent protein kinase kinase 2 (CaMKK2) is a calcium-activated regulator of energy homeostasis in many cell types, including neurons and hepatocytes. In these cells, CaMKK2 connects calcium signaling to several ubiquitous energy and metabolism pathways such as AMPK, CaMKI, and CaMKIV. Tumor cells often express CaMKK2 ectopically, commandeering this enzyme to promote survival, proliferation, and metastasis across a wide variety of cancers. Recent work has established additional roles for CaMKK2 in tumor immunity. Notably, expression of this enzyme promotes M2 polarization of tumor-associated macrophages and facilitates the development of myeloid-derived suppressor cells, indirectly promoting tumor growth. Thus, there has been considerable interest in developing CaMKK2 inhibitors, including competitive kinase antagonists and ligand-directed degraders (LDDs), as potential cancer therapeutics. Indeed, the classic competitive inhibitor STO609 has been shown to reduce primary breast tumor growth in mice. However, the role of CaMKK2 in most cellular compartments within the tumor immune environment remains unknown, which is a significant impediment to the clinical development of these agents. To develop a complete understanding of the effects of CaMKK2 inhibition on the tumor environment, we set out to systematically delineate which cells express CaMKK2 and for what purpose.

Our most significant finding is that natural killer (NK) cells upregulate CaMKK2 expression in the tumor environment, conferring a fitness advantage that improves anti-tumor immune activity. We report that CaMKK2 is expressed at low levels in NK cells isolated from murine spleens but that its expression is dramatically increased in NK cells isolated from tumors or exposed to tumor conditions. A series of *in vitro* functional assays showed that CaMKK2 expression suppresses apoptosis and promotes proliferation of NK cells without affecting the cytotoxic efficacy of individual cells. These findings were highly

intriguing as NK cells play a critical role in the anti-tumor immune response, especially in controlling metastatic disease. As such, we demonstrated that NK cell-intrinsic deletion of CaMKK2 increases metastatic progression across several murine models, establishing a critical role for this enzyme in NK cell tumor immunity. Interestingly, ablation of the CaMKK2 protein, but not inhibition of its kinase activity, resulted in decreased NK cell survival, a result which reveals a unique scaffold function for this enzyme. Finally, we identified lactic acid as a key driver of CaMKK2 upregulation under tumor conditions, an interesting finding given the immune suppressive nature of lactic acid. Intracellular importation of lactic acid through the MCT channels, and not general acidification, is necessary for CaMKK2 upregulation in NK cells. These results suggest that CaMKK2 upregulation in tumor-infiltrating NK cells is an adaptive mechanism by which these cells mitigate the deleterious effects of a lactate-rich tumor environment.

This work will inform strategies to manipulate the CaMKK2 signaling axis as a therapeutic approach in cancer. Because CaMKK2 acts as a scaffold in NK cells, competitive inhibitors and LDDs are likely to have distinct therapeutic utilities. Our work suggests that competitive inhibitors may be broadly preferable in the clinical setting, and we aim to test this hypothesis in mouse tumor models once suitable LDDs become available. We are also working to identify components of the CaMKK2 scaffold complex and elucidate the downstream pathways, which may yield further insights into how this pathway can be manipulated in NK cells. Moreover, because intracellular lactate import is necessary for CaMKK2 upregulation, there may be liabilities associated with the emerging use of MCT1 inhibitors in cancer therapy, which we intend to explore in mouse models. Our findings also raise the possibility that NK cells can be modified to constitutively express CaMKK2 as a proactive shield against suppressive tumor factors, and we are working to replicate our core findings in human NK cells. Overall, our work holds significant implications for the therapeutic manipulation of tumor immunity.

# Contents

# List of figures

# List of tables

# Abbreviations

| | |
|---|---|
| 27HC | 27-hydroxycholesterol |
| αCHC | α-cyano-4-hydroxycinnamic acid |
| ADCC | Antibody-dependent cellular cytotoxicity |
| AGR2 | Anterior gradient 2 |
| AMPK | AMP-activated protein kinase |
| BMDM | Bone marrow-derived macrophage |
| CaMKI | Calcium/calmodulin-dependent protein kinase type 1 |
| CaMKIV | Calcium/calmodulin-dependent protein kinase type 4 |
| CaMKK2 | Calcium/calmodulin-dependent protein kinase kinase 2 |
| CAR | Chimeric antigen receptor |
| CCL4 | Chemokine ligands 4 |
| CCR5 | C-C chemokine receptor type 5 |
| CFSE | Carboxyfluorescein succinimidyl ester |
| CLP | Common lymphoid progenitor |
| CML | Chronic myelogenous leukemia |
| CNS | Central nervous system |
| CREB | cAMP response element-binding protein |
| CRISPR | Clustered regularly interspaced short palindromic repeats |
| DN | Double negative |
| eGFP | Enhanced green fluorescent protein |
| EMT | Epithelial-mesenchymal transition |
| FPN | Ferroportin |
| FSP1 | Ferroptosis suppressor protein 1 |
| GPCR | G protein-coupled receptor |

| | |
|---|---|
| GRHL2 | Grainyhead-like protein 2 |
| HCC | Hepatocellular carcinoma |
| HDAC | Histone deacetylase |
| HEPES | 4-(2-hydroxyethyl)-1-piperazineethanesulfonic acid |
| HER2 | Human epidermal growth factor receptor 2 |
| HIF1α | Hypoxia-inducible factor 1α |
| HLA | Human leukocyte antigen |
| IFNγ | Interferon gamma |
| IL-2 | Interleukin 2 |
| IL-10 | Interleukin 10 |
| IL-15 | Interleukin 15 |
| IVIS | In vivo imaging system |
| ITAM | Immunoreceptor tyrosine-based activation motif |
| ITIM | Immunoreceptor tyrosine-based inhibitory motif |
| KIR | Killer immunoglobulin-like receptor |
| KO | Knock-out |
| LAG-3 | Lymphocyte activation gene 3 |
| LDD | Ligand-directed degrader |
| LYPD3 | Ly6/PLAUR domain-containing protein 3 |
| LKB1 | Live kinase B1 |
| mAb | monoclonal antibody |
| M-CSF | Macrophage colony-stimulating factor |
| MCT | Monocarboxylate transporter |
| MHC I | Major histocompatibility complex class I |
| MICA/B | MHC class I chain-related protein A and B |
| mTOR | Mammalian target of rapamycin |

| | |
|---|---|
| NAD | Nicotinamide adenine dinucleotide |
| NCR | Natural cytotoxicity receptor |
| NFAT | Nuclear factor of activated T cells |
| NK | Natural killer cell |
| NKT | Natural killer T cell |
| NM | Normal media |
| NSG | NOD.Cg-Prkdc$^{scid}$ Il2rg$^{tm1Wjl}$/SzJ |
| Nu/nu | athymic nude |
| PIPES | Piperazine-N,N′-bis (2-ethanesulfonic acid) |
| TAM | Tumor-associated macrophage |
| TCM | Tumor-conditioned media |
| TCR | T cell receptor |
| TGF-β | Transforming growth factor beta |
| TLR4 | Toll-like receptor 4 |
| TNBC | Triple negative breast cancer |
| TRAIL | Tumor necrosis factor-related apoptosis-inducing ligand |
| TSC1/2 | Tuberous sclerosis protein 1/2 |
| ULBP | UL16 binding protein 1 |
| UMAP | Uniform Manifold Approximation and Projection |
| VASP | Vasodilator-stimulated phosphoprotein |
| VEGF | Vascular endothelial growth factor |
| xCT | Cystine/glutamate transporter |

# Acknowledgements

I am thankful for the exceptional support I've received throughout my PhD studies, especially from my lead mentors Donald McDonnell and Luigi Racioppi. I also want to thank Ching-Yi Chang and Debarati Mukherjee for their guidance and for all my colleagues in the McDonnell lab for their help, advise, and friendship. I am grateful for the support of the Duke Medical Scientist Training Program, the Pharmacology and Cancer Biology Department, and my thesis committee. Funding for my work came from several sources, including the National Cancer Institute, the Department of Defense, and the Susan G. Komen Breast Cancer Foundation. Key reagents were kindly provided by our friends at Bristol-Myers Squibb and by Dr. David Drewry at the University of North Carolina.

On a personal note, I want to thank my wife Hannah Juras for her unwavering support in all aspects of life. I am similarly grateful for the devotion of parents Barry and Laura Juras and my sister Josselin Juras, as well as my in-laws Mark and Gayle Miele. Finally, I want to thank my brothers and sisters at Pilgrim Orthodox Presbyterian Church for their friendship and faithfulness, which has kept my eyes fixed on the things that matter most.

# 1 Introduction

## *1.1 Overview*

Great advances have been made in cancer treatment over the last two decades, contributing to a 27% reduction in the cancer death rate in the United States[1]. Recent innovations include improved techniques in surgical and radiation oncology[2,3], novel targeted therapies such as PARP and MET inhibitors[4,5], and sequencing-based stratification of tumor subtypes, enabling more effective use of traditional chemotherapies[6]. Perhaps the greatest paradigm shift has been the emergence of cancer immunotherapies that harness the innate anti-tumor capabilities of the immune system. Monoclonal antibodies (mAbs) have been developed to block critical tumor signaling pathways or mark tumor cells for immune destruction, and these therapies are now standard-of-care for many cancers, including rituximab for B-cell lymphomas, trastuzumab for HER2+ breast tumors, and nivolumab for several advanced cancers[7-10]. T-cells have been engineered to express chimeric antigen receptors (CARs), unleashing potent cellular cytotoxicity against specific targets[11], and oncolytic viral therapies are rapidly emerging[12]. Despite the advent of such promising new therapies, cancer remains the second-leading cause of death in the United States after cardiovascular disease[1], and specific types of cancer are still associated with very poor outcomes. Tumor subtypes that lack targeted therapies confer worse outcomes, one example being triple-negative breast cancer (TNBC), which lacks expression of the targetable markers HER2, estrogen receptor, and progesterone receptor. TNBC accounts for 12% of breast cancer diagnoses and carries a 5-year survival rate about 15% lower than other breast cancers, with particularly high mortality in advanced metastatic cases[13]. Pancreatic adenocarcinoma and bile duct cancers are still associated with 5-year survival rates of less than 20%[14,15]. Drug resistance is also an emerging problem as a wide variety of initially effective treatments are followed

by recurrent drug-resistant disease with poor outcomes[16]. Thus, new insights into the workings of tumor cells and tumor immunity are urgently needed to develop additional treatment options.

Our work lies at the intersection of three emerging fields within the cancer biology space: natural killer cell immunity, CaMKK2 signaling, and lactic acid metabolism. Specifically, we identify a novel mechanism by which natural killer (NK) cells adapt to and survive the metabolic stresses of the tumor environment: upregulation of CaMKK2. This thesis details the effects of CaMKK2 expression on NK cellular biology and immune surveillance, sheds light on the mechanisms by which CaMKK2 expression is modulated, and explores the translational significance of these findings.

## *1.2 Natural killer cells*

### 1.2.1 Background

Natural killer cells occupy a distinct niche in the immune system, performing a range of unique anti-pathogen and anti-tumor functions. Like T and B-cells, NK cells arise from common lymphoid progenitors in the bone marrow before trafficking to the lymphoid organs, yet NK cells adopt a distinct granular morphology and function as part of the innate immune system. As such, NK cells are not antigen-specific, do not undergo diversification and selection processes, and do not require activation signals from antigen-presenting cells. Rather, NK cells directly integrate activation and suppression signals through germline-encoded cell-surface receptors that are paired with cytoplasmic ITIM and ITAM motifs to trigger effector activity[17]. Most activating receptors belong to the natural cytotoxicity receptor (NCR) family, which includes the prominent complexes NKG2D, NKp46, and NKp30[18,19]. Conversely, most inhibitory receptors belong to the killer immunoglobulin-like receptor (KIR) family, which recognize a variety of MHC class I alleles

(HLA in humans), a complex expressed on all healthy nucleated cells. Robust expression of the proper MHC class I allele labels a cell as “self” and strongly inhibits NK cell cytotoxicity[20]. Upon proper stimulation, NK cells mediate cytotoxic killing in the same manner as CD8 T-cells. NK cells release pre-formed granules containing perforin, which forms channels in the membrane of the target cells, and granzyme, which enters those channels and directly cleaves caspase 3, triggering apoptosis[21]. NK cells also produce FasL and TRAIL, which trigger the extrinsic apoptosis pathway if the cognate receptors remain intact on the target cell[21].

The primary function of NK cells is to eliminate cells that have lost or downregulated MHC class I and are thus missing “self” markers. Indeed, the foundational studies of NK cell biology showed that cells engineered to lose MHC class I expression were readily cleared in mice, a function dependent on the natural killer population[22]. Loss of normal MHC class I expression is an important marker of pathological transformation as this complex is the primary means by which CD8 T cells surveil cytoplasmic peptide content. Several DNA viruses, including cytomegalovirus and Epstein Barre virus, suppress expression of MHC Class I by interfering with the antigen presentation process[23,24]. By reducing MHC Class I, a virus-infected cell is able to “hide” its viral antigens from CD8 T-cell surveillance and evade killing[24].

### 1.2.2 Development and subpopulations

NK cells arise from common lymphoid progenitors (CLPs) in the bone marrow and differentiate into a variety of subpopulations with distinct functions. CLPs become committed to NK differentiation upon expression of CD122 (IL-2Rβ)[25,26], and subsequent development in the bone marrow is largely driven by IL15 signaling[27]. In the bone marrow, NK cells undergo the “licensing” or “education” process by which they gain cytotoxic effector capabilities contingent on expression of inhibitory KIR receptors, preventing autoimmune sequelae[28]. After leaving the bone marrow, peripheral NK cells continue to

progress through additional stages of maturation in which effector capacity in augmented. In mice, “immature” NK cells are $CD11b^{-}/CD27^{+}$, whereas mature type 1 cells are $CD11b^{+}/CD27^{+}$, and the highly cytolytic mature type 2 cells are $CD11b^{+}/CD27^{-}$ [29]. Human NK cells also express CD11b and CD27, but a more dependable maturation schematic uses CD16 (FcγRIII) and the human-specific marker CD56. Human NK cells gain increasing cytolytic function as they progress from $CD56^{bright}CD16^{-}$ to $CD56^{dim}CD16^{dim}$ to $CD56^{dim}CD16^{bright}$ [30]. To acquire specific functions, subsets of NK cells will pause at particular maturation stages or embark on entirely divergent pathway. For example, $CD56^{bright}CD16^{dim}$ NK cells are prolific producers of cytokines and chemokines, activating and recruiting a variety of immune cells[31]. NK cells may serve unique tissue-specific roles, such as their role in placenta vascularization during pregnancy. These “decidual” NK cells reside at the placenta-uterine interface and produce copious amounts of pro-angiogenic factors such as the VEGF family[32]. Natural killer T (NKT) cells are most often classified as a subpopulation of T cells, but this thesis will treat them as an NK subset. NKT cells undergo thymic development and express a TCR like T cells, yet these cells are innately cytotoxic, express most canonical NK receptors, and their classic TCR is an invariant ligand of CD1d that essentially functions as an NK activation receptor[33-35]. Our work reveals additional similarities between the NK lineage and NKT cells, bolstering this classification.

**Table 1: NK cell subtypes and select functional markers**

| Immature | Regulatory (mature 1) | Cytotoxic (mature 2) |
|---|---|---|
| CD11b- | CD11b+/- | CD11b+ |
| CD27+/- | CD27+ | CD27- |
| $CD56^{bright}$ | $CD56^{bright}$ | $CD56^{dim}$ |
| KIR- | KIR+/- | KIR+ |

| Activating receptors | | |
|---|---|---|
| **Receptor** | **Family** | **Ligand** |
| NKG2D | CLR | MICA/B |
| CD16 | Fc | IgG Fc |
| NKp44 | NCR | MLL5 |
| NKp46 | NCR | Numerous |
| NKp30 | NCR | B7-H6 |

| Inhibitory receptors | | |
|---|---|---|
| **Receptor** | **Family** | **Ligand** |
| NKG2A | CLR | HLA-E (h) |
| KIR2DL1 | KIR | HLA-C2 (h) |
| KIR3DL2 | KIR | HLA-A (h) |
| Ly49C | KIR | $H2^{b}$ (m) |
| Ly49G2 | KIR | $H2^{k}$ (m) |
| KLGR1 | Checkpoint | E-cadherin |
| PD1 | Checkpoint | PD-L1 |
| LAG3 | Checkpoint | MHC II |

NCR= natural cytotoxicity receptor
KIR= killer immunoglobulin-like receptor
CLR= C-type lectin receptor

### 1.2.3 Role in tumor immunity

Tumor cells adopt a similar strategy to hide their mutated neo-antigens from T-cell surveillance, reducing MHC Class I expression through genomic and epigenomic modifications to various steps in the MHC Class I antigen presentation pathway[36]. Thus, NK cells serve as a critical complement to T-cell immunity, killing tumors that evade T cells through MHC Class I downregulation. However, NK cells also require engagement of activation receptors to mediate cytotoxic release. Activating ligands include an assortment of DNA damage markers, such as MICA, MICB, and ULBP1-3, which are commonly expressed on tumor cells[37]. NK cells play a particularly important role in controlling the metastatic dissemination of tumor cells[38,39]. This heightened sensitivity is largely driven by cellular changes that occur during the epithelial-mesenchymal transition (EMT)[40], changes that often cause upregulation of NK cell activation ligands[41,42] and downregulation of MHC Class I[43]. However, tumors may become resistant to NK cell killing if they downregulate expression of critical activating receptors or lose the receptors through proteolytic shedding[44], highlighting the importance of diverse anti-tumor immune mechanisms.

Since their initial discovery, several additional functions have been ascribed to NK cells. NK cells and monocytes are the principal mediators of antibody-dependent cellular cytotoxicity (ADCC), the process by which antibody-opsonized cells are lysed. NK cells detect the constant domain (Fc) of cell-bound IgG antibodies via their Fc receptors (CD16), producing a powerful activation signal that leads to degranulation[45]. Indeed, the activity of several monoclonal antibody therapies is ascribed to NK cell-mediated ADCC[46-50]. Certain subsets of NK cells are specialized for cytokine signaling rather than direct cytotoxicity, especially the $CD56^{bright}CD16^{-}$ subset of human NK cells[51]. These cells are major producers of IFNγ, which increases MHC Class I expression across cell types while promoting activation and differentiation of various immune cells[52-54]. NK cells also produce Flt3L, an important chemoattractant for dendritic cells[55]. Some tumors have co-opted the decidual NK cell phenotype discussed earlier, programming “decidual-like” NK cells that promote tumor growth through VEGF production[56]. Another subset of NK cells, termed “regulatory” NK cells and defined by CD73 expression, promotes tumor growth by producing immune suppressive cytokines such as IL10 and expressing checkpoint markers like LAG-3[57].

### 1.2.4 Regulatory pathways

The metabolic state and effector function of NK cells is regulated, in large part, by the competing effects of the AKT/mTOR and AMPK pathways. The AKT/mTORc1 pathway promotes an activated glycolytic state characterized by enhanced glucose uptake, increased oxidative phosphorylation, elevated production of IFNγ and Granzyme B, and augmented effector activity against tumor cells[58-61]. Together with the IL15/JAK/STAT5 pathway, the AKT/mTORc1 pathway regulates maturation of NK cells into later effector stages[62,63], and mTOR regulates the “education” process that maintains NK cell reactivity through frequent MHC I engagment[64]. A variety of activation receptors, including NKG2D, CD16, IL15, and IL10, activate the mTORc1 pathway by triggering PI3K

and AKT signaling[59,61,65,66]. AKT may regulate some processes independently of mTOR, such as promoting cell-cycle progression through regulation of cyclin D3 transcription, E2F activation, and cytoplasmic sequestration of p27[67,68].

Conversely, the AMPK pathway promotes an inactive, quiescent state in response to energy deprivation or suppressive signals. AMPK activation in NK cells is characterized by suppressed IFNγ production, decreased activation marker expression, reduced proliferation, and diminished ex vivo cytotoxic activity[69-71]. AMPK is canonically activated by an elevated AMP/ATP ratio, attenuating energy-demanding cellular functions when energy is in short supply[72], but in NK cells, AMPK is also activated by adiponectin signaling and engagement of certain inhibitory receptors such as KLGR1[70,71]. The suppressive effects of AMPK are mediated through inhibition of NF-κB signaling and through antagonism of the mTOR pathway[71-73]. The TSC1/TSC2 complex is a major negative regulator of mTOR that integrates competing signals from the AKT1 and AMPK pathways. AMPK phosphorylates TSC2 at Thr1227 and Ser1345, driving TSC2 activation and mTOR inhibition, whereas AKT1 phosphorylates TSC2 at Ser939 and Thr1462, driving TSC2 inhibition and mTOR activation[73,74]. The AKT/mTOR and AMPK pathways are critical competing regulators of NK cell function, and kinases that modulate these pathways could play a central role in the anti-tumor activity of NK cells.

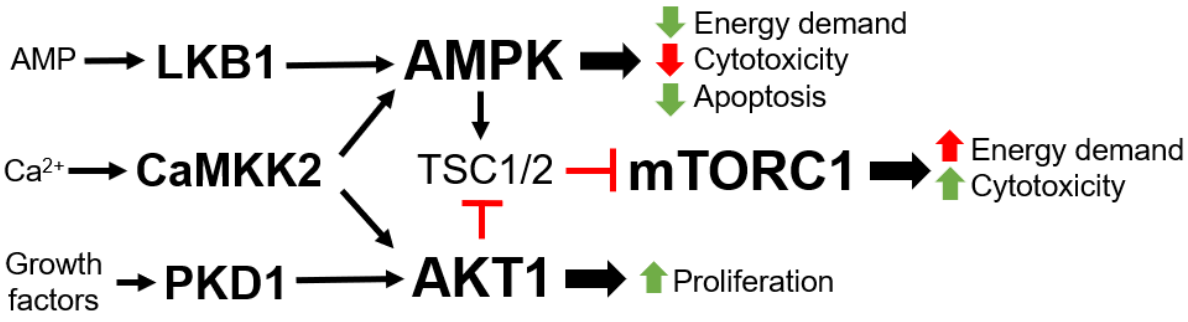


**Figure 1: Key metabolic regulatory pathways in NK cells.** A series of metabolic "sensors" regulate the AMPK and AKT1 pathways, which control the metabolic and cytolytic status of NK cells.

### 1.2.5 Therapeutic utility

Given the importance of NK cells in tumor immunity, NK cell-based cancer therapies have garnered considerable interest. Autologous NK cell transfusions were an early approach in which a patient's own NK cells were harvested, activated ex vivo, and then re-transfused. A variety of ex vivo stimulants have been employed to activate the primary NK cells, including IL2 and IL12 cytokine pulses and co-cultures with irradiated tumor cells[75-78]. These early approaches produced enhanced activation states among circulating NK cells but demonstrated no efficacy against tumor progression, often due to poor infiltration of solid tumors or strong immune suppression within the tumor environment[76,78,79]. However, autologous transfusions are being revisited as improved retroviral transfection techniques enable genetic engineering of primary NK cells[80]. Lentiviral strategies have been used to knock-down the inhibitory receptor NKG2A and overexpress the activating receptor NKG2D in primary human NK cells, modifications that significantly reduce tumor growth in mouse xenograft models[81,82].

Allogeneic NK cell transfusions have also gained traction, especially using CAR-NK cells or variants of the NK92 cell line. NK cells can be fitted with chimeric antigen receptors (CARs) in the same manner as T-cells to mediate cytotoxicity against specific antigen targets. CAR-NK therapies against NHL (CD19) and AML (CD33) are currently in clinical trials[83]. Because CAR-NK cells lack a TCR and have a limited lifespan in circulation, they carry a reduced risk of graft-versus-host disease, cytokine release syndrome, and neurotoxicity compared to CAR-T cells[84]. CAR-NK cells can be engineered from primary NK cells or from cell lines such as NK92, a constitutively active human NK cell lymphoma line with attenuated expression of the KIR inhibitory receptors[85]. NK92 cells are also employed in ways other than CAR modification. Clinical transfusion studies with unmodified NK92 cells showed limited efficacy in cancer patients, in part due to immune-mediated rejection of the foreign cells, but engineered variants of NK92 show greater

potential[86]. Important modifications include deletion of MHC Class I expression, which reduces T-cell mediated immune rejection[87], and overexpression of activation receptors such as DNAM-1 and NKG2D[88].

While early applications focused on hematological malignancies, attention has recently turned toward solid tumors, which are more difficult to treat with NK cell therapies given the hypoxic, nutrient-depleted, immune suppressive qualities of the tumor microenvironment[79]. To combat effects of the tumor environment, NK92 cells were recently engineered to lose expression of the TGF-β receptor, a major suppressor of NK cell activity within solid tumors[60]. This modification broadly enhances NK cell anti-tumor activity and attenuates tumor growth in mouse xenograft models[89]. As additional NK regulatory networks are elucidated, it will be important to identify receptors or enzymes that specifically improve NK cell survival or effector activity in the conditions created by solid tumors. These targets can be amplified or deleted in NK cells using techniques already developed.

## *1.3 Calcium/calmodulin-dependent protein kinase kinase 2*

### 1.3.1 Function and physiological importance

CaMKK2 is a calcium-activated serine/threonine kinase that regulates metabolism and energy homeostasis across many tissue types. CaMKK2 is activated by a cytoplasmic calcium influx that triggers calmodulin binding, similar to other members of the calcium/calmodulin-dependent kinase family[90]. Calmodulin binding triggers conformational changes that expose target-binding domains[90,91], allowing CaMKK2 to phosphorylate downstream targets such as CaMKI, CaMKIV, AKT, and AMPK[92,93]. Indeed, CaMKK2 directly activates AMPK via phosphorylation of Thr172, coupling the ubiquitous AMPK energy homeostasis pathway to calcium signaling[94]. Although

canonically activated by calcium/calmodulin binding, CaMKK2 exhibit basal activity autonomous of calcium signaling[95]. CaMKK2 is negatively regulated via activation of the cAMP/PKA pathway, which phosphorylates CaMKK2 at three critical serine residues, precluding calmodulin binding while promoting association with the inhibitory 14-3-3γ protein[96]. 14-3-3 binding constrains the conformational flexibility of CaMKK2, reducing its capacity to phosphorylate downstream targets[97]. CaMKK2 is a critical amplifier of calcium signaling and lies at the nexus of several key metabolic pathways.

CaMKK2 expression is most prevalent in the central nervous system (CNS) where it activates the CaMKI and CaMKIV pathways to regulate neuronal development and survival. CaMKK2 promotes neuron elongation and branching through CaMKI signaling, with different CaMKK2 isoforms favoring distinct neuron morphologies[98,99]. Inclusion of exon 16 in CaMKK2 promotes neuron branching, whereas exclusion of exon 16 promotes elongation[99]. Cerebellar granule cell neurons rely on the CaMKK2/CaMKIV pathway to transcribe and phosphorylate CREB, a critical neuronal survival factor that also drives migration to the inner granule cell layer[100]. CaMKK2 is required for some types of long-term hippocampal memory formation[101], and irregular CaMKK2 signaling has been linked to the emergence of bipolar disorder, anxiety disorders, and schizophrenia[102-105]. The CaMKK2/CaMKIV cascade is particularly important under ischemic conditions, as deletion or inhibition of CaMKK2 worsens stroke outcomes in mice[106,107]. CaMKK2 protects against cerebrovascular ischemic injury by increasing CREB survival signaling, attenuating inflammation, and maintaining integrity of the blood-brain barrier[106,107].

CaMKK2 is expressed in several tissues outside the CNS where it regulates both cellular and whole-body metabolism, largely via the AMPK pathway. CaMKK2 expression in the hypothalamus is critical for production of hormone neuropeptide Y, a potent appetite stimulant that specifically favors carbohydrate intake[108]. In pancreatic β-islet cells, CaMKK2 regulates insulin release by sensing calcium fluctuations[109], and CaMKK2

promotes gluconeogenesis in hepatocytes, likely by coupling catecholamine signaling to the AMPK pathway[110]. Together, these activities impact whole-body intake and utilization of glucose[109]. CaMKK2 also plays a role in skeletal homeostasis, enabling osteoblast activation via sympathetic neuronal signaling while directly inhibiting osteoclast differentiation[111,112]. Indeed, CaMKK2 deletion protects against ovariectomy-induced osteoporosis in mice[112]. Moreover, CaMKK2 signaling attenuates the differentiation of adipose and muscle tissue, preventing myoblast and pre-adipocytes from initiating differentiation programs[113 114].

### 1.3.2 Pathological relevance

CaMKK2 signaling is often coopted to facilitate disease processes, including metabolic syndrome, non-alcoholic fatty liver disease (NAFLD), and a variety of cancers. Given its role in regulating appetite, insulin secretion, and hepatic gluconeogenesis, it is unsurprising that CaMKK2 contributes to metabolic derangements when caloric intake is excessive. Deletion or inhibition of CaMKK2 reduces food intake, weight gain, insulin resistance, and hepatic steatosis in mice fed a high-fat diet[108,109,115]. Tumor cells of diverse origins ectopically express high levels of CaMKK2, which confers a variety of selective advantages. In many tumors, CaMKK2 bypasses PDK1 and directly activates the AKT pathway, promoting tumor cell survival in prostate tumors[116] while enabling carboplatin resistance and apoptosis suppression in ovarian cancers[93,117]. In LKB1-deficient lung cancer, CaMKK2 is upregulated by the PLAG1 transcription factor to suppress anoikis and enable metastatic dissemination[118]. In breast cancer, CaMKK2 expression promotes tumor cell migration through VASP signaling and filopodia regulation (currently unpublished), and in prostate cancer, CaMKK2 is required for androgen-mediated tumor cell migration[119]. CaMKK2 also regulates golgi trafficking in prostate tumors, preventing ER dysfunction and preserving proliferative capacity[120]. In hepatocellular carcinoma (HCC), CaMKK2 promotes proliferation by providing a scaffold upon which CaMKIV, S6,

S6K, and mTOR can assemble and regulate the cell cycle[121]. Recent work has even connected CaMKK2 to ferroptosis, demonstrating that CaMKK2 expression in melanoma cells reduces lipid peroxidation and ferroptotic cell death through NRF2/AMPK activation[122].

### 1.3.3 Role in immunity

CaMKK2 is expressed in hematopoietic stem and progenitor cells in the bone marrow where it maintains quiescence and suppresses differentiation[123,124]. Indeed, CaMKK2 expression in acute promyelocytic leukemia reduces the effectiveness of all-trans retinoic acid therapy by impeding differentiation of the promyelocytes[125]. CaMKK2 expression acts as a lineage switch in granulocyte-monocyte progenitor cells, favoring monocyte differentiation over granulocytes[123,126]. However, CaMKK2 remains functionally important in terminally differentiated macrophages, coupling TLR4 stimulation to pro-inflammatory effects such as increased phagocytosis and cytokine production[127]. In the tumor context, CaMKK2 expression in the monocyte lineage promotes pro-tumor immune phenotypes, including enhanced accumulation of myeloid-derived suppressor cells both in the tumor and in secondary lymphoid organs.[128] CaMKK2 expression also favors M2 polarization of tumor-associated macrophages (TAMs), a phenotype reversed by CaMKK2 deletion[129]. Indeed, treatment with CaMKK2 inhibitor STO609 reduces primary breast tumor growth in mice while increasing the prevalence of inflammatory M1 macrophages[129]. Thus, CaMKK2 plays a multi-faceted role in the immune system, regulating differentiation of progenitor cells and governing the phenotype of various myeloid-derived immune populations.

### 1.3.4 Pharmacology

Given its role in various disease processes, CaMKK2 has become a popular target for inhibitory compounds. The classic CaMKK2 antagonist is STO609, a competitive

inhibitor of ATP binding that has shown efficacy in mouse models of breast cancer and NAFLD[115,129]. However, STO609 has a relatively low binding affinity for CaMKK2, with half-maximal inhibition achieved at 1 μM in HeLa cells[130]. STO-609 also mediates several off-target effects, including direct inhibition of AMPK[130]. Recent initiatives in industry and academia have generated a new generation of selective, high-affinity kinase inhibitors including GSK1901320, GSK650934, 4t, YL-36, SOB8-17-3, and CC8977[129,131,132]. 4t is the first CaMKK2 inhibitor able to cross the blood-brain barrier and shows promise in promoting satiety and weight loss in mouse models[132].

A second class of antagonists called ligand-directed degraders (LDDs) is also being developed against CaMKK2. LDDs are bi-specific molecules that feature a target-binding domain paired with a ubiquitin ligase recruitment domain. By bringing the E3 ubiquitin ligase in close proximity to CaMKK2, the kinase is polyubiquitylated and degraded through the proteasomal pathway, thus eliminating the entire protein rather than selectively inhibiting the kinase domain[133]. Compared to classic kinase inhibitors, LDDs offer distinct advantages such as increased target selectivity and activity against inhibitor-resistant tumors. LDD binding is not restricted to catalytic sites or specific allosteric motifs, enabling drug developers to target peptide domains unique to particular proteins[134]. For example, LDDs have allowed isoform-specific degradation of SGK3[135] and decoupling of CDK4 inhibition from CKD6 inhibition[136]. Recent work identifies LDDs as promising treatments for inhibitor-resistant cancer. For example, BTK signaling in ibrutinib-resistant C481S CLL tumors can be disrupted using a LDD against BTK[137], and LDDs can degrade imatinib-resistant BCR-ABL1 in CML[138]. Other routes for inhibiting CaMKK2 have also been suggested, including the administration of fungus-derived fusicoccins, which stabilizes interactions between CaMKK2 and the inhibitory regulator 14-3-3γ[97].

## *1.4 Lactic acid and tumor metabolism*

### 1.4.1 Background

Lactic acid is the chief byproduct of anaerobic metabolism and is among the most common metabolites in solid tumors, reaching concentrations of 10-40 mM within the tumor microenvironment[139,140]. Under hypoxic conditions, mitochondrial respiration is unable to regenerate the NAD+ required to maintain glycolysis, so cells switch to anaerobic respiration, a process by which lactate dehydrogenase regenerates NAD+ by converting pyruvate to lactic acid. Due to rapid, disorganized cell growth that outstrips vascularization, solid tumors often become hypoxic, triggering lactate production. However, even well-oxygenated tumors with active mitochondrial respiration often produce abundant lactic acid, a seemingly paradoxical phenomenon called the Warburg Effect[141]. Lactate is exported en-masse from tumor cells into the surrounding microenvironment through the monocarboxylate transporters (MCTs), a family of passive bidirectional lactate transporters[142]. Once conceptualized as a waste product, this mass of exported lactic acid is now known to play a critical role in developing the tumor niche and promoting tumor progression[143]. Indeed, high expression of lactate dehydrogenase is a negative prognostic factor in breast tumors[144], and MCT1 inhibitors are in phase I clinical trials to reduce lactate export from tumor cells[145].

### 1.4.2 Effects on tumor-associated cells

Through direct signaling and acidification, lactic acid affects almost every compartment of the tumor environment. Tumors cells often adapt to the lactate-rich environment, developing mechanisms to use lactate for mitochondrial respiration[146,147] or aggressively export lactate from the cytosol[148]. Lactic acid plays a key role in co-opting fibroblasts and vascular endothelial cells to support tumor growth. Via modulation of the ETS1/AP1 transcription factor, lactate promotes fibroblast differentiation and TGF-β

production[149,150], and it modulates Iκβα in vascular endothelial cells to drive a CXCL8 paracrine loop responsible for vascular formation[151]. The suppressive effects of lactic acid on tumor-associated immune cells are particularly strong. Lactic acid has been shown to polarize macrophages toward a pro-tumor M2 phenotype through HIF1α signaling[152], promote the development of myeloid-derived suppressor cells[153], prompt immunosuppressive IL23 production by tumor cells[154], and reduce the activation and survival of T-cells and monocytes[155,156].

In NK cells, lactic acid suppresses effector activity and induces apoptosis, broadly dampening NK-mediated tumor immunity. Lactic acid accumulation reduces intracellular pH, leading to mitochondrial dysfunction and apoptosis, with certain tissue-resident NK sub-populations being particularly vulnerable[157,158]. Lactic acid-mediated acidification of the tumor environment has also been shown to suppress the master mTOR activation pathway in NKT cells[159]. Lactic acid reduces IFNγ production in NK cells by suppressing expression of the NFAT transcription factor[155]. Interestingly, systemic buffering via oral bicarbonate is sufficient to reactivate NK cells and reduce NK cell-sensitive lymphoma progression in mouse models[160]. Thus, novel methods for reducing the suppressive effects of lactic acid may disrupt tumor growth and improve anti-tumor immune function, including the performance of NK cells.

### 1.4.3 Lactate as a transcriptional regulator

Lactic acid broadly alters the transcriptional state of cells, and studies have only begun elucidating the full effects. Recent work has shown that intracellular lactate directly reacts with lysine residues, producing “lactylated” histones with distinct epigenetic properties. Lactylation directly competes with acetylation and may constitute a “glycolytic switch” that comprehensively changes metabolic programs[161 162]. The effects of lactylation have yet to be elucidated in most cell types, though the modification has been shown to drive M1 polarization in macrophages[161]. At high cytoplasmic concentrations, lactic acid

also acts as a competitive inhibitor for many HDAC enzymes, broadly altering transcriptional signatures in HTC116 cells[163]. Moreover, lactate has been shown to modulate the activity of the NRF2 and HIF-1α transcription factor through accumulation of ROS[149], affecting macrophage polarization, among other functions. Lactate binds the cell-surface G protein-coupled receptor (GPCR) GPR81, leading to transcriptional upregulation of PDL1 via TAZ induction in human lung cancers[164]. Several GPCRs also detect lactate-induced acidification of the extracellular environment and activate compensatory transcriptional programs, including GPR4, GPR65, GPR68, and GPR132[165]. Thus, lactate is a far-reaching epigenetic regulator with many activities that remain to be identified.

The work presented in this thesis establishes that intracellular lactic acid mediates transcriptional upregulation of CaMKK2 in all subsets of tumor-infiltrating NK cells. We then elucidate the ways in which CaMKK2 alters the biology and anti-metastasis activity of NK cells, with significant implications for the clinical use of drugs that modulate CaMKK2 activity and lactate transport. Ultimately, our work ties together lactic acid biology, CaMKK2 signaling, and NK cell tumor immunity to demonstrate a novel mechanism by which NK cells respond to metabolic stresses in the tumor environment.

# 2 CaMKK2 expression as a fitness adaptation in NK cells

## *2.1 Preceding work*

Until recently, cancer-related studies of CaMKK2 were limited to investigations of its cancer cell-intrinsic actions. These studies have consistently shown that CaMKK2 expression benefits tumor cells, and ongoing studies continue to elucidate the mechanisms underlying this biology. Notable recent studies from our group demonstrated that CaMKK2 increases PDE1A expression, which increases the hydrolysis of cGMP, decreasing PKG1-mediated phosphorylation of VASP. Reduced VASP phosphorylation promotes filopodia formation, reorganizing the architecture of the cytoskeleton to enable tumor cell migration and metastasis (currently unpublished). However, our group has become increasingly interested in the role of CaMKK2 in non-cancer cells within the tumor environment, and how these "cancer-cell extrinsic" roles of CaMKK2 impact tumor pathobiology. Tumor-associated cells play key roles in tumor development, and our group has investigated CaMKK2 signaling in fibroblasts, macrophages, and monocytes. To identify immune populations that express CaMKK2, we employed a CaMKK2-eGFP reporter system. CaMKK2-eGFP reporter mice contain a mouse artificial bacterial chromosome in which the coding sequence of eGFP has been inserted at the start codon for the CaMKK2 gene[166]. The initial screen with this model showed expression of eGFP, the CaMKK2 surrogate, in many myeloid populations but little expression in lymphoid cells. Further studies revealed that specific ablation of CaMKK2 in myeloid cells, or inhibition of the enzyme using small molecule inhibitors, skews macrophages toward a pro-inflammatory M1 phenotype, resulting in decreased growth of primary tumors[129]. We are currently investigating ways to exploit these data for therapeutic benefit.

The initial eGFP screen, however, contained a restricted panel of immune markers, limiting our ability to identify CaMKK2 expression in many important immune populations.

Publicly available databases, such as the Immunological Genome Project (ImmGen), only feature bulk mRNA sequencing data, which prevents subpopulation analysis. Moreover, existing data was limited to immune cells from one or two specific tissue types in healthy mice, typically spleen or bone marrow, even though tissue type and disease state can affect the phenotype of immune cells. Given the limitations of existing data sets, we conducted a second screen of immune cells from CaMKK2-eGFP reporter mice using additional immune markers and tissue types, with a particular interest in identifying immune cells, other than those of the myeloid lineage, that express CaMKK2.

## *2.2 Results*

### 2.2.1 NK cells express low basal levels of CaMKK2

Immune cells were recovered from eight different tissues in healthy CaMKK2-eGFP reporter mice and gated for ten distinct immune populations or subpopulations in each tissue. Our gating strategy is a modified version of a previously published approach used to simultaneously analyze myeloid and lymphoid populations **(Fig. 3B)**[167]. As expected, robust expression of the CaMKK2-eGFP reporter was observed in macrophages and monocytes, with expression being low or undetectable in most lymphoid subpopulations **(Fig. 2A)**. The only splenic lymphoid population that showed evidence of eGFP expression was a subset of $CD11b^+$ NK cells, although eGFP fluorescence levels in these cells were lower than that observed in the monocyte controls **(Fig. 2A)**. However, this $eGFP^+$ subset represented at least 30% of $CD11b^+$ NK cells in every tissue analyzed except the mesenteric lymph nodes **(Fig. 2B)**. CD11b is a typical myeloid marker, but its expression is also found in NK cells at later maturation stages **(Table 1)**. The association of CaMKK2 expression with mature effector NK cells was particularly intriguing and warranted further investigation. In contrast, eGFP expression was not observed in $CD11b^-$ NK cells, B cells, or any subset of T-cells in any tissues analyzed **(Fig. 3A)**, suggesting

that mature NK cells are unique among lymphocytes in expressing CaMKK2. Interestingly, a subset of NKT cells also exhibited eGFP expression, especially in the blood and bone marrow **(Fig. 3A)**, which reflects the pattern seen in the general NK population. The similar expression pattern in NK and NKT cells likely indicates a conserved regulatory mechanism in these related cell types, and going forward, we chose to conceptualize NKT cells as a subset of NK cells for the purpose of our studies.

Another novel finding from this screen was the identification of eGFP in double negative (DN) thymocytes. About half of the DN population was positive for eGFP fluorescence, whereas no other thymocyte subsets, including double and single-positive populations, showed any evidence of expression **(Fig. 2C)**. Furthermore, eGFP expression in DN thymocytes was correlated with CD44 **(Fig. 2C)**, a marker of the DN1 and DN2 substages[168]. Double negative thymocytes represent the first stage of T-cell development during which unique T-cell receptors are generated and the canonical T-cell marker CD3 is first expressed. Interestingly, the end of the DN2 stage is exactly when VDJ recombination begins[169], and the loss of CaMKK2 expression at this juncture suggests a possible regulatory role for CaMKK2 in this process. CaMKK2 expression is known to act as a "checkpoint" in the differentiation of various immune progenitor cells, including HSPCs and GMPs in the bone marrow[123,126], raising the possibility that CaMKK2 restricts the progression of T-cell progenitors in a similar manner. Given our focus on tumor immunity, we were primarily interested in the role of CaMKK2 in peripheral effector immune cells and did not pursue the thymocyte findings any further. However, it would be interesting to elucidate the impact of CaMKK2 ablation on T-cell development in young mice (4-6 weeks old). In such a study, the prevalence of peripheral T-cells in WT and CaMKK2-/- mice, including "recent thymic emigrant" T-cells that are $Q2a^{low}/CD24^{high}$ [170], could be measured at weekly intervals during development. The results of such studies would shed light on the possible role of CaMKK2 in thymocyte progression.

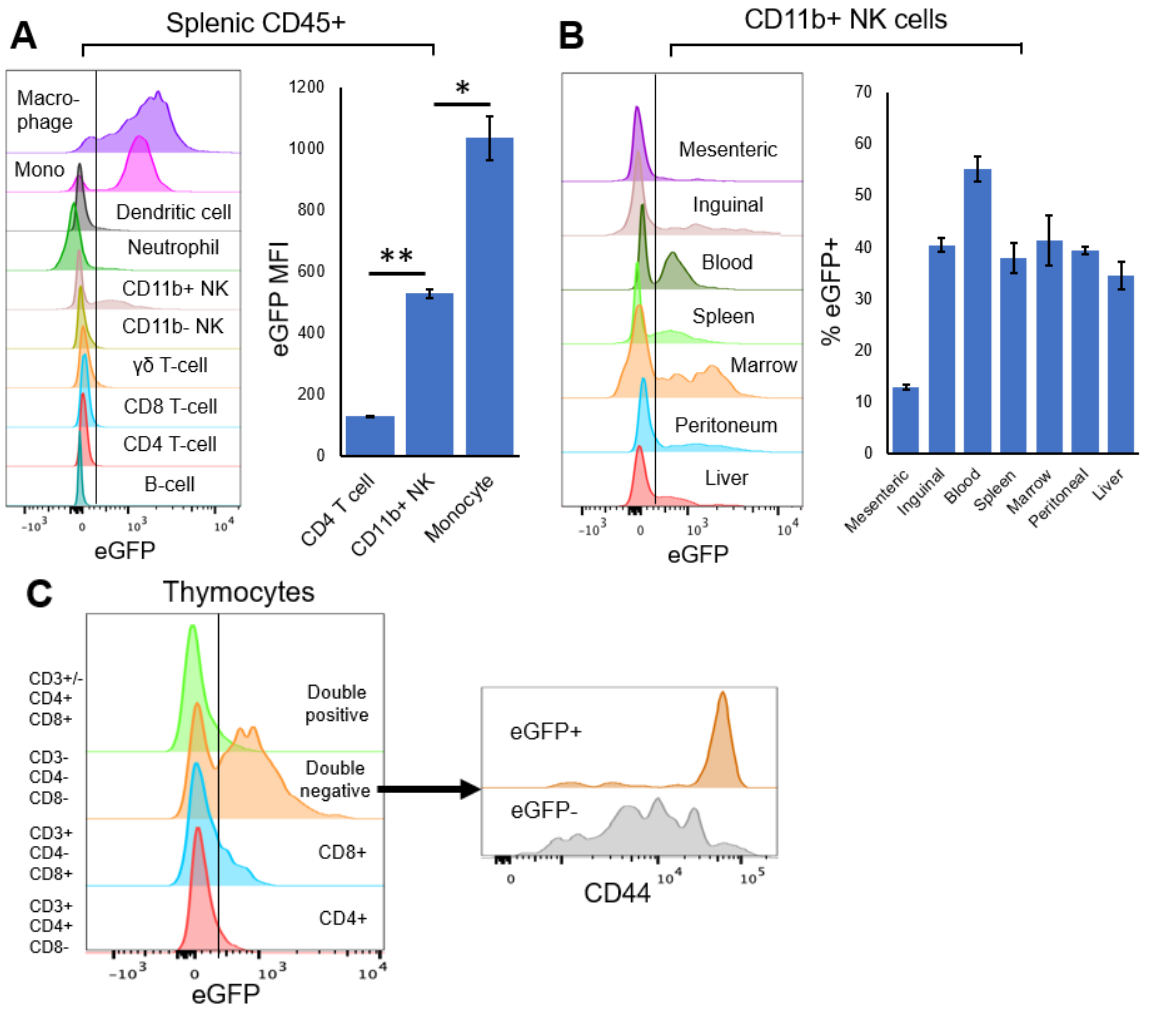


**Figure 2: CaMKK2 is expressed in CD11b$^+$ NK cells and double-negative thymocytes.** (A) Splenic immune cells from healthy CaMKK2-eGFP reporter mice were harvested and analyzed for eGFP fluorescence using flow cytometry. Each distribution represents >500 cells. The eGFP median fluorescence intensity (MFI) among the eGFP$^+$ subset of monocytes and the eGFP$^+$ subset of CD11b$^+$ NK cells (see depicted cut-off line) was compared to the eGFP MFI in all CD4 T-cells. N=2, standard error is shown. (B) Mature NK cells (NK1.1$^+$/CD11b$^+$) were isolated from various tissues of healthy CaMKK2-eGFP reporter mice and analyzed for eGFP fluorescence using flow cytometry. Each distribution represents >1000 cells. The percentage of CD11b$^+$ NK cells that are eGFP+ (see depicted cut-off line) is compared across tissues. N=2, standard error is shown. (C) Thymocytes were harvested from healthy CaMKK2-eGFP reporter mice and analyzed for eGFP fluorescence using flow cytometry. The double negative thymocyte fraction (CD3-/CD4$^-$/CD8$^-$) was divided into eGFP$^+$ and eGFP$^-$ subpopulations, which were further analyzed for CD44 expression. Each distribution represents >250 cells; data is representative of 2 mice.

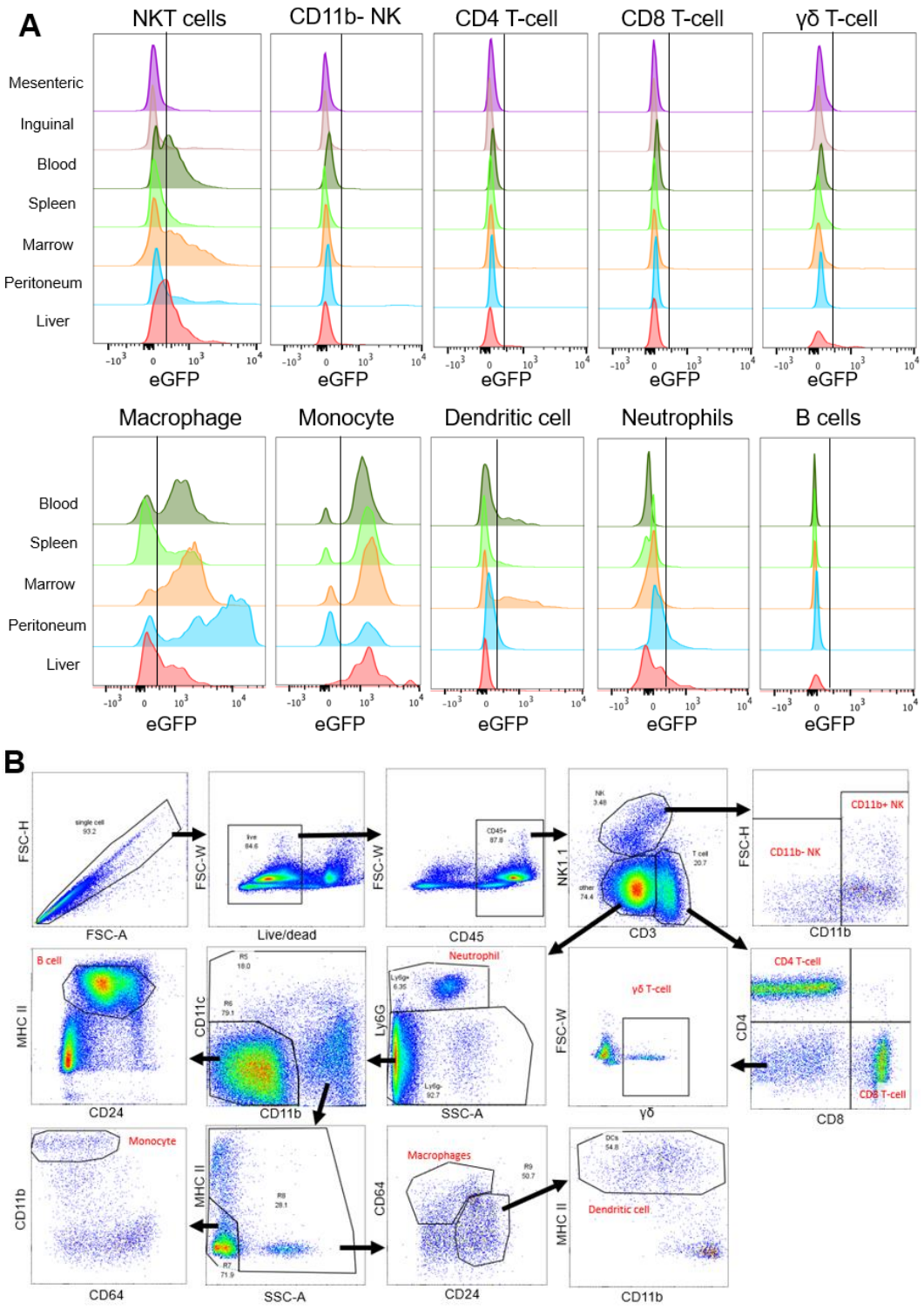


**Figure 3: NK cells are the only cells from the lymphoid lineage that express CaMKK2**. (A) Various tissues were harvested from healthy CaMKK2-eGFP reporter mice, and several immune subsets were stained for flow cytometry analysis of eGFP fluorescence. Each distribution represents >500 cells; data is representative of two mice. (B) The flow cytometry gating strategy is shown for data presented in Figures 1,2A, and 13D.

### 2.2.2 CaMKK2 is upregulated in NK cells under tumor conditions

The initial screen to identify CaMKK2-expressing immune cells was conducted in healthy mice. To explore the effects of the tumor environment on this enzyme, we repeated the earlier study under conditions that mimicked the tumor microenvironment and subsequently in tumor-bearing animals. We first performed an *ex vivo* study in which splenic NK cells from CaMKK2-eGFP reporter mice were cultured in tumor-conditioned media (TCM) from EO771 cells. TCM is spent media recovered from tumor cell cultures, and it approximates the chemical composition of the tumor environment. IL2 and IL15 were added to the culture to maintain NK cell viability. Flow cytometry was used to analyze the NK cells 24 hours and 72 hours after plating. In this manner, we made the surprising observation that eGFP fluorescence was dramatically increased at 72 hours, whereas no expression was observed at 24 hours **(Fig. 4A)**. This was the first data to suggest that a factor in the tumor environment modulates CaMKK2 expression levels.

To validate these results in an animal tumor model, subcutaneous EO771 tumors were propagated in CaMKK2-eGFP reporter mice and harvested for flow cytometry-based immune profiling. Notably, eGFP expression was significantly higher in tumor-infiltrating NK cells than in NK cells from the spleens of the same mice **(Fig. 4B)**. Indeed, the level of eGFP fluorescence in the tumor-infiltrating NK cells approached that of macrophages, which served as a positive control **(Fig. 4C)**. Moreover, splenic NK cells from tumor-bearing mice did not show an appreciable increase in eGFP expression compared to splenic NK cells from healthy mice **(Fig. 4D)**, suggesting that the local tumor environment mediates CaMKK2 upregulation, not systemic factors in tumor-bearing animals. Under basal conditions, CaMKK2 expression was confined to mature $CD11b^{+}$ NK cells, but in the tumor environment, even immature $CD11b^{-}/CD27^{+}$ NK cells were found to express the

eGFP reporter, albeit at a lower level than the $CD11b^{+}/CD27^{-}$ subset **(Fig. 4E)**. Using a panel of markers, including inhibitory KIR receptor Ly49c, activating receptor NKp46, activation marker Granzyme B, and NKT marker CD3, we did not identify any correlation between NK cell functionality and eGFP expression **(Fig. 4F)**. CaMKK2, represented by the eGFP surrogate, was expressed at similar levels across all these subsets. Thus, tumor-associated upregulation of CaMKK2 is not specific to any NK cell subset but occurs broadly throughout the natural killer population, including NKT cells, which are often characterized as a separate cell type. In contrast, T-cells showed no evidence of elevated eGFP expression in the tumor environment **(Fig. 4C)**, suggesting that CaMKK2 upregulation is specific to NK cells rather than generalizable across the lymphoid lineage. These findings were repeated in a second independent primary tumor study.

The CaMKK2-eGFP reporter model is a surrogate for transcription as it reflects activity of the CaMKK2 promoter, but a more direct measurement of the enzyme was required to confirm its expression (i.e. Western immunoblots). NK cells are not abundant enough in the tumor environment to use tumor-derived NK cells for immunoblotting. Instead, we isolated splenic NK cells from WT BL/6 female mice to culture *ex vivo* in normal growth media (NM) or tumor-conditioned media (TCM). Splenic T-cells were also harvested from WT mice and cultured in the same manner as NK cells. As positive and negative controls for CaMKK2 expression, bone marrow was harvested from WT and CaMKK2-/- (KO) mice and differentiated into bone marrow-derived macrophages (BMDMs) using M-CSF stimulation. The Western immunoblot confirmed robust CaMKK2 expression in the TCM-treated NK cells, but not in the NK cells grown in normal media **(Fig. 4G)**, indicating that factors within the tumor context enables CaMKK2 upregulation. T-cells exhibited no CaMKK2 expression under either condition **(Fig. 4G)**, which reinforces earlier data and demonstrates that the regulatory mechanisms observed in NK cells are

not generalizable among lymphocyte populations. CaMKK2 expression in TCM-treated NK cells was confirmed in a second independent Western immunoblot.

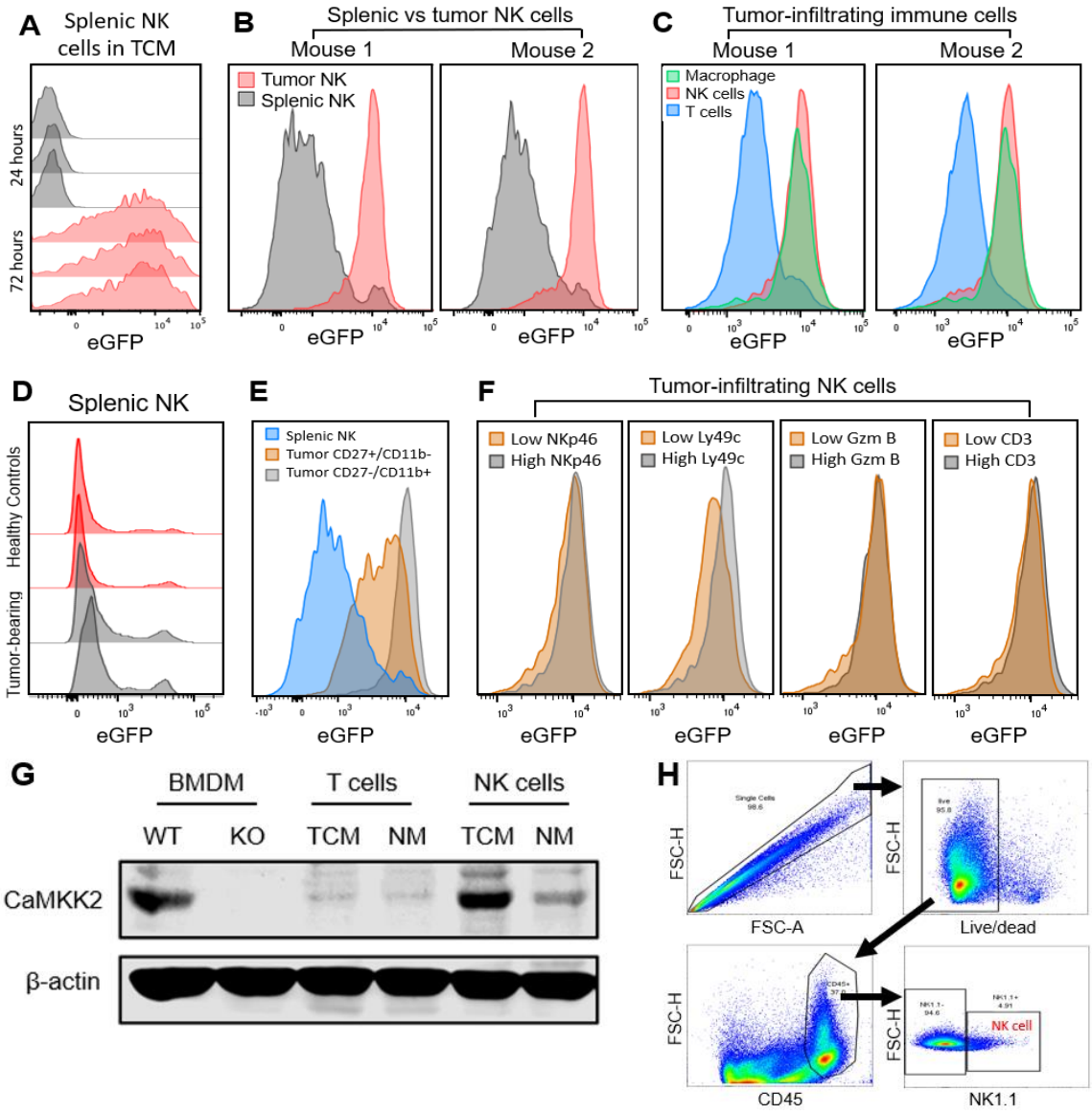


**Figure 4: CaMKK2 expression is upregulated in tumor-infiltrating NK cells.** (A) Splenic NK cells were harvested from CaMKK2-eGFP reporter mice, cultured in 50% EO771 TCM for 24-72 hours, and analyzed for eGFP fluorescence via flow cytometry. (B-C) Fourteen-day subcutaneous EO771 tumors were harvested from two CaMKK2-eGFP reporter mice along with spleens. (C) NK cells from tumor and spleen, or (D) NK cells, T-cells, and macrophages from the tumor were analyzed for eGFP fluorescence. (E) Splenic NK cells were harvested from CaMKK2-eGFP reporter mice bearing fourteen-day subcutaneous EO771 tumors and from healthy control reporter mice, and eGFP fluorescence was analyzed. (E-F) Fourteen-day subcutaneous EO771 tumors were harvested from CaMKK2-eGFP reporter mice, and eGFP expression was analyzed in a

variety of NK cell subsets. Each distribution represents >1000 cells; data is representative of 2 mice. (G) Bone marrow-derived macrophages (BMDMs), splenic T-cells, and splenic NK cells harvested from WT and CaMKK2-/-(KO) BL/6 female mice were cultured in 50% EO771 tumor-conditioned media (TCM) or normal growth media (NM) for 72 hours. CaMKK2 and the β-actin control were measured via Western immunoblotting on a 7.5% acrylamide gel. (H) The flow cytometry gating strategy for panels A-F is depicted.

### 2.2.3 CaMKK2 promotes NK cell survival and proliferation *in vitro*

Upon establishing that CaMKK2 is expressed in tumor-infiltrating NK cells, we began dissecting the mechanisms by which this enzyme influences NK cell biology using a series of *in vitro* models. Two models of CaMKK2 ablation were used in these studies: (1) splenic NK cells harvested from WT and CaMKK2 KO mice, and (2) pharmacologic degradation of CaMKK2 in WT NK cells using a specific, high-affinity CaMKK2 LDD (CC3240). This LDD degrades about 75% of the CaMKK2 protein in primary mouse NK cells **(Fig. 5D)**. To approximate tumor conditions *in vitro*, NK cells were cultured in 50% EO771 TCM. Using this model, the effects of CaMKK2 ablation on a range of NK cell processes were assessed, including apoptosis, proliferation, activation marker expression, direct cytotoxic activity, and migration.

Both the KO and CC3240-treated NK cell groups, when cultured in TCM, exhibit a significant reduction in total live cells compared to the WT and DMSO controls **(Fig. 5A, 5E)**. This reduction in total live NK cells was likely driven by a combination of reduced NK cell survival and reduced proliferation. When cultured in TCM, both KO and CC3240-treated NK cells exhibited reduced viability **(Fig. 5B, 4F)** and elevated levels of the pre-apoptosis marker Annexin V, compared to controls **(Fig. 5C, 4G)**. Thus, increased apoptosis is likely the driver of reduced NK cell viability in the CaMKK2-deficient groups, rather than other forms of cell death. A significant reduction in viability was also observed when CC3240-treated NK cells were cultured in A7C11 TCM **(Fig. 5H)**, indicating that the pro-survival effects of CaMKK2 are generalizable beyond the EO771 TCM model.

Importantly, no changes in viability and Annexin V expression were seen in the CaMKK2-deficient NK cells grown in normal media **(Fig. 5A-C, 4E-G)**, reflecting the necessity of tumor conditions to upregulate CaMKK2.

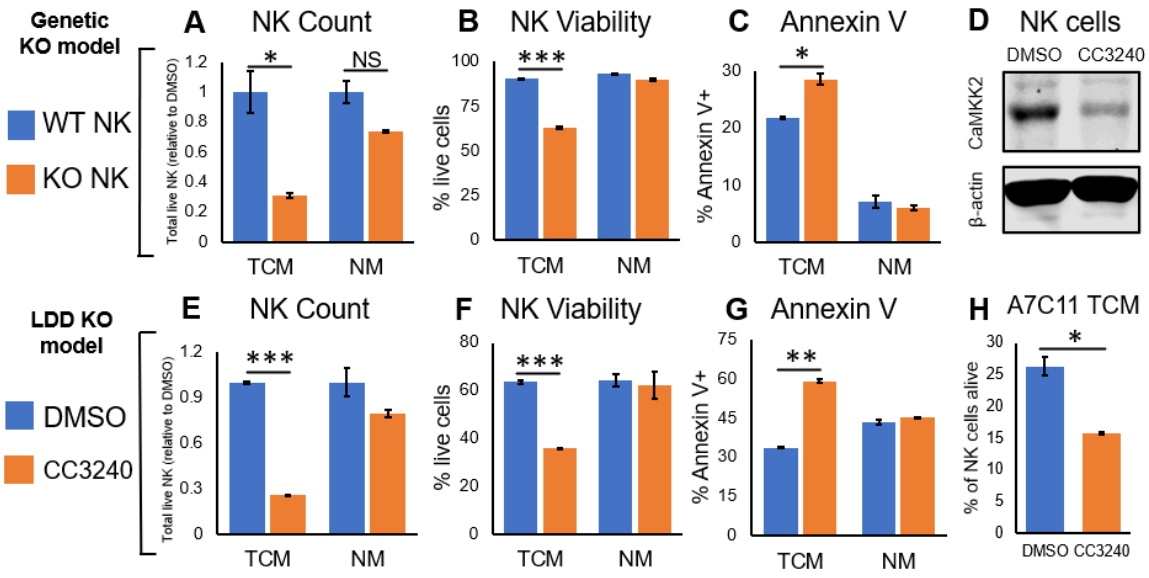


**Figure 5: CaMKK2 ablation reduces NK cell viability.** (A-C) Splenic NK cells were isolated from WT or CaMKK2 KO BL/6 females and cultured for 96 hours in 50% EO771 TCM or normal growth media (NM). Flow cytometry was used to determine, (A) the total number of live NK cells as a proportion of the DMSO control, (B) the viability of the NK cells, (C) and Annexin V staining on the NK cells. (D) Splenic NK cells were harvested from WT BL/6 females and cultured for 72 hours in 50% EO771 TCM containing 2.5 μM CC3240 or DMSO vehicle. CaMKK2 and the β-actin control were measured via Western immunoblotting on a 7.5% acrylamide gel. (E-G) Splenic NK cells were isolated from WT BL/6 females and cultured for 72 hours in 50% EO771 TCM or normal growth media (NM) containing 2.5 μM CC3240 or DMSO vehicle. Flow cytometry was used to determine, (E) the total number of live NK cells as a proportion of the DMSO control, (F) the viability of the NK cells, and (G) Annexin V staining on the NK cells. (H) Splenic NK cells were isolated from WT BL/6 females and cultured for 72 hours in 50% A7C11 TCM containing 2.5 μM CC3240 or DMSO vehicle. Flow cytometry was used to determine NK cell viability. For all panels: N=3, and standard error is shown.

We next studied the effects of CaMKK2 expression on NK cell proliferation. CaMKK2 KO NK cells cultured in TCM exhibited reduced expression of the proliferation marker Ki67 compared to WT NK cells **(Fig. 6A)**. To directly measure proliferation, WT NK cells were stained with the amine-reactive vital dye CFSE and cultured in TCM with CC3240 or DMSO vehicle. CFSE is diluted with each round of cell division, so reduced CFSE fluorescence serves as a proxy for proliferation. We found that the CC3240-treated NK cells were significantly less likely to undergo division compared to those treated with the DMSO control **(Fig. 6B).** These findings suggest that CaMKK2 expression preserves the proliferative capacity of tumor-conditioned NK cells. As with the survival phenotype, exposure to TCM was required to elicit changes in proliferation upon CaMKK2 ablation **(Fig 6A-B)**.

The effects of CaMKK2 expression on *in vitro* NK cell migration were also assessed. To this end, NK cells were cultured for 72 hours in EO771 TCM with CC3240 or DMSO vehicle, at which point equal numbers of live cells from each group were placed into the upper inserts of a migration chamber containing the CCL4 chemokine in the lower well. After three hours, it was observed that significantly fewer CC3240-treated NK cells had migrated to the bottom chamber compared to the DMSO control **(Fig. 6C)**. CCL4-mediated chemotaxis was markedly reduced, but so too was the baseline level of random migration, suggesting a broad dysfunction in the cell movement machinery of CaMKK2-deficient NK cells. WT and KO NK cells express CCR5, the CCL4 receptor, at comparable levels **(Fig. 6D)**. These data, together with that from the proliferation and cell survival studies, suggest that CaMKK2 expression confers a general fitness advantage on NK cells under the stressful conditions of the tumor environment.

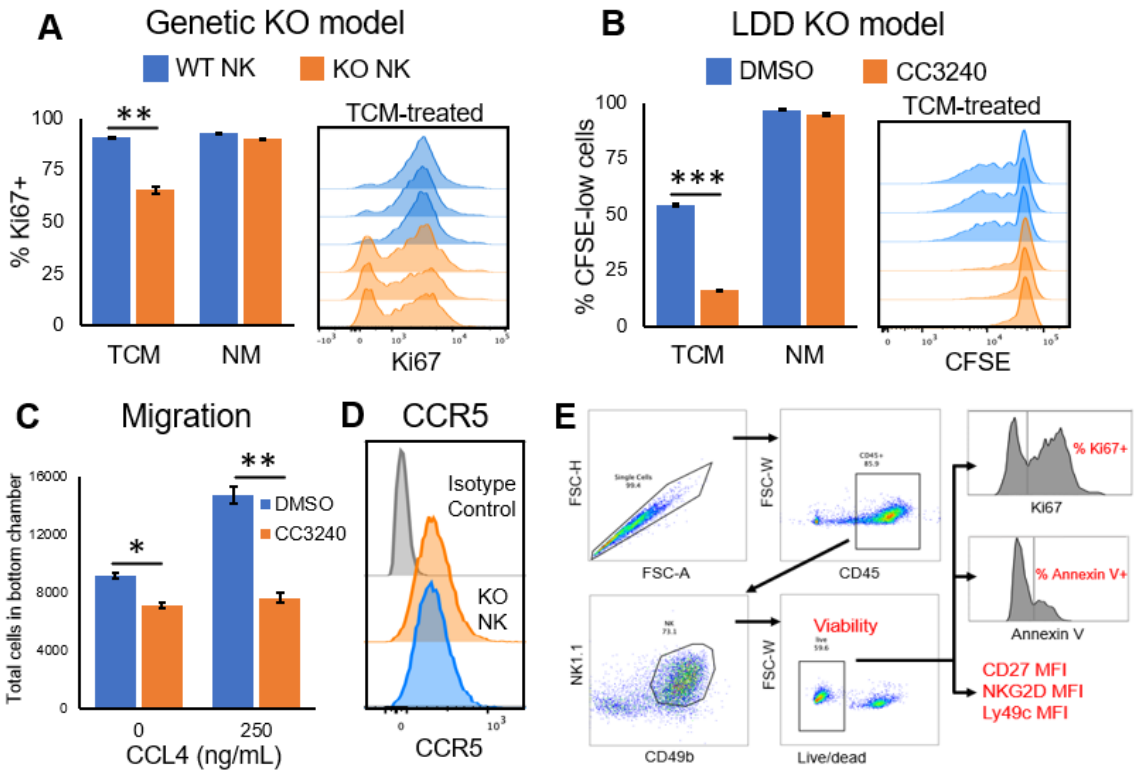


**Figure 6: CaMKK2 ablation reduces NK cell proliferation and migration.** (A) Splenic NK cells were isolated from WT or CaMKK2 KO BL/6 females and cultured for 96 hours in 50% EO771 TCM or normal growth media (NM). Flow cytometry was used to determine Ki67 staining. N=3, standard error shown. (B) Splenic NK cells were isolated from WT BL/6 females, stained with CFSE, and cultured for 72 hours in 50% EO771 TCM or NM containing 2.5 μM CC3240 or DMSO vehicle. Flow cytometry was used to measure dilution of the CFSE dye. N=3, standard error shown. (C) Splenic NK cells were isolated from WT BL/6 females and cultured for 72 hours in 50% EO771 TCM containing 2.5 μM CC3240 or DMSO vehicle. 500k live NK cells were transferred to the upper chambers of a migration plate, separated from CCL4-containing media by a barrier with 5 μm pores. After 3 hours, cell number in the bottom chamber was measured via flow cytometry. N=3, standard error shown. (D) Splenic NK cells were harvested from WT or CaMKK2 KO BL/6 females and cultured for 96 hours in normal growth media containing 100 ng/mL IL2 and IL15. CCR5 expression was measured via flow cytometry and compared to an isotype control. (E) The flow cytometry gating strategy for Figures 5-7 is shown.

The effects of CaMKK2 expression on the cytotoxic actions of NK cells were assessed through functional marker expression and *ex vivo* cytotoxicity assays. Flow cytometry profiling of TCM-cultured NK cells showed that CaMKK2 ablation had no effect on the expression of several markers indicative of cytotoxic function, including CD27, NKG2D, and KIR receptor Ly49c **(Fig. 7A)**. Granzyme B stained poorly in these cells and is not shown. These results were not surprising given the lack of correlation between eGFP fluorescence and functional marker expression in the CaMKK2 reporter experiments **(Fig. 3F)**. We also evaluated the direct cytotoxicity of KO or CC3240-treated NK cells. Specifically, NK cells were cultured for 72 hours in TCM with CC3240 or DMSO vehicle, then co-cultured with YAC-1 target cells at various ratios. YAC-1 is an MHC I-negative cell line classically used in NK cell cytotoxicity assays. YAC-1 survival was measured using flow cytometry[171]. In this manner, it was determined that neither pharmacologic ablation of CaMKK2 **(Fig. 7B)** nor genetic ablation **(Fig. 7C)** affects the cytotoxicity of NK cells against YAC1 tumors. Taken together, our *in vitro* assays show that CaMKK2 regulates apoptosis, proliferation, and migration in tumor-conditioned NK cells, but does not directly affect cytotoxic potency of individual cells.

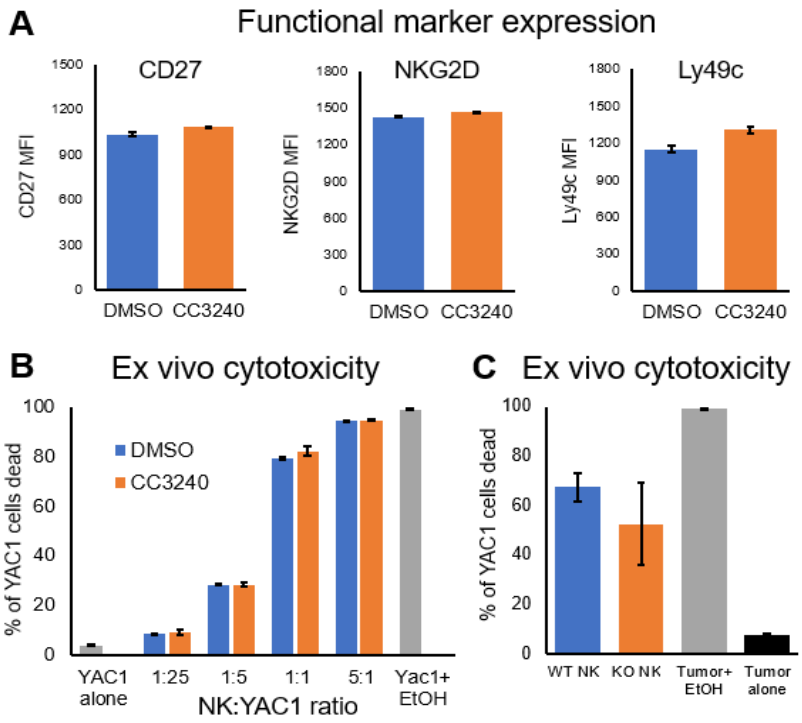


**Figure 7: CaMKK2 ablation does not affect NK cell cytotoxic potency.** (A-B) Splenic NK cells were isolated from WT BL/6 females and cultured for 72 hours in 50% EO771 TCM containing 2.5 μM CC3240 or DMSO vehicle. (A) The median fluorescence intensity (MFI) of key functional markers was measured using flow cytometry. N=2, standard error shown. (B) Live NK cells were co-cultured with CFSE-stained YAC-1 cells at the stated ratios for 4 hours, and YAC-1 viability was measured using flow cytometry. YAC-1 cells were also cultured alone (YAC-1 alone) or with 25% ethanol (YAC1 + EtOH). N=3, standard error is shown. (C) Splenic NK cells were harvested from WT or CaMKK2 KO mice and cultured in 50% EO771 media for 96 hours. Live NK cells were co-cultured with CFSE-stained YAC-1 cells at a 1:5 ratio for 4 hours, and YAC-1 viability was measured via flow cytometry. N=3, standard error is shown.

### 2.2.4 CaMKK2 regulates NK cell biology through a scaffold mechanism

To study the mechanism by which CaMKK2 regulates NK cell function, we compared the effects of several functionally distinct CaMKK2-modulating compounds. CC8977, YL-36, and GSKi are competitive inhibitors of CaMKK2, whereas the LDDs CC3240 and CC3756 recruit the E3 ubiquitin ligase cereblon to degrade the CaMKK2 protein, mimicking genetic KO of CaMKK2 (currently unpublished). All five compounds are highly specific for CaMKK2 and bind with high affinities[129,131]. Interestingly, both LDDs but none of the competitive inhibitors reduce viability and Ki67 expression in TCM-cultured NK cells **(Fig. 8A-B)**, suggesting that the CaMKK2 protein scaffold, but *not* its kinase function, is important for NK cell regulation. All five compounds reduced AMPK phosphorylation at Thr172, the classic CaMKK2-binding site, confirming that the drugs are active in primary murine NK cells **(Fig. 8C)**. These findings rule out the AMPK pathway as the primary mediator of the pro-survival, pro-proliferation phenotype associated with CaMKK2 expression. Rather, our data highlight an important scaffold function for this enzyme in regulating NK cell biology. We also treated tumor-conditioned NK cells with the most widely used competitive CaMKK2 kinase inhibitor STO609, but this drug was found to reduce NK cell survival even under normal media conditions **(Fig. 8D)**, likely reflecting toxicity or lack of specificity at the high concentrations (10 μM) necessary for CaMKK2 inhibition[130].

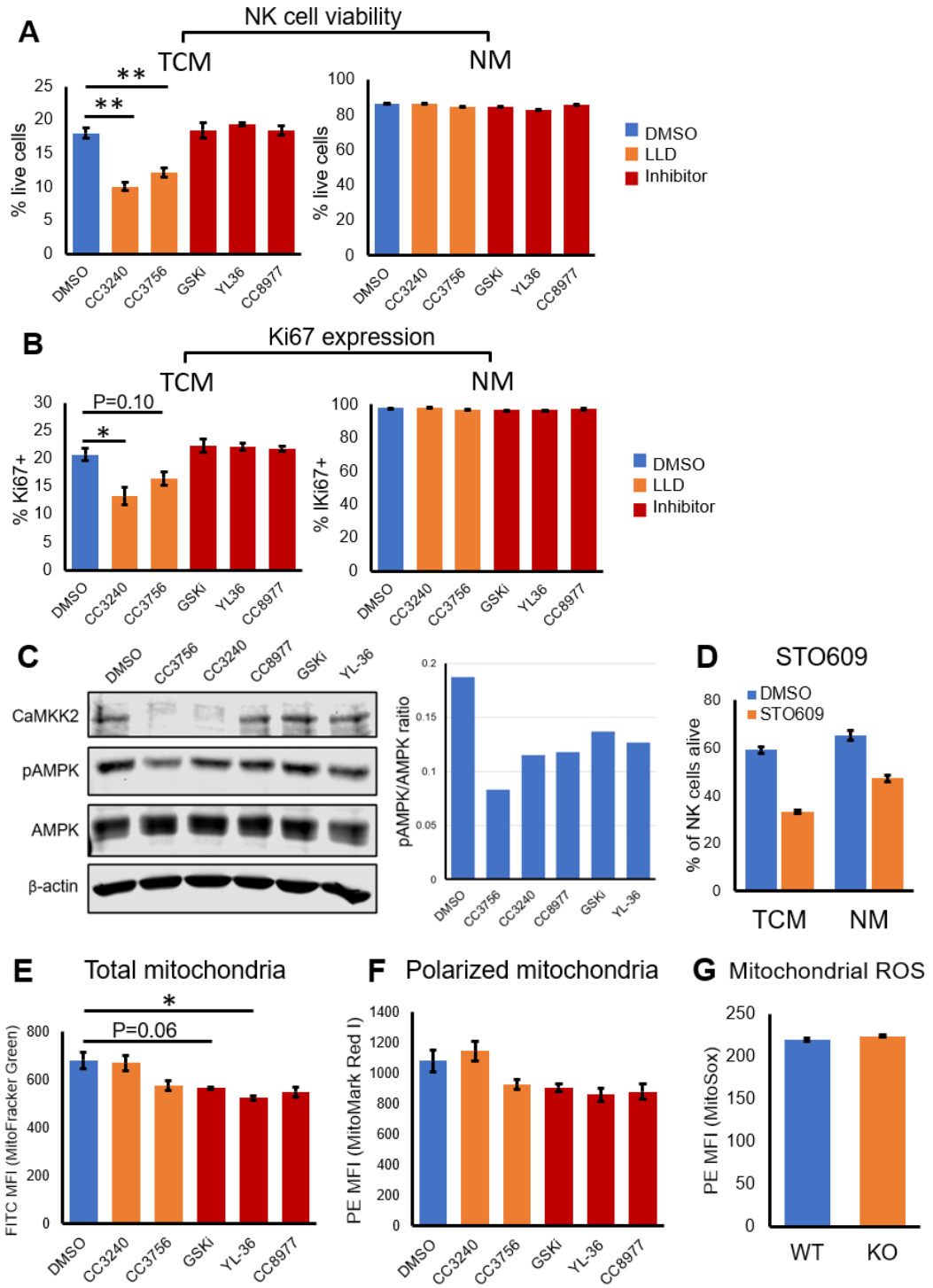


**Figure 8: CaMKK2 LDDs, but not competitive inhibitors, reduce NK cell fitness**. (A-B) Splenic NK cells isolated from WT BL/6 females were cultured for 96 hours in 50% EO771 TCM or normal growth media (NM) containing DMSO vehicle, the LDD CC3240 or CC3756 (1 μM), or the competitive inhibitor GSKi, YL36, or CC8977 (1 μM). (A) NK cell viability and (B) expression of Ki67 were measured using flow cytometry. N=3, standard error shown. (C) Splenic NK cells isolated from WT BL/6 females were cultured for 96 hours in normal media containing 10 mM lactic acid and either the DMSO vehicle, the LDD CC3240 or CC3756 (1 μM), or the competitive inhibitor GSKi, YL36, or CC8977 (1 μM). A

Western immunoblot was then used to analyze expression of CaMKK2, AMPKα, phospho-Thr172-AMPKα (pAMPK), and β-actin (7.5% acrylamide gel, 45 μg protein loaded per well). (D) Splenic NK cells were isolated from WT BL/6 females and cultured for 72 hours in 50% EO771 TCM or normal growth media containing 10 μM STO609 or DMSO vehicle. NK cell viability was measured via flow cytometry. N=2, standard error shown. (E-G) Splenic NK cells isolated from WT BL/6 females were cultured for 96 hours in 50% EO771 TCM containing DMSO vehicle, the LDD CC3240 or CC3756 (1 μM), or the competitive inhibitor GSKi, YL36, or CC8977 (1 μM). (D) CaMKK2, AMPK, pAMPK (Thr172), and β-actin expression were measured by Western immunoblotting following resolution of proteins on a 7.5% acrylamide gel. (E) MitoTracker Green FM staining was measured via flow cytometry to determine total mitochondria mass, and (F) MitoMark Red I staining was measured via flow cytometry to determine the mass of polarized mitochondria. N=3, standard error shown. (G) Splenic NK cells harvested from WT or KO BL/6 females were cultured for 96 hours in 50% EO771 TCM, stained with the MitoSox ROS dye, and analyzed using flow cytometry. N=2, standard error is shown.

As a primary source of energy and reactive-oxygen species, the mitochondria play an important role in the survival and proliferation of most cell types, including NK cells. The structural integrity, biogenesis, and turnover of mitochondria is tightly regulated as imbalanced mitochondrial activity leads to cellular dysfunction and death[172]. Interestingly, CaMKK2 has been shown to regulate mitochondrial activity in multiple tumor cell lines through modulation of the SDH enzyme complex[173], raising the possibility that CaMKK2 enhances NK cell fitness through effects on the mitochondria. To explore this possibility, splenic NK cells were cultured in EO771 TCM for 96 hours and treated with a CaMKK2 inhibitor, LDD, or the DMSO vehicle. NK cells were then stained with three fluorescent mitochondrial dyes that were measured using flow cytometry: (1) MitoTracker Green, which stains all mitochondria and measures total mitochondrial mass, (2) MitoMark Red I, a dye whose fluorescence depends on mitochondrial membrane potential, and (3) MitoSox, which measures mitochondrial reactive oxygen species. None of the CaMKK2 inhibitors or LDDs affected total mitochondria mass **(Fig. 8E)**, mitochondrial membrane potential **(Fig. 8F)**, or production of mitochondrial reactive oxygen species **(Fig. 8G)** in the TCM-treated NK cells. Given these results, we ruled out mitochondrial regulation as the principal mechanism by which CaMKK2 preserves NK cell fitness.

### 2.2.5 CaMKK2 expression enhances NK cell anti-tumor immunity

NK cells play many roles in tumor immunity, including detection of *de novo* tumor formation, clearance of metastatic cells, and recruitment/activation of other immune cells. However, NK cells are a particularly critical component of the anti-metastasis response, and our animal studies focused on this aspect of tumor biology. Changes during the epithelial-mesenchymal transition, which is critical for metastasis, render tumor cells especially vulnerable to NK cell activity[40,41]. Indeed, NK cells have a significant impact on the dissemination of tumor cells and the growth of metastatic lesions[39]. Conversely, NK cells typically show poor infiltration into primary tumors[174,175], and evidence for the role of NK cells in primary tumor progression is mixed[176,177]. From a translational perspective, metastatic disease is highly relevant as 70% of cancer mortality is attributed to metastasis[178]. For these reasons, our animal studies focused on metastatic disease rather than primary tumor progression. Specifically, we use intravenous metastasis models in which tumor cells are injected through the lateral tail veins of mice. Although intravenous tumor injection bypasses the early intravasation step, this model preserves the circulation, extravasation, and colonization steps during which NK cells exert the greatest influence. Tail vein models are widely employed in the cancer biology field as a relevant metastasis model[179-181].

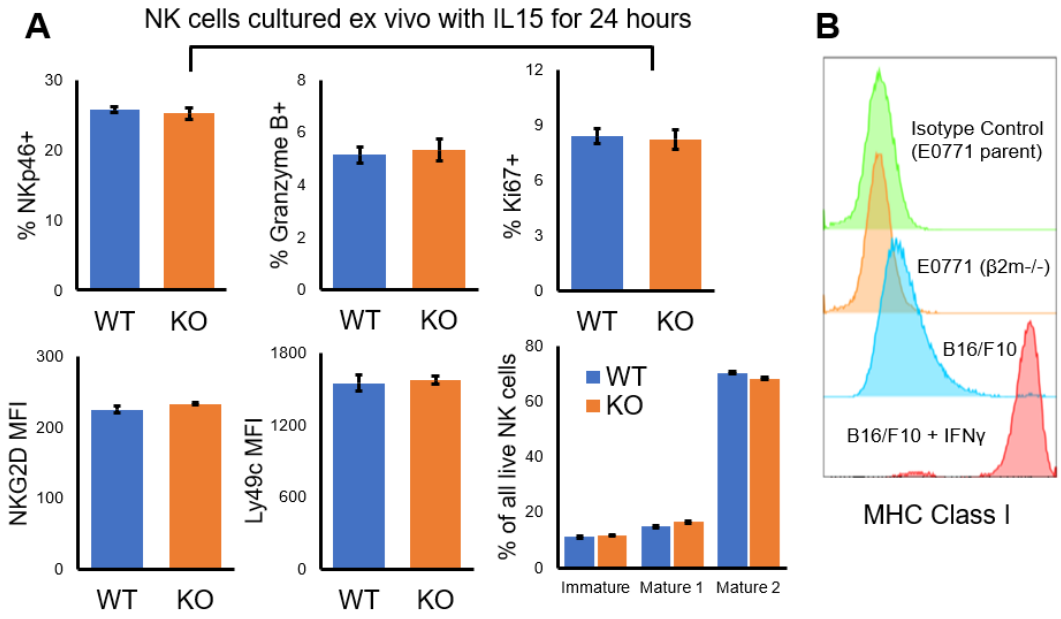


**Figure 9: Profile of NK cells and tumor cells used in metastasis studies.** (A) Splenic NK cells were harvested from WT and CaMKK2 KO BL/6 females and cultured for 24 hours in normal media containing 100 ng/mL IL15. Various functional markers were characterized via flow cytometry. The prevalence of immature NK cells ($CD27^+/CD11b^-$), mature 1 NK cells ($CD27^+/CD11b+$), and mature 2 NK cells ($CD27^-/CD11b^+$) was also measured. N=4, standard error shown. (B) β2m-/- EO771 cells, B16-F10 cells, and B16-F10 cells treated with 100 ng/mL IFNγ for 48 hours were analyzed for MHC Class I expression via flow cytometry. Fluorescence was compared to EO771 parent cells stained with an isotype control antibody.

To limit CaMKK2 ablation to the NK cell compartment, our initial metastasis experiments utilized NSG mice engrafted with NK cells isolated from WT or CaMKK2 KO hosts. NSG mice completely lack endogenous NK cells due to the deletion of the IL-2 receptor γ chain. Thus, NK cells harvested from the spleens of WT or CaMKK2 KO mice can be transfused into NSG hosts in lieu of endogenous NK cells. However, NK cell viability must be maintained by exogenous administration of recombinant IL-2. At the time of transfusion, WT and CaMKK2 KO NK cells were qualitatively similar as measured by the expression of several activation and maturation markers **(Fig. 9A)**. To increase tumor cell sensitivity to NK cell activity, the EO771 tumor subline we employed was engineered to eliminate MHC I expression using a CRISPR-based approach to delete both alleles of

β2m **(Fig. 9B)**. β2m serves as the common heavy chain of MHC I and is required for the stabilization and cell surface expression of the complex[182]. The EO771 cells were also modified to express luciferase, enabling systemic monitoring of tumor burden in live animals using a luciferin-based *in vivo* imaging system (IVIS). The modified EO771 cells were injected via tail vein, and within two weeks, mice engrafted with CaMKK2 KO NK cells exhibit a significantly larger systemic EO771 metastatic burden than mice engrafted with WT NK cells **(Fig. 10A-C)**. These results suggest that ablation of CaMKK2 impairs the anti-metastasis and surveillance functions of NK cells.

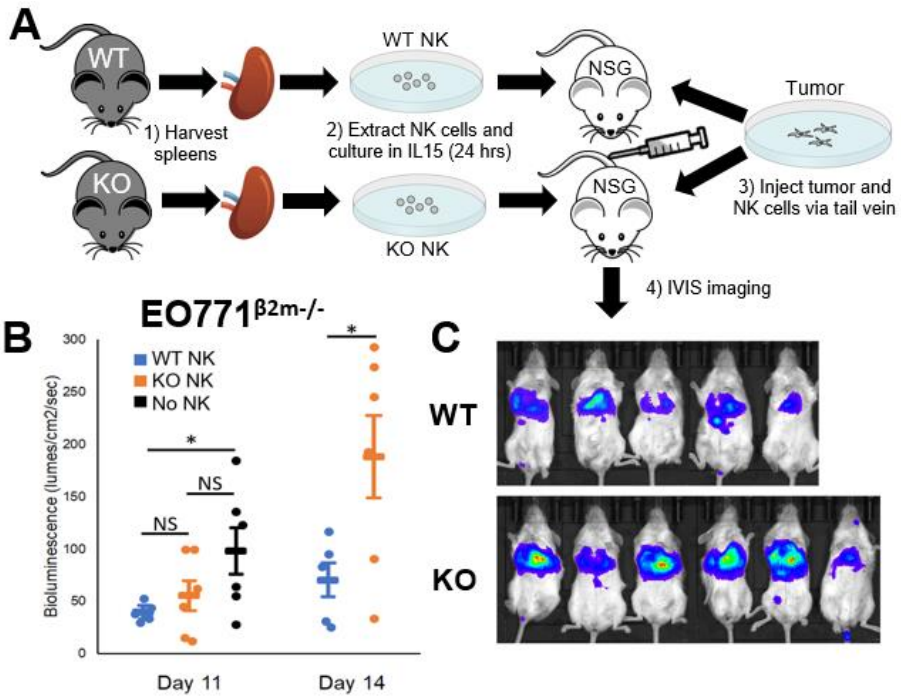


**Figure 10: NK cells from a CaMKK2 KO background show reduced activity against EO771 metastases.** (A) Splenic NK cells from WT or CaMKK2 KO BL/6 females were isolated, cultured in media containing IL15 for 24 hours, and intravenously transfused into NSG mice. Two days later, luciferase-expressing β2m-/- EO771 breast tumor cells were also transfused. A positive control group received only tumor cells and no NK cells. (B) Whole-body metastatic burden in the EO771 study was measured using luciferin bioluminescence imaging at days 11 and 14 post-tumor injection. Camera exposure time was 3 minutes. N=5-6, standard error is shown. (C) Raw bioluminescence data from the day 14 imaging session is shown.

The metastasis study was repeated using the B16-F10 melanoma model, which expresses low levels of MHC I at baseline **(Fig. 9B)**. As observed in the EO771 model, mice engrafted with CaMKK2 KO NK cells exhibited a significantly larger metastatic B16-F10 burden compared to their WT counterparts **(Fig 11A-B)**. Post-mortem flow cytometry analysis of the lung tissue, which was the dominant site of metastasis, showed a significant reduction in the prevalence and total number of live NK cells in the lungs of the KO group, likely driven in part by the observed reduction in NK cell viability **(Fig. 11C)**. However, the WT and KO groups exhibited no differences in NK cell activation or maturation markers **(Fig. 11D)**, suggesting that NK cell viability, but not cytotoxic function, is compromised upon CaMKK2 ablation. These results reinforce earlier *in vitro* studies showing reduced viability when CaMKK2 is ablated in TCM-cultured NK cells.

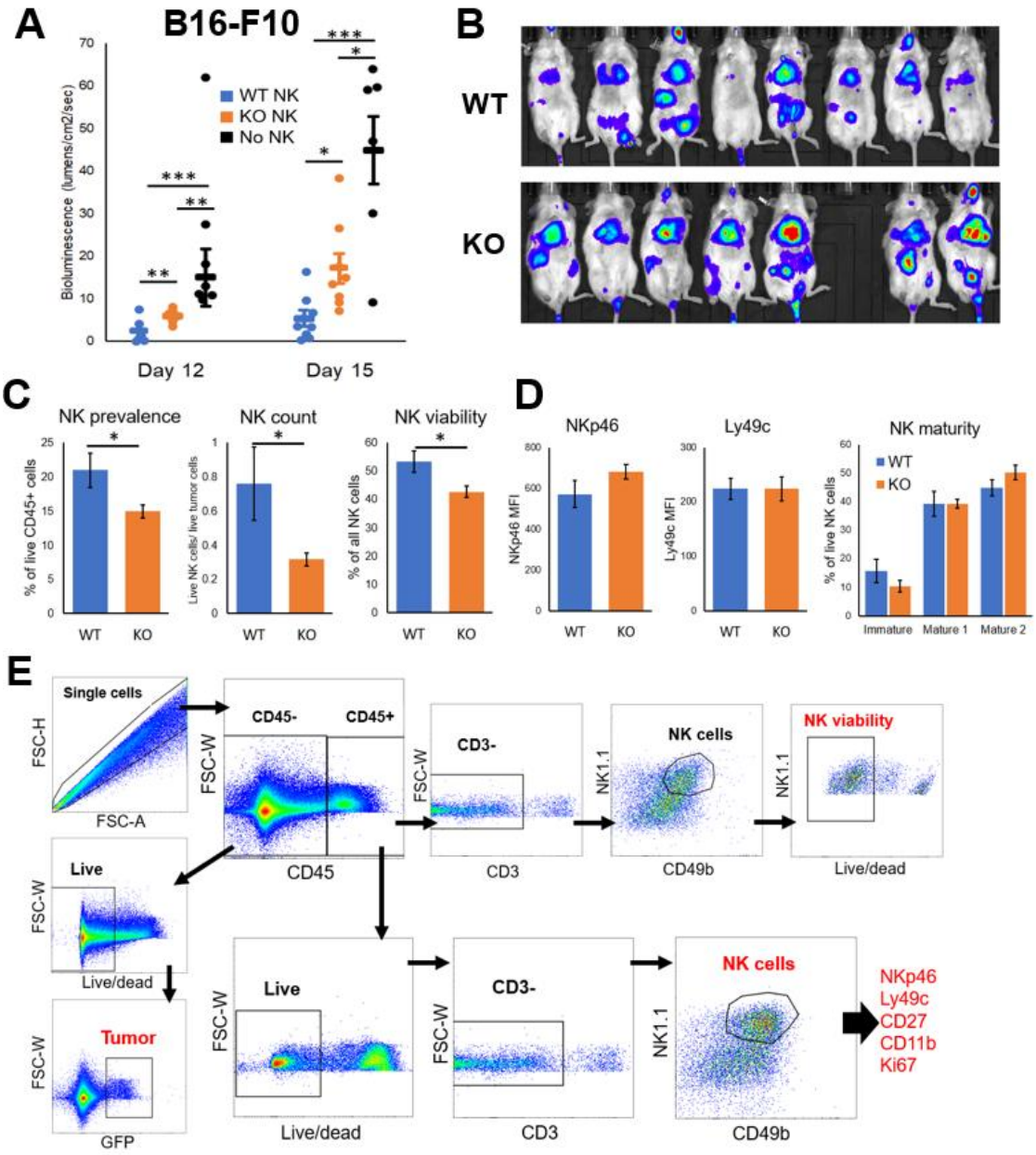


**Figure 11: NK cells from a CaMKK2 KO background show reduced activity against B16-F10 metastases.** (A) NSG mice were engrafted with NK cells from WT or KO mice and injected with luciferase-expressing B16-F10 tumor cells. Whole-body metastatic burden was measured using luciferin bioluminescence imaging. Results were collected 12 and 15 days post-injection. Camera exposure time was two minutes. N=7-8, standard error shown. (B) Raw bioluminescence data from Day 15 is shown. (C-D) NK cells were recovered post-mortem from the lungs of each mouse and analyzed using flow cytometry. (C) Live NK cells as a portion of $CD45^+$ cells (NK prevalence), total live NK cells as a fraction of live tumor cells (NK count), and the fraction of all NK cells that are alive (NK viability) were measured. (D) Median fluorescence intensity (MFI) of NKp46 and Ly49c on NK cells was measured. The distribution of immature, Mature 1 NK cells, and Mature 2 NK cells was measured. N=7-8, standard error shown. (E) The flow cytometry gating strategy is shown for Figures 10-12.

The NK cells transfused in the first set of metastasis studies were harvested from animals with a germline deletion of the CaMKK2 locus, raising the possibility of confounding developmental or compensatory factors. CaMKK2 is expressed in several immune cell precursors in the bone marrow where it regulates lineage commitment and downstream development[126]. CaMKK2 also affects the function of macrophages which in-turn influences NK cells through complex cross-talk interactions[183]. To control for these potential confounders, and to clearly delineate the significance of NK cell-*intrinsic* functions of CaMKK2, we repeated the metastasis experiments using a tamoxifen-inducible CaMKK2 KO model. This model features constitutive expression of a cre-ERT2 fusion protein that translocates to the nucleus upon tamoxifen induction, excising the floxed CaMKK2 alleles **(Fig. 12A)**. Splenic NK cells were harvested from $ERT2^{+}$ and $ERT2^{-}$ controls after one week of tamoxifen administration, and the NK cells were co-transfused with luciferase-expressing, $GFP^{+}$ B16/F10 cells into NSG hosts. Knockdown of CaMKK2 in BMDMs from $ERT2^{+}$ mice, but not in the $ERT2^{-}$ mice, was confirmed by Western immunoblot **(Fig. 12B)**. Within two weeks of tumor injection, mice reconstituted with the $ERT2^{+}$ NK cells showed a significantly larger systemic B16-F10 tumor burden compared to the $ERT2^{-}$ controls **(Fig. 12C-D)**, confirming the importance of CaMKK2 in metastatic progression.

Post-mortem flow cytometry analysis showed a dramatic increase in MHC I expression on tumor cells isolated from the lungs of $ERT2^{-}$ mice compared to the $ERT2^{+}$ group **(Fig. 12E)**. MHC I expression protects tumors from NK killing, so MHC I upregulation is likely the result of selective pressure exerted on the tumor cells by NK cells. Thus, persistently low MHC I expression on the tumors provides direct evidence of reduced immunoediting when NK cells lose CaMKK2 expression. Flow cytometry profiling of the immune cell repertoire in the lungs showed a reduction in total live NK cells in the $ERT2^{+}$

group compared to that observed in ERT2$^{-}$ mice **(Fig. 12F),** as was observed in prior studies using the germline CaMKK2 KO model. The reduction in live NK cells is likely driven by reduced proliferation, reflected in lower Ki67 expression among ERT2$^{+}$ NK cells, and by a reduction in NK cell viability in the ERT2$^{+}$ group **(Fig. 12F)**.

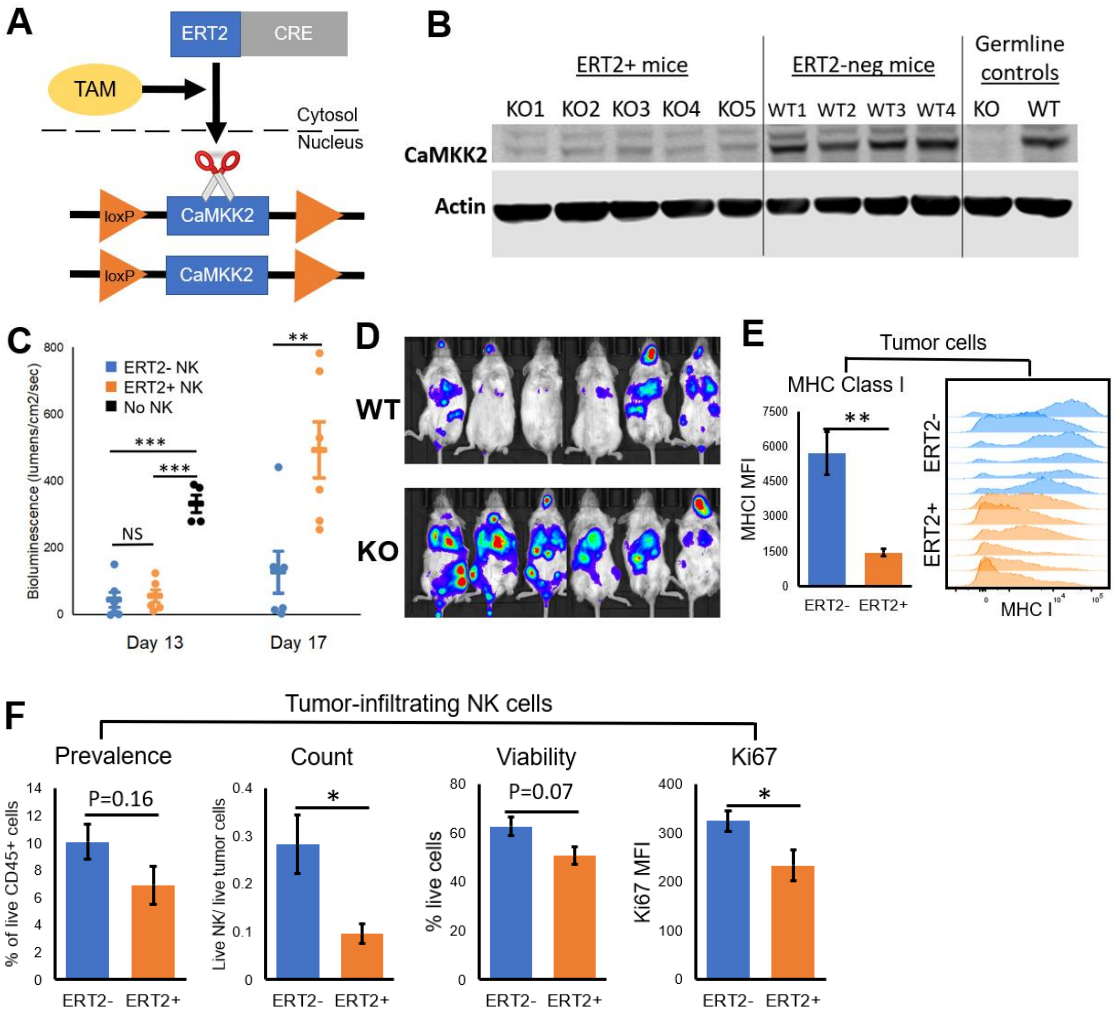


**Figure 12: NK cells from an inducible CaMKK2 KO background show reduced activity against B16-F10 metastases.** (A) NK cells were harvested from the spleens of tamoxifen-treated CaMKK2$^{fl/fl}$:ERT2$^{+}$ mice or CaMKK2$^{fl/fl}$:ERT2$^{-}$ mice and co-injected into the tail veins of NSG mice along with luciferase-expressing GFP$^{+}$ B16-F10 tumor cells. The CaMKK2$^{fl/fl}$:ERT2$^{+}$ mice express a fusion cre-ERT2 protein that translocates to the nucleus upon tamoxifen binding, excising the floxed CaMKK2 alleles. (B) After one week of tamoxifen dosing, BMDMs were recovered from the ERT2$^{+}$ mice and ERT2-negative controls to confirm CaMKK2 ablation via Western immunoblot on a 7.5% acrylamide gel. (C) Whole-body luciferin bioluminescence was measured at days 13 and 17 post-tumor cell injection. Camera exposure time was 2 minutes. N=6, standard error shown. (D) The raw bioluminescence data from day 17 is shown. (E) GFP+ tumor cells were harvested

from the lungs of each mouse 17 days post-injection, and MHC Class I expression was analyzed using flow cytometry. N=6, standard error shown. (F) NK cells were harvested from lungs of each mouse 17 days post-injection. Flow cytometry was used to measure the prevalence of NK cells among live $CD45^+$ cells (prevalence), the number of live NK cells as a proportion of live tumor cells (count), the percentage of all NK cells that are alive (viability), and Ki67 expression among NK cells (Ki67).

The metastasis studies conducted up to this point have utilized immune deficient animals in which transfused NK cells are the only functional bone marrow-derived immune population. However, many other immune populations are normally present in the tumor environment, and these populations may affect the overall phenotype or be impacted by the loss of CaMKK2 in NK cells. Thus, we developed a model in which CaMKK2 was selectively ablated in NK cells in immune competent animals **(Fig. 13A)**. Specifically, we crossed mice with floxed CaMKK2 alleles to mice expressing *cre* under the control of the Ncr1 (NKp46) promoter, which is only active in NK cells. Experimental and control mice both express one copy of the Ncr1-cre construct, but only the experimental group contain floxed CaMKK2 alleles. Experimental and control mice were injected via tail vein with luciferase-expressing, $GFP^+$ B16-F10 tumor cells, and tumor burden was monitored via IVIS. Within two weeks of tumor injection, the group with floxed CaMKK2 alleles exhibited a significantly greater systemic B16-F10 metastatic tumor burden than control mice **(Fig. 13B-C)**. These studies reveal that ablation of CaMKK2 in the NK cell compartment reduces immune surveillance even in immune competent animals. An extensive immune profiling of post-mortem lung tissue was performed, but we did not identify any downstream immunologic changes resulting from CaMKK2 ablation in NK cells. As expected, the total number of NK cells was reduced in the $CaMKK2^{fl/fl}$ group, but the prevalence of B-cells, neutrophils, dendritic cells, T-cell subsets, and macrophage subsets were unaltered **(Fig. 13D)**. Thus, the reduced tumor burden associated with CaMKK2 expression in NK cells is likely mediated by direct changes in the size of the effector NK cell population.

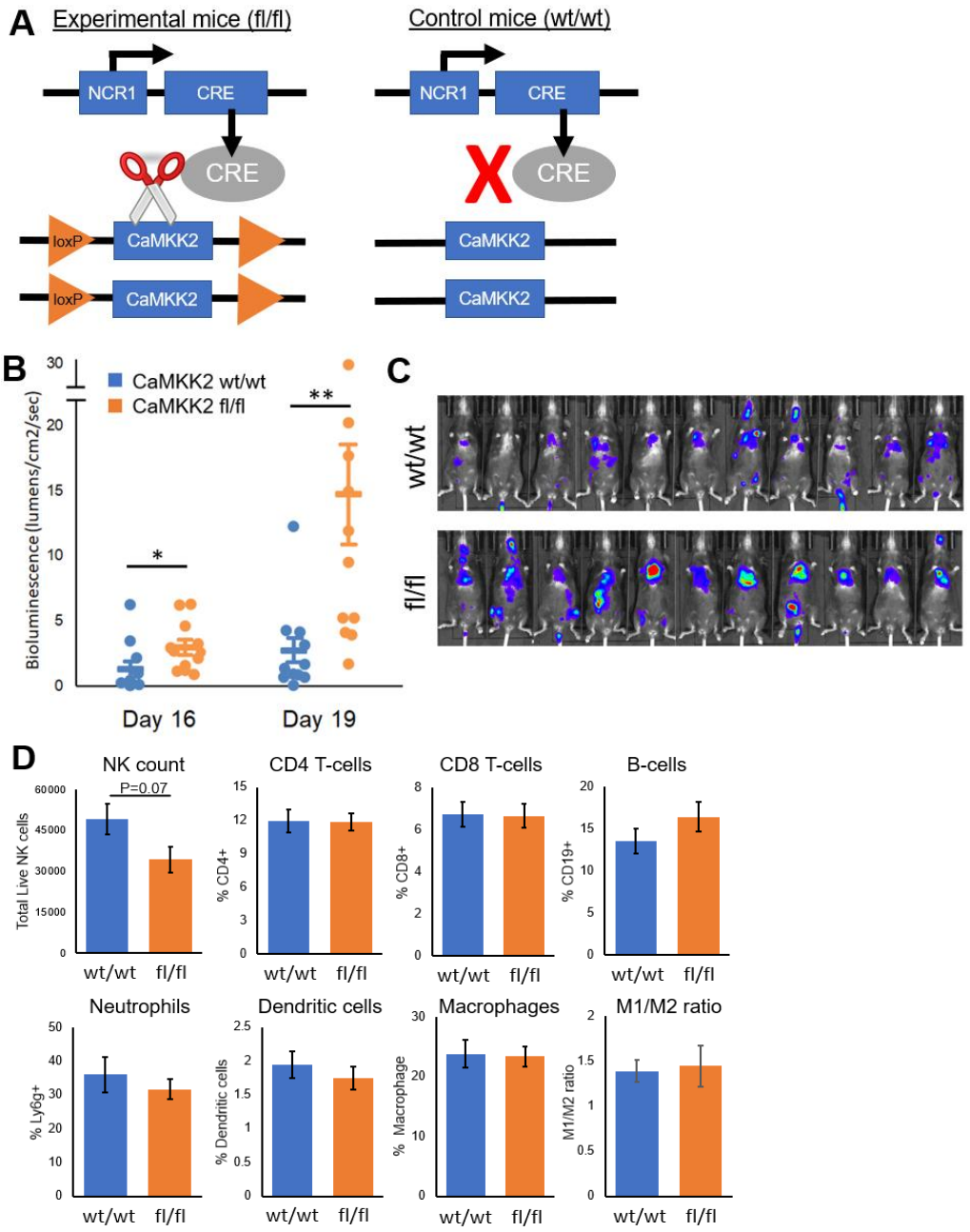


**Figure 13: NK cell-specific CaMKK2 ablation produces increased metastatic progression in immune-competent mice.** (A) Mice were bred that express Cre under the Ncr1 (NKp46) promoter and contain either CaMKK2$^{fl/fl}$ (fl/fl) alleles or CaMKK2 wt/wt alleles, and luciferase-expressing B16-F10 tumor cells were injected via tail vein into these two groups. (B) Whole-body luciferin bioluminescence was measured at days 16 and 19 post-tumor injection. Camera exposure time was 3 minutes. N=11, standard error shown. (C) Raw bioluminescence data from day 19 is shown. (D) NK cells were harvested from the lungs of each mouse 19 days post-injection. Flow cytometry was used to measure the absolute number of live NK cells and the prevalence of various other immune populations within the lungs. M1 macrophages were defined as MHC Class II+/CD206-, and M2 macrophages were defined as MHC Class II$^{-}$/CD206$^{+}$. The flow cytometry gating strategy is shown in Figure 2B. N=11, standard error is shown.

### 2.2.6 CaMKK2 upregulation is driven by a small molecule tumor factor

To tie together our findings, we needed to establish a mechanism by which the tumor environment influences CaMKK2 expression in NK cells. Many components of the tumor environment could trigger this transcriptional event, including cell-cell interactions or soluble factors. Proteins expressed on tumor cells or other tumor-associated cells may engage specific membrane receptors on NK cells, triggering signaling pathways that alter transcriptional state. For example, when the KLGR1 receptor binds E-cadherin, AMPK dephosphorylation is inhibited, which leads to increased telomerase expression in NK cells[70]. Similarly, soluble factors in the extracellular tumor environment could alter transcription. The two major classes of soluble factors are (1) proteins, which includes cytokines and chemokines, and (2) small molecules, which includes metabolites, hormones, and lipids. A wide range of soluble factors are known to alter the transcriptional state of NK cells, including IL15, TGF-β, and picolinic acid[184-186]. Previous experiments showed that TCM exposure was sufficient to upregulate CaMKK2 in a pure population of NK cells, negating cell-cell interactions as a likely driver of CaMKK2 expression. Thus, we focused on identifying soluble factors sufficient to upregulate CaMKK2.

To distinguish between protein and non-protein factors, we compared the effects of normal TCM and heat-inactivated TCM on NK cells *in vitro*. By heating TCM to 50 degrees for 30 minutes, most proteinaceous factors are denatured and lose their normal signaling capacities, but in general small molecules retain their structures and functions. Thus, if TCM loses its capacity to upregulate CaMKK2 when heat-inactivated, then it is implied that a protein factor(s) must be required for upregulation. Interestingly, heat-inactivated EO771 TCM produced the same drop in viability as normal TCM when NK cells are treated with the CC3240 LDD **(Fig. 14A)**. These data indicate that small molecule factors are sufficient to mediate CaMKK2 upregulation, and protein factors are uninvolved.

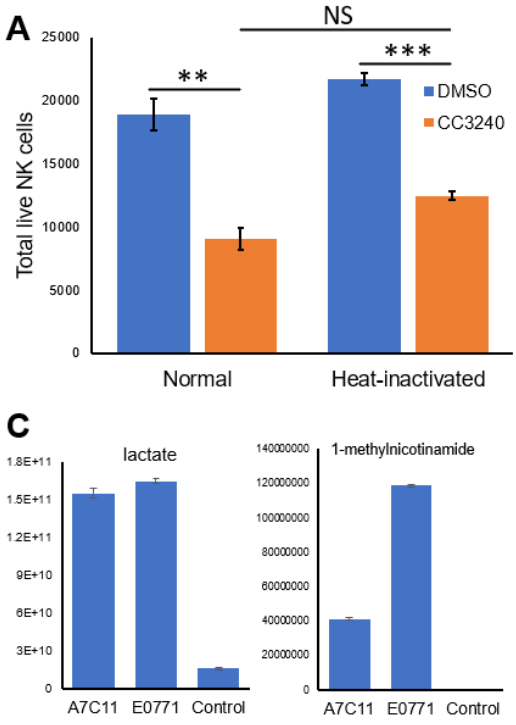


B

| | Metabolite | Fold-enrichment vs NM | |
|---|---|---|---|
| | | A7C11 TCM | E0771 TCM |
| > 8-fold enrichment | 1-methylnicotinamide | * | * |
| | 2-oxoglutarate(2-) | * | * |
| | 3-hydroxyhexadecenoylcarnitine | * | * |
| | N-Acetylmethionine | 364.055 | 93.232 |
| | dopaminochrome | 68.641 | 137.058 |
| | pyridoxal | 63.241 | 127.968 |
| | G6P/F6P | 127.094 | 47.781 |
| | N2-Formyl-N1-(5-phospho-D-ribosyl)glycinamide | 39.247 | 40.927 |
| | ketoleucine | 31.431 | 39.826 |
| | UMP | 29.646 | 29.211 |
| | lactate | 9.757 | 10.382 |
| | Glycerol 3-phosphate | 8.770 | 18.163 |
| > 2-fold enrichment | D-Glucosamine 6-phosphate | 20.075 | 6.151 |
| | estrone 3-sulfate | 7.647 | 8.916 |
| | palmitate | 7.527 | 7.344 |
| | trans-caffeate/3-(4-hydroxyphenyl)pyruvate | 3.022 | 7.660 |
| | malate(2-) | 4.186 | 5.149 |
| | CTP | 3.213 | 5.503 |
| | L-alanine | 2.544 | 4.905 |
| | 6-Phosphogluconic acid | 3.292 | 3.561 |
| | UTP | 2.958 | 3.775 |
| | omega hydroxy dodecanoate | 3.994 | 2.377 |
| | sarcosine | 2.178 | 4.116 |
| | margarate | 2.579 | 2.696 |
| | 3-methyl-2-oxobutanoate | 2.281 | 2.369 |

* Metabolite undetectable in normal media

**Figure 14: A small molecule tumor factor(s) promotes CaMKK2 upregulation.** (A) Splenic NK cells from WT BL/6 females were cultured in 50% E0771 TCM (Normal) or 50% E0771 TCM that had been incubated at 56 degrees for 30 minutes (Heat-inactivated). Cells were treated with either 2.5 μM CC3240 or DMSO vehicle for 72 hours, and total number of live NK cells was measured via flow cytometry. N=2, standard error shown. (B) A7C11 TCM, E0771 TCM, and normal growth media (control) were analyzed via mass spectrometry for 217 common metabolites. Twelve metabolites, highlighted at the top of the chart, were significantly elevated by a factor of eight or more in both A7C11 TCM and E0771 TCM compared to the normal media (NM) control. N=3, standard error shown. (C) The relative levels of two metabolites known to influence tumor immunity are shown. N=3, standard error shown.

To identify candidate small molecule factors affecting CaMKK2 expression, we conducted a metabolomics screen of tumor-conditioned media. Our previous data demonstrated that both EO771 TCM and A7C11 TCM facilitate CaMKK2 upregulation in NK cells *ex vivo* **(Fig. 4G, 5F, 5H)**. Thus, we used mass spectrometry to compare the metabolite composition of these two TCM types against normal media. Our collaborators in The Duke Molecular Physiology Institute used liquid chromatography mass spectrometry to identify the relative abundance of 217 small molecule metabolites. We

then ran a statistical test to prioritize specific metabolites for further investigation, selecting metabolites that were increased in *both* EO771 and A7C11 TCM compared to normal media by a statistically significant factor of two-fold or more ($p<0.05$). This screen produced 25 candidate factors, which was narrowed to 12 factors by increasing the threshold to an eight-fold increase. These 12 factors included the vitamin derivatives 1-methylnicotinamide and pyridoxal, the catecholamine metabolite dopaminochrome, the amino acid derivatives ketoleucine, 2-oxyglutarate, and N-acetylmethionine, the ribonucleotides UMP and N2-Formyl-N1-(5-phospho-D-ribosyl)glycinamide, and the anaerobic fermentation byproduct lactate.

### 2.2.7 Intracellular lactic acid accumulation drives CaMKK2 upregulation

The metabolites 1-methylnicotinamide and lactate immediately stood out as both compounds have established mechanistic roles in tumor immunity. 1-methylnicotinamide is known to induce TNFα production by tumor-infiltrating T cells[187], and lactate is known to affect the survival, activity, and functional phenotype of most immune populations in the tumor environment[152,155,156]. None of the other candidate factors have known roles in tumor immunology. Given lactate's multifaceted role in tumor pathobiology, we elected to evaluate its role in NK cell function before proceeding to a more comprehensive study of the other metabolites identified. Splenic NK cells harvested from CaMKK2 reporter mice were cultured in 50% EO771 TCM, normal media containing 10 mM lactic acid, or normal media alone, and eGFP fluorescence was measured via flow cytometry as a surrogate for CaMKK2 expression. A lactic acid concentration of 10 mM is representative of a typical solid tumor in humans[139]. At 24 hours, there was no change in eGFP expression in the TCM and lactic acid groups **(Fig. 15A).** However, by 96 hours, both the TCM and lactic acid-treated NK cells showed a significant increase in eGFP expression compared to the normal media control **(Fig. 15B).** A Western immunoblot confirmed these results, showing

that exposure to 10 mM lactic acid for 96 hours was sufficient to produce robust CaMKK2 expression, whereas NK cells cultured in normal media show minimal expression **(Fig. 15C)**.

Lactic acid and TCM cause similar phenotypes in CaMKK2-deficient NK cells, providing further evidence that lactic acid is the key component of TCM driving increased CaMKK2 expression. CaMKK2 ablation has no effect on NK cells cultured in normal media because the enzyme is minimally expressed under these conditions. In lactic acid-treated NK cells, however, CaMKK2 ablation produces a significant reduction in NK cell viability and proliferation state, identical to the phenotype observed in TCM-treated NK cells **(Fig 15 D-E**). Finally, the fact that the CaMKK2-eGFP reporter model shows the same rapid expression increase as Western blots indicates that transcriptional changes drive CaMKK2 upregulation, rather than increased post-translational protein stabilization. If protein stabilization were responsible for increased CaMKK2 levels, there would be no parallel increase in the eGFP reporter protein.

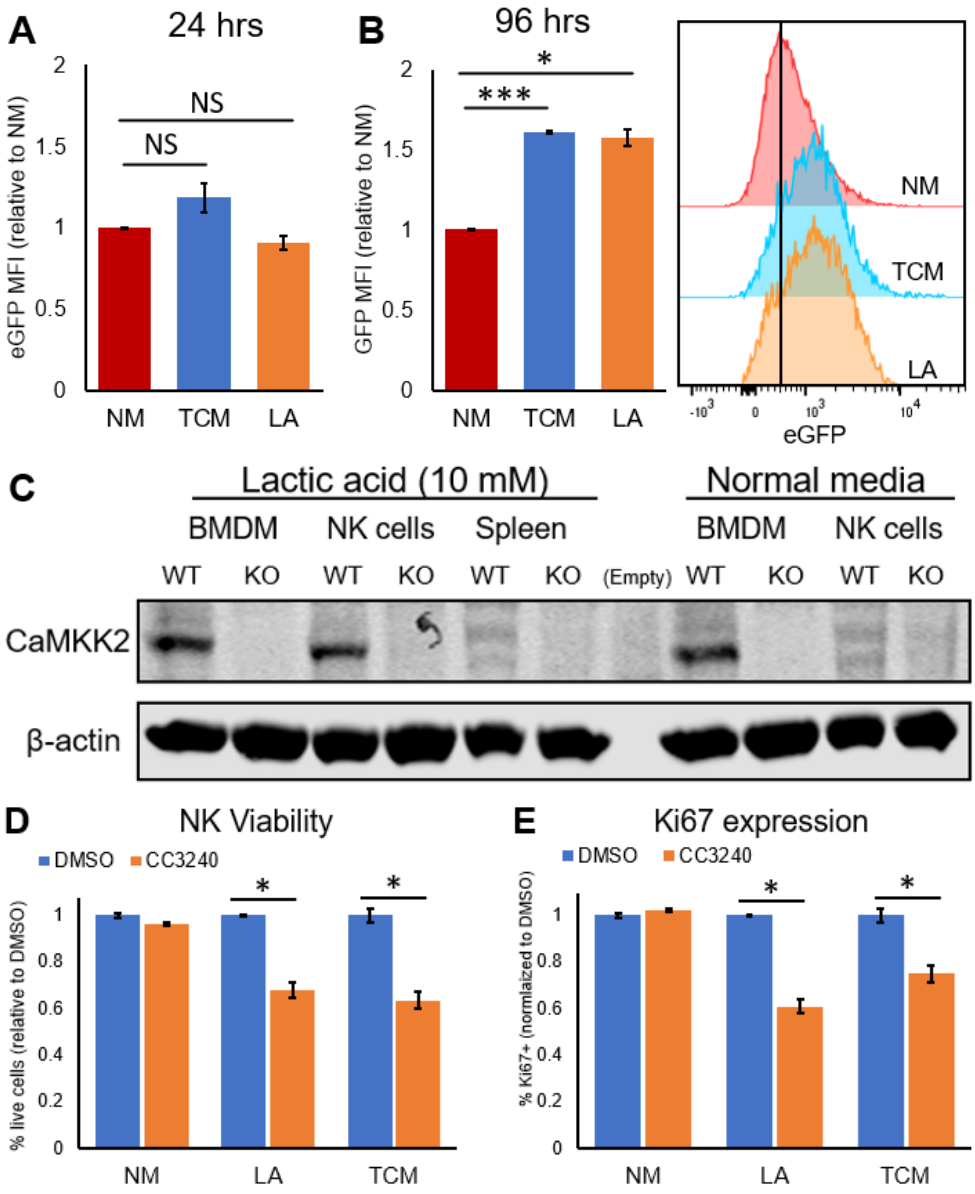


**Figure 15: Lactic acid exposure is sufficient to mediate CaMKK2 upregulation in NK cells.** (A-B) Splenic NK cells isolated from CaMKK2-eGFP reporter mice were cultured for 24-96 hours in normal growth media (NM), 50% EO771 tumor-conditioned media (TCM), or normal media with 10 mM lactic acid (LA). Flow cytometry was used to measure the level of eGFP expression relative to the NM group at (A) 24 hours in culture, or (B) 96 hours in culture. The raw eGFP fluorescence peaks at 96 hours are also shown. N=3, standard error shown. (C) Mixed splenocytes, pure splenic NK cells, and bone marrow-derived macrophages (BMDMs) were harvested from WT or CaMKK2 KO mice and cultured in normal media with or without 10 mM lactic acid for 96 hours. Protein from each cell type was resolved on a 7.5% acrylamide gel, and CaMKK2 or β-actin was detected via Western immunoblotting. (D-E) Splenic NK cells from WT BL/6 females were cultured in normal media (NM), 50% E0771 TCM (TCM), or normal media with 10 mM lactic acid (LA), along with 2.5 μM CC3240 or DMSO vehicle. (D) NK cell viability and (E) expression of Ki67 are shown at 96 hours. N=3, standard error shown.

Our next goal was to elucidate the mechanism by which lactic acid modulates CaMKK2 transcription. Possible mechanisms include signaling through GPR81, a cell-surface G protein-coupled receptor (GPCR) activated by high concentrations of extracellular lactate. According to the Immgen database, however, NK cells do not express detectable levels of GPR81 **(Fig. 16A)**. Alternatively, lactate can enter cells and directly modulate transcriptional activity. As discussed earlier, intracellular lactic acid is known to activate the HIF1α and NRF2 transcription factors, inhibit various HDAC enzymes, and directly modify histone activity through "lactylation" of lysine residues. Indeed, NK cells express low-to-moderate levels of the classic lactate shuttles MCT1 and MCT4 **(Fig. 16D-E)**, suggesting a mechanism by which lactate can be imported into the cells. Through acidification of the tumor environment, lactic acid can indirectly trigger pH-sensing GPCRs or cause intracellular acidification, which alters many signaling pathways[188]. Interestingly, NK cells express at least two of the four known pH-sensing GPCRs, GPR65 and GPR132 **(Fig. 16B-C)**, raising the possibility of CaMKK2 regulation through pH-mediated transcriptional effects.

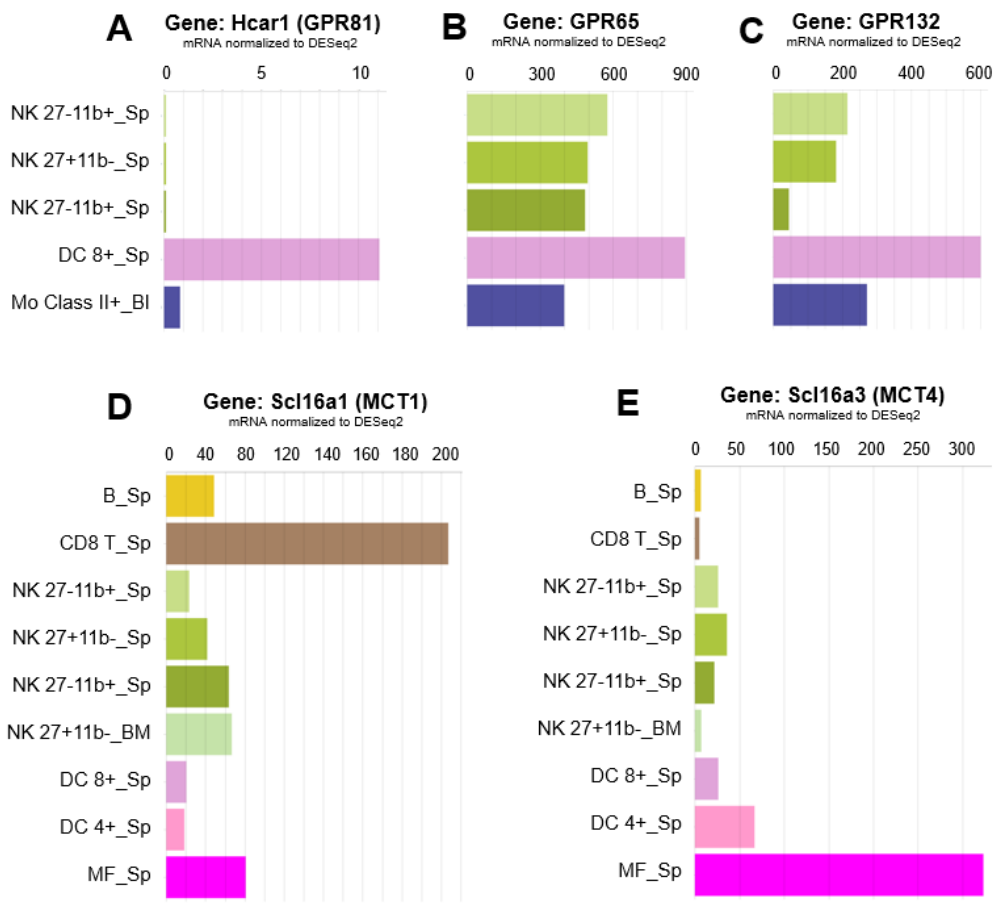


**Figure 16: NK cells express pH sensors and lactate import channels.** mRNA sequencing data from the Immunological Genome Project (ImmGen) was used to interrogate expression of (A) the GPR81 lactate sensor, (B-C) the GPR65 and GPR132 pH sensors, and (D-E) the MCT1 and MCT4 lactate transporters in various immune cells. Sp= spleen, Bl= Blood, BM= bone marrow, Mo= monocyte, MF=macrophages.

Our mechanistic studies began by probing the importance of intracellular lactate import through the MCT1 and MCT4 channels. The monocarboxylate transporter family requires a proton gradient to passively shuttle lactate and pyruvate across the cell membrane. Due to enhanced acidity and proton availability, the MCT family is particularly active in the tumor environment[189]. To test whether these transporters play a role in lactate-mediated CaMKK2 expression, we cultured CaMKK2-eGFP reporter NK cells in 10 mM lactic acid, with or without the MCT1 inhibitor AZD3965. AZD3965 is an MCT1-selective competitive inhibitor currently being explored as a treatment for a variety of

cancers[190]. As in prior studies, reporter NK cells treated with lactic acid showed a significant increase in eGFP fluorescence compared to normal media conditions, but in this study, we demonstrated that treatment with AZD3965 completely blocked this effect **(Fig. 17 A-B)**. These data suggest that MCT1-mediated intracellular import of lactate plays an important role in CaMKK2 upregulation. Interestingly, NK cells treated with sodium lactate exhibited no increase in eGFP expression **(Fig. 17 A-B)**, likely because a proton gradient is required to power MCT import activity.

To confirm these results in a WT model, we conducted Western immunoblots on WT splenic NK cells cultured with lactic acid and MCT inhibitors. Data from the reporter model suggest that acidification is not responsible for CaMKK2 upregulation as intracellular import of the lactate molecule is necessary for this response, not exposure to free protons generated by the dissociation of lactic acid. To definitively control for pH effects, however, this experiment used heavily buffered media containing 25 mM HEPES and 25 mM PIPES with a fixed pH of 7.4. Media pH was identical in all samples throughout the experiment, except for one sample whose pH was set to 6.4 **(Fig. 17C)**. The immunoblot demonstrates that 10 mM lactic acid is sufficient to drive CaMKK2 protein upregulation in NK cells, but this upregulation is significantly reduced by MCT1 inhibitor AZD3965 and by pan-MCT inhibitor α-cyano-4-hydroxycinnamic acid (αCHC) **(Fig. 17C)**. The more complete reduction of CaMKK2 expression in the αCHC group compared to the AZD3965 group may reflect the added effects of MCT4 inhibition. Importantly, media acidification alone does not affect CaMKK2 expression levels **(Fig. 17C)**, and acidified media does not replicate the effects of TCM on the survival of CaMKK2-deficient NK cells **(Fig. 17D)**. These data rule out a specific role for acidification in the regulation of CaMKK2 expression while confirming the necessity of intracellular lactate import.

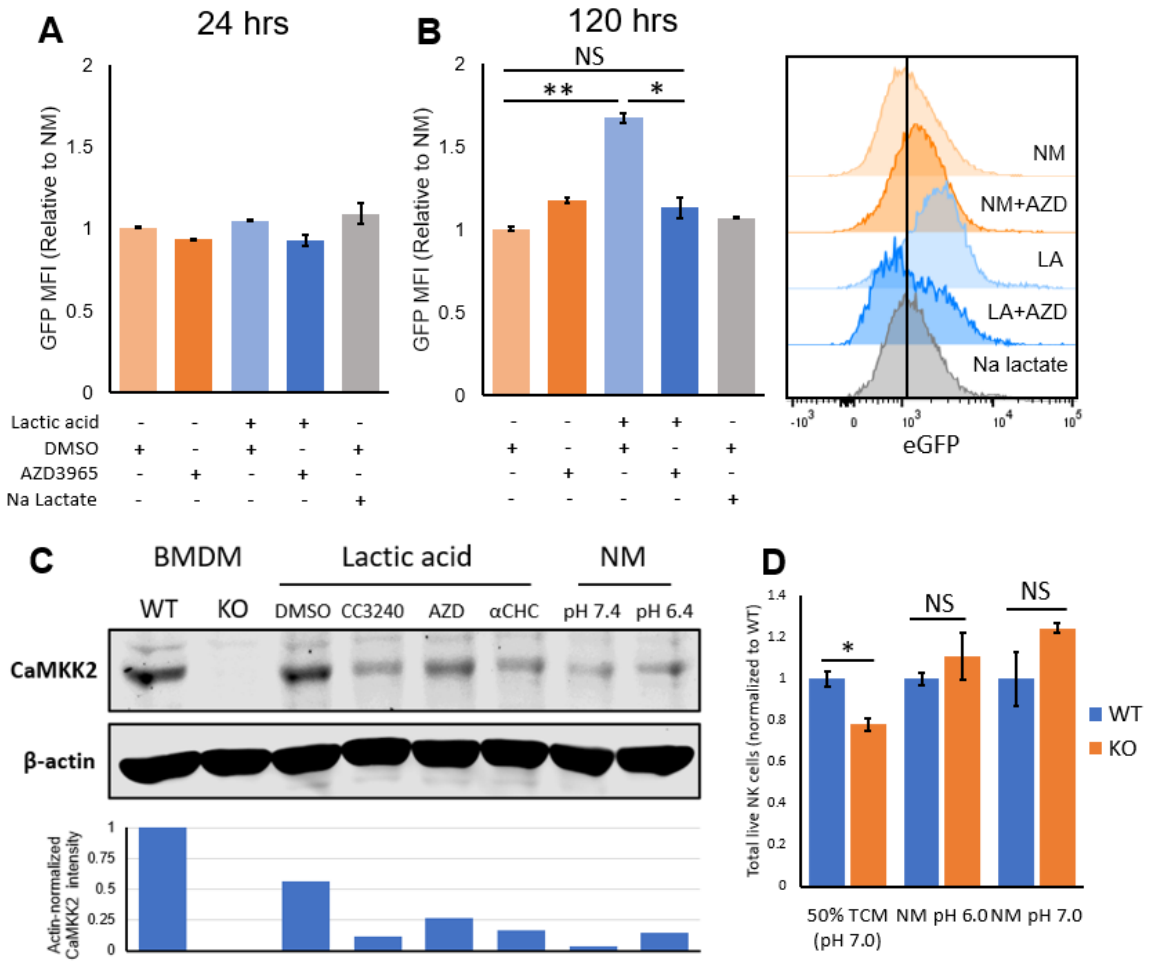


**Figure 17: Intracellular lactate import is necessary for CaMKK2 upregulation.** (A-B) Splenic NK cells from CaMKK2-eGFP reporter mice were cultured in normal media, normal media containing 10 mM lactic acid, or normal media containing 10 mM sodium lactate (Na lactate). Cells were also treated with 500 nM AZD3965 (AZD) or DMSO. Flow cytometry was used to measure eGFP expression relative to the NM group at (A) 24 hours in culture and (B) at 120 hours in culture. The raw fluorescence peaks at 120 hours are shown. N=3, standard error shown. (C) Bone marrow-derived macrophages (BMDMs) were harvested from WT and CaMKK2 KO mice and differentiated in normal media with M-CSF. Splenic NK cells were harvested from WT BL/6 females and cultured in heavily buffered normal media with a fixed pH of 6.4 or 7.4 ("NM" lanes) or in heavily buffered normal media with a fixed pH of 7.4 containing 10 mM lactic acid ("Lactic acid" lanes). Various samples of lactic acid-cultured NK cells were simultaneously cultured with 2.5 μM CC3240, 500 nM AZD3965 (AZD), 5 mM αCHC (αCHC), or DMSO vehicle. CaMKK2 and the β-actin control were measured via Western immunoblotting on a 7.5% acrylamide gel (45 ug protein per lane). (D) Splenic NK cells were harvested from WT and CaMKK2 KO BL/6 females and cultured for 96 hours in 50% EO771 TCM, heavily buffered normal media with a pH of 6.0, or heavily buffered normal media with a pH of 7.0. The total number of live NK cells, normalized to the WT level, was measured via flow cytometry. N=2, standard error shown.

## *2.3 Discussion*

### 2.3.1 Interpretation of results

CaMKK2 has been studied extensively in the context of tumor cells and myeloid immune cells, but this enzyme was not previously known to play a role in NK cell immunity. Our work demonstrates that a subset of $CD11b^+$ NK cells express CaMKK2 at baseline, though this subset lacks a specific identity as CaMKK2 expression does not closely correlate with common NK cell functional markers. $CD11b^+$ NK cells demonstrate a binary pattern of CaMKK2 expression as reporter cells are either completely negative or distinctly positive for eGFP. Thus, the mechanism(s) regulating CaMKK2 levels may involve a "threshold effect" whereby exposure to a specific level of a stimulating factor increases transcription, causing some cells to stochastically express the enzyme while others do not. Upon exposure to tumor conditions, CaMKK2 is robustly expressed in *all* subsets of NK cells, including immature $CD11b^-$ NK cells and NKT cells. Thus, a regulatory apparatus is likely conserved across the extended NK cell family, enabling CaMKK2 transcription when the proper stimulus is detected. $CD11b^+$ NK cells may simply be more sensitive to this stimulus, explaining the mixed baseline expression. Increased CaMKK2 expression is likely due to transcriptional upregulation rather than protein stabilization because the eGFP reporter model shows the same increase as Western blots. Finally, CaMKK2 expression is not observed in any post-thymic T-cell subset, indicating that CaMKK2 modulation is specific to the NK cell lineage as other closely related lymphoid populations never express this enzyme.

*In vitro* functional assays demonstrate that CaMKK2 expression improves the general fitness of tumor-conditioned NK cells through a novel scaffold mechanism. Ablation of CaMKK2 through genetic means or ligand-directed degradation increases apoptosis and reduces viability in tumor-conditioned NK cells. CaMKK2 ablation also

causes cell cycle quiescence, restricts proliferation, and reduces chemotaxis under tumor conditions. However, CaMKK2 ablation does not affect the cytotoxic potency of individual tumor-conditioned NK cells. Considering the mitochondria's multifaceted role in regulating apoptosis, cell cycle progression, and even chemotaxis, we hypothesized that CaMKK2 could be influencing NK cell fitness through mitochondrial regulation. However, CaMKK2 ablation has no effect on mitochondria mass, membrane potential, or reactive oxygen species, which suggests a non-mitochondrial mechanism by which CaMKK2 influences NK cell biology. In contrast to genetic ablation or ligand-directed degradation of CaMKK2, competitive inhibition of this enzyme has no effect on tumor-conditioned NK cells, indicating that CaMKK2 serves a unique scaffold function independent of its kinase activity. The nature and implications of this scaffold function are discussed in greater detail later in this section.

Metastasis studies consistently show increased metastatic progression in mice with CaMKK2-deficient NK cells, establishing an important role for CaMKK2 in NK cell tumor immunity. These results were repeated using three models of NK cell-intrinsic CaMKK2 ablation and two different NK cell-sensitive tumor models, B16-F10 and EO771$^{\beta 2m-/-}$. Tumor cells recovered from the lungs of mice with CaMKK2-deficient NK cells showed significantly lower MHC I expression than WT controls, an immunoediting phenotype consistent with reduced NK cell anti-tumor activity. Moreover, immune profiling showed that total NK cell counts were significantly lower in the lungs of the CaMKK2-deficient groups despite their larger tumor burdens, and the NK cells that were present showed reduced viability and proliferative capacity. This *in vivo* immune profiling data is consistent with the *in vitro* data generated using tumor-conditioned media. Even in fully immune competent mice with several intact mechanisms of anti-tumor immunity, NK cell-specific ablation of CaMKK2 led to increased metastatic burden. Extensive immune profiling of lung tissue from this study failed to show changes in the infiltration or

polarization of any immune populations besides NK cells, highlighting (1) the importance of effector NK cell activity in controlling certain tumor types and (2) the importance of CaMKK2 in preserving NK cell function.

Based on the data presented thus far, we posit that CaMKK2 expression reduces metastatic progression by improving the fitness of NK cells within metastatic nodules, not by increasing NK cell recruitment to tumors or by enhancing NK cell anti-tumor surveillance in circulation. CaMKK2 is only expressed at appreciable levels in NK cells exposed to tumor conditions for at least 72 hours, and peripheral NK cells isolated from tumor-bearing mice showed no evidence of CaMKK2 upregulation in the eGFP reporter model. Thus, NK cells in circulation should not express CaMKK2, and WT and CaMKK2 KO NK cells in circulation should not display any phenotypic differences, including their ability to migrate to the tumor or mediate cytotoxic activity in circulation. Indeed, three of the four metastasis studies showed a growing divergence between the WT and KO groups as the metastatic tumors grew larger, with two of the studies developing differences in metastatic burden only at the latest timepoint **(Fig. 10B, 12C)**. These results are consistent with our hypothesis that NK cells must be conditioned by an established tumor environment before CaMKK2 is upregulated and begins to play an important role in NK immunity. Moreover, in the EO771$^{\beta 2m-/-}$ model, NK cells were intravenously injected 48 hours *after* the tumor cells, meaning that many tumor cells had already extravasated and begun colonizing tissues by the time NK cells were introduced into the system. Thus, NK cell activity against circulating EO771 cells is unlikely to explain the large differences in metastatic progression between the WT and CaMKK2-deficient groups.

Although NK cell recruitment from the periphery to tumor nodules is unlikely to explain the metastasis phenotype, impaired *intra*-tumoral migration may contribute to increased metastatic growth in the CaMKK2-deficient groups. The *in vitro* migration assay showed that CaMKK2 ablation impairs baseline migration and CCL4 chemotaxis in tumor-

conditioned NK cells. These findings could translate to reduced infiltration of CaMKK2-deficient NK cells into deep, less-vascularized portions of a tumor nodule. To test this hypothesis *in vivo*, we could conduct immunohistochemistry staining on large lung nodules recovered from mice with WT or CaMKK2-deficient NK cells, looking for reduced "deep tumor" infiltration in the CaMKK2-deficient group. Given the current data, however, the best explanation for differences in metastatic progression in the WT versus CaMKK2-deficient mice involves the survival and proliferation of NK cells within the local tumor environment.

CaMKK2 upregulation in tumor-infiltrating NK cells is driven by exposure to lactic acid, an abundant tumor metabolite. We have shown that addition of lactic acid to normal growth media is sufficient to increase CaMKK2 expression in a pure population of NK cells *in vitro*. Furthermore, inhibition of the key MCT lactate import channels prevents CaMKK2 upregulation even in lactic acid-rich media, indicating that intracellular lactic acid import is necessary for upregulation to occur. Sodium lactate does not substitute for lactic acid, likely because a proton gradient is required to drive the critical MCT channels. We have not identified the exact mechanism by which lactic acid alters CaMKK2 transcription, but we have ruled out several possibilities. The need for intracellular lactic acid import negates any role for the cell surface lactate receptor GPR81. Moreover, acidic media is neither necessary nor sufficient to upregulate CaMKK2, negating indirect pH effects as the driver of CaMKK2 modulation. As discussed earlier, lactic acid can directly alter transcription through histone lactylation, HDAC inhibition, and HIF1α activation, among other examples. High concentrations of lactic acid could also alter cellular metabolism and mitochondrial respiration rates, causing indirect effects on transcriptional state, though the abundance of glucose in all *in vitro* experiments should prevent such a metabolic shift. In any case, it will be difficult to further elucidate lactate's specific mechanism given the wide range of possibilities and our limited understanding of lactate's multifaceted role in cellular

biology. However, we have established lactic acid as the key driver of CaMKK2 upregulation, highlighting a novel adaptive mechanism by which NK cells respond to and mitigate the deleterious effects of this ubiquitous tumor metabolite.

### 2.3.2 Translational implications

This work has significant therapeutic implications as it reveals potential liabilities associated with inhibition of CaMKK2 and MCT1, while suggesting novel strategies for enhancing NK cell immunity. We have previously shown that CaMKK2 inhibition has beneficial effects in tumor cells and in TAMs[129], but the detrimental effects of LDD-mediated CaMKK2 ablation on NK cells could attenuate these benefits. Importantly, we did not observe any negative effects of competitive CaMKK2 inhibitors on NK cell function, and we posit that it is specifically the loss of the CaMKK2 scaffold function that is deleterious to NK cell immunity. Thus, competitive inhibitors of CaMKK2 may be clinically preferable to LDDs in clinical applications where preservation of NK cell function is essential. CaMKK2 LDDs have yet to be adapted for *in vivo* use, but when suitable compounds become available, the relative efficacy of these two drug classes in NK cell-sensitive mouse tumor models will be explored. In a similar manner, MCT1 inhibitors are currently in clinical trials as cancer therapeutics[190], but this class of drugs may carry liabilities similar to CaMKK2 LDDs. By blocking the accumulation of intracellular lactate in NK cells, MCT1 inhibitors could reduce CaMKK2 upregulation, limiting the utility of this class of drugs in NK cell-sensitive tumors. However, if MCT1 inhibitors are highly successful at preventing lactic acid export from tumor cells, then the benefits of the drug may outweigh the liabilities. AZD3965 is suitable for *in vivo* use, and it would be straightforward to test whether MCT1 inhibition negatively effects the progression of NK cell-sensitive metastatic tumors.

NK cell transfusions are being investigated as a cancer therapy, and our findings suggest that modification of these immune cells to constitutively express CaMKK2 may confer proactive resistance to the toxic effects of the tumor environment. We found that the human NK lymphoma cell line NK92, which is being explored clinically, already expresses CaMKK2 at robust levels and is unlikely to benefit from enhanced expression **(Fig. 18A)**. Indeed, constitutive expression in NK92 cells may reflect the selective advantages of improved survival and proliferation conferred by CaMKK2. However, primary human NK cells are also used for allogeneic and autologous transfusions. Primary NK cells have been modified via retroviral transfection to overexpress proteins beneficial to anti-tumor activity, such as NKG2D and IL15[82,191], and CaMKK2 could be constitutively expressed using the same techniques. Upon entering the tumor environment, NK cells require time to fully activate defensive adaptations like the CaMKK2 pathway, creating a window of high vulnerability. Constitutive CaMKK2 expression may confer protection in this critical early entry period.

### 2.3.3 Ongoing work

#### 2.3.3.1 Elucidating scaffold components and downstream pathways

Our work comparing CaMKK2 degraders and competitive inhibitors strongly suggests that CaMKK2 is functioning as a scaffold in NK cells, and we are working to elucidate the components of this scaffold complex and determine the affected downstream pathways. The only known scaffold function for CaMKK2 is in hepatocellular carcinoma (HCC) where CaMKK2 nucleates a complex containing CaMKIV and components of mTOR, promoting tumor cell proliferation[121]. The specific complex reported in HCC is unlikely to mediate the effects seen in NK cells because its activity requires both the scaffold and kinase functions of CaMKK2, whereas only the scaffold function is necessary in NK cells. However, this work in HCC demonstrates that the mTOR complex can directly

associate with CaMKK2. Given mTOR's established role in regulating NK cell metabolism and effector activity, we are investigating the effects of CaMKK2 expression on mTOR activity. mTORC1 directly phosphorylates S6 kinase (SK6), which in turn phosphorylates several downstream targets, including S6 at Ser235/236.

If S6 phosphorylation is significantly altered by CaMKK2, we will determine whether the changes in mTOR activity regulated by this enzyme are relevant to the survival and proliferation phenotypes observed in NK cells. Changes in a signaling pathway do not necessarily imply a causative role in the phenotype of interest. For example, competitive CaMKK2 inhibitors reduce AMPK phosphorylation but have no effect on NK cell survival and proliferation, which rules out a role for the AMPK pathway. If an mTOR inhibitor such as everolimus can reverse or replicate the effects of CaMKK2 ablation on NK cell survival and proliferation, then we should be able to establish a cause-and-effect relationship between mTOR and the CaMKK2- mediated phenotypes observed. At that point, we would also need to confirm a physical association between mTOR and CaMKK2. If mTOR activity is not affected by CaMKK2 expression or if we fail to demonstrate an association between mTOR and CaMKK2, then we plan to conduct a broader screen for proteins associated with CaMKK2 in NK cells. Specifically, we will optimize an immunoprecipitation protocol to pull-down CaMKK2 from a pure population of NK cells and identify associated proteins through mass spectrometry.

#### 2.3.3.2 Tying CaMKK2 to human NK cell biology

Human and murine NK cells are quite similar, with analogous developmental patterns, effector mechanisms, and functional markers. Thus, we expect our findings in mice to translate to human biology. Interestingly, we found that the human NK cell lymphoma line NK92 constitutively expresses robust levels of CaMKK2 **(Fig. 18A)**, confirming that human NK cell derivatives are capable of CaMKK2 expression. However,

ligand-directed degradation of CaMKK2 with CC3240 had no effect on the survival, proliferation, or activation of NK92 cells, even under stressful TCM conditioning **(Fig. 18B)**. CC3240 degrades about 75% of the CaMKK2 protein in NK92 cells **(Fig. 18C)**, which is similar to the reduction in primary mouse NK cells. Though clearly expressed in NK92, CaMKK2 does not serve the purpose we expected based on our work with murine NK cells. Tumor cells like NK92 undergo many rounds of mutation and selection, and perhaps CaMKK2 expression was critical at an early stage of tumor development but became unnecessary or redundant when additional pathways were mutated later in the evolutionary process. Alternatively, CaMKK2 may simply play a different role in the NK92 line than in primary NK cells. Given the broad discordance between NK92 cells and primary NK cells, we will focus on primary NK cells going forward.

Through clinical collaborations on projects unrelated to CaMKK2, our lab acquired single cell RNA sequencing data for tumor-infiltrating human immune cells. Through UMAP dimension reduction techniques, we were able to plot and analyze a diverse repertoire of immune cells recovered from three primary human breast tumors, including NK cell populations. The NK cell cluster was identified by high expression of Ncr1 (NKp46) mRNA, **(Fig. 18D)**, and this cluster was then analyzed for evidence of CaMKK2 expression. The study was valid as CaMKK2 mRNA was observed in the macrophage cluster, but very little CaMKK2 was detected in the tumor-infiltrating NK cells **(Fig. 18E)**. However, this study has several limitations, including the small sample size, limited NK cell infiltration, relatively low sequencing penetrance, and unknown lactic acid concentrations within the tumor environment. As discussed earlier, NK cell infiltration in primary tumors is generally quite poor, and the small number of NK cells recovered from these three specific samples may not have penetrated the tumor capsule or been exposed to interior regions with pronounced lactic acid accumulation. Moreover, CaMKK2 detection in the macrophage cluster is rather sparse, suggesting that the expression threshold for

detection was quite high in this study. Going forward, we will conduct additional single cell RNA sequencing analyses as more tumors become available, with a particular interest in metastatic nodules. In the meantime, we may purchase primary human NK cells from a vendor or acquire primary human cells from colleagues in the Duke Hematology department. In either case, we will culture these cells in TCM from a human tumor line or in lactic acid and use Western immunoblotting to detect CaMKK2 protein expression.

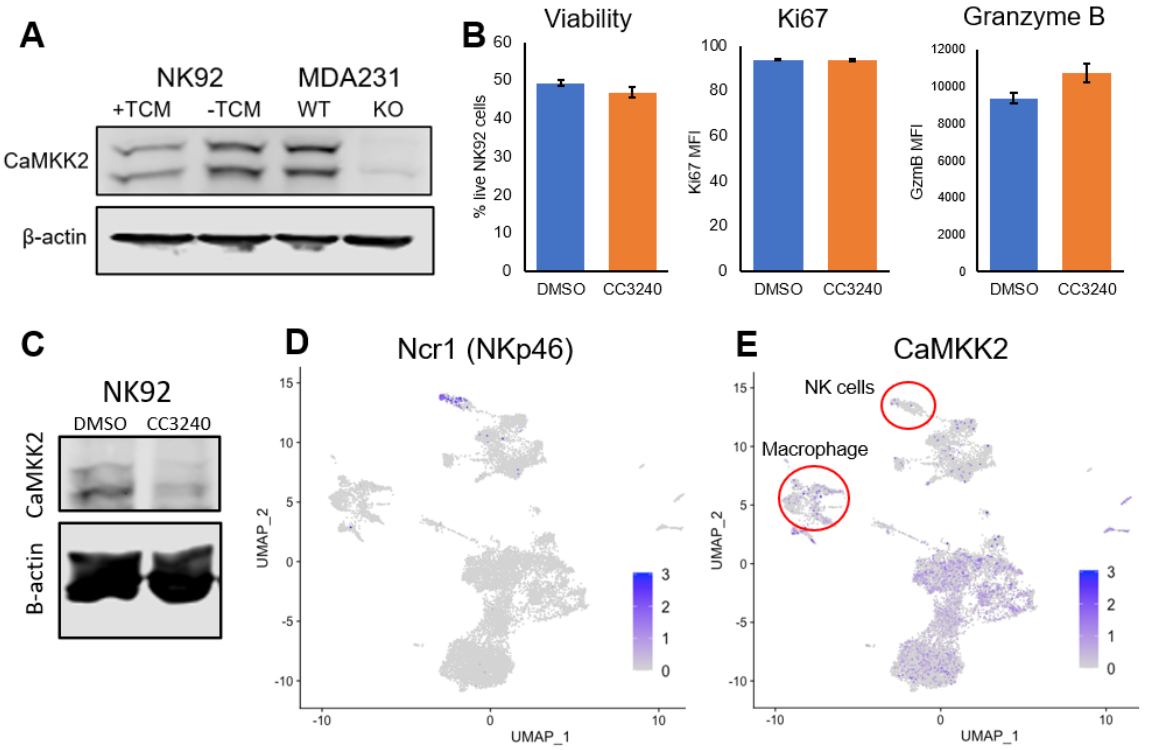


**Figure 18: The role of CaMKK2 in human NK cells is unclear.** (A) NK92 cells were cultured in normal growth media or 50% MDA-231 TCM for 96 hours, and CaMKK2 and β-actin levels were measured using a Western immunoblot (7.5% acrylamide gel). WT MDA231 and CaMKK2 KO MDA231 cells were run on the same Western. (B-C) NK92 cells were cultured in 50% MDA-231 TCM for 96 hours with CC3240 or a DMSO vehicle. (B) Flow cytometry was used to determine viability, Ki67 expression, and Granzyme B levels. N=2, standard error shown. (C) CaMKK2 and β-actin levels were measured using a Western immunoblot (7.5% acrylamide gel). (D-E) Immune cells from three primary human breast tumors were subjected to single cell RNA sequencing, and the resulting data was concatenated and plotted using the UMAP dimension reduction technique. (E) Cells expressing Ncr1 (NKp46) mRNA were highlighted, and (F) cells expressing CaMKK2 mRNA were highlighted.

#### 2.3.3.3 Effects of CaMKK2 ablation on peripheral NK cells

Most of our work up to this point has focused on tumor-infiltrating NK cells, not peripheral NK cells in tumor-bearing animals. This is largely due to early experiments in which tumor-bearing CaMKK2-eGFP reporter mice failed to show upregulation of CaMKK2 in splenic NK cells. However, in two of the metastasis studies, we recovered NK cells from spleens as well as tumors, and we were surprised to find a significant reduction in total NK cell numbers in the spleens of the CaMKK2-deficient group **(Fig. 19A-B)**. In these studies, WT and KO splenic NK cells exhibited comparable levels of viability **(Fig. 19A-B)**, implying that variations in total cell number are not driven by differences in survival. Differences in proliferation rate may explain these results, but we cannot draw any firm conclusions about proliferation because Ki67 staining was not performed. These findings complicate our previous conclusion that only tumor-infiltrating NK cells upregulate CaMKK2, and that the trafficking of peripheral NK cells into the tumor is not responsible for the elevated rates of metastatic progression in CaMKK2 KO mice. Indeed, such significant differences in peripheral NK cell numbers likely contribute to differences in tumor growth rate.

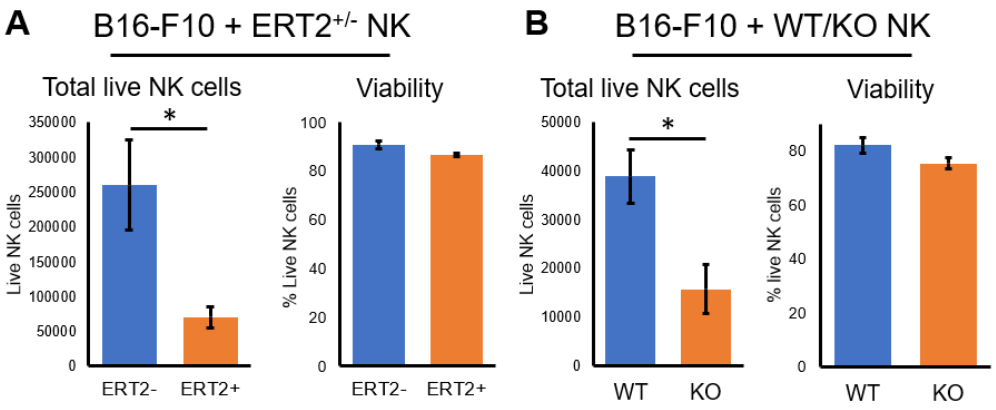


**Figure 19: Tumor-bearing mice engrafted with CaMKK2-deficient NK cells have fewer splenic NK cells.** (A) NSG mice were intravenously administered B16-F10 tumor cells and NK cells with tamoxifen-induced CaMKK2 ablation (ERT2+) or a WT control (ERT2-). After 17 days, spleens were recovered from these mice, and the total number and viability of splenic NK cells was measured using flow cytometry. N=6, standard error shown. (B) NSG mice were intravenously administered B16-F10 tumor cells and WT or CaMKK2 KO NK cells. After 15 days, spleens were recovered from these mice, and the total number and viability of splenic NK cells was measured using flow cytometry. N=7-8, standard error shown.

There are several possible explanations for these differences in splenic NK cell counts, and for inconsistencies between the CaMKK2-eGFP reporter data and the metastasis studies. First, the tumor-bearing reporter mice whose splenic NK cells showed minimal eGFP expression were inoculated with subcutaneous primary tumors, not metastatic tumors. Disseminated metastatic lesions may exert a much greater systemic influence than a single, structurally superficial primary tumor. Thus, we will conduct a metastasis study in CaMKK2-eGFP reporter mice to directly test whether splenic NK cells upregulate CaMKK2. If CaMKK2 upregulation is observed in this study, then we must determine what factors are responsible. We have shown that lactic acid exposure is sufficient to increase CaMKK2 expression, but it is questionable whether systemic lactic acid levels could rise high enough in tumor-bearing mice to trigger upregulation in the spleen. However, we have not conducted a lactic acid titration curve to determine the exact concentrations required to cause CaMKK2 upregulation. It is possible that relatively

low levels of lactic acid trigger upregulation, levels that could be achieved systemically in mice with advanced metastatic tumor burdens. Alternatively, a second tumor factor may cause CaMKK2 expression, and unlike lactic acid, perhaps this second factor can act at distal sites at low concentrations. This theoretical factor could directly influence CaMKK2 transcription, or it could work through the lactic acid mechanism. For instance, the factor could alter the metabolism of peripheral NK cells to increase intracellular lactic acid (e.g. antagonize mitochondrial respiration), which in turn increases CaMKK2. In either case, we will continue exploring the effects of tumor growth on CaMKK2 expression in peripheral NK cells and determine whether differences in splenic NK cell counts contribute to the pro-metastasis phenotype observed upon ablation of NK cell-intrinsic CaMKK2.

# 3 LYPD3 as a regulator of ferroptosis

## *3.1 Background*

Our overarching goal is to identify clinically translatable methods to modulate anti-tumor immunity, with a particular focus on the CaMKK2 pathway in NK cells. However, regulatory pathways in tumor cells can also be manipulated to undermine tumor defenses and enhance anti-tumor immunity. Tumors are highly susceptible to ferroptosis, a unique iron-dependent cell death mechanism driven by unrestricted accumulation of lipid peroxides. Indeed, T cells and NK cells are able to “prime” tumor cells for ferroptosis by releasing IFNγ, which antagonizes critical anti-ferroptosis defenses such as those that engage GPX4 and SCL7A11 (xCT)[192]. The tumor cell then proceeds to release damage-associated molecular patterns such as HMGB1[193], which engages TLR4 in dendritic cells to promote immune activation[194]. Moreover, heavily peroxidated membrane lipids promote phagocytosis of tumor cell components by macrophages[195], potentially boosting antigen presentation and the adaptive immune response. Indeed, ferroptosis appears to share many similarities with necrosis and pyroptosis in its tendency to expose inflammatory factors and tumor antigens[196]. The effects of IFNγ may be accentuated if combined with additional ferroptosis enhancement strategies. Thus, there is significant interest in identifying methods that allow specific activation of this cell death mechanism in tumor cells, both to attenuate tumor cell survival and to broadly enhance anti-tumor immunity.

LY6/PLAUR Domain Containing 3 (LYPD3), known as C4.4A in humans, is a cell-surface protein expressed in the suprabasal layers of squamous epithelia, especially during early development[197]. Structurally, LYPD3 is a glycosylphosphatidylinositol (GPI)-anchored protein that lacks transmembrane and intracellular domains[198]. Low levels of LYPD3 expression are retained in the oral and esophageal epithelia, but the protein is otherwise absent under normal physiological conditions, and the specific functions of this

protein are unknown[197]. However, LYPD3 is upregulated significantly in many squamous carcinomas of the head and neck[199], and this protein is often expressed ectopically in squamous cell carcinoma and adenocarcinoma of the lung where it is associated with poor prognoses[200,201]. Two former graduate students in our lab, Kim Cocce and Taylor Krebs, demonstrated that endocrine therapy-resistant luminal breast cancers are often characterized by upregulation of grainyhead like transcription factor 2 (GRHL2), which mediates upregulation of LYPD3[202]. Thus, our lab initially focused on LYPD3 as a therapeutic vulnerability in endocrine therapy-resistant breast cancers.

Our laboratory has generated a significant amount of data from studies that explored the biology of LYPD3 in breast cancer. Using the human MCF7 and mouse PY230 breast tumor lines, it was shown that LYPD3 is expressed at higher levels in more aggressive tumors. WS8, an estrogen-independent MCF7 variant, exhibits greater LYPD3 expression than the MCF7 parent line, and TamR, a tamoxifen-resistant variant of WS8, expresses even higher LYPD3 levels **(Fig. 20A)**. The 27-hydroxycholesterol (27HC) metabolite normally suppresses tumor cell proliferation, but more aggressive tumors develop resistance to these effects. Resistance to 27HC is also correlated with higher LYPD3 expression in the PY230 model, but interestingly, this is only observed in tumors cells that have been passaged through mice **(Fig. 20B)**. These results suggest that LYPD3 provides a fitness advantage to cells *in vivo*. Using the Cancer Therapeutics Response Portal (CTRP) from the Broad Institute, it was demonstrated across a variety of human tumor cell lines that LYPD3 expression correlates with resistance to xCT inhibitors **(Fig. 20C)**. xCT is a critical glutamate import channel that provides glutathione precursors to the GPX4 anti-ferroptosis pathway. Thus, these data suggest that LYPD3 plays a role in preventing ferroptosis, either directly through the xCT/GPX4 pathway or through another mechanism. This hypothesis was explored experimentally by generating an shRNA knock-down system that reduces LYPD3 expression in PY230 cells by over 80% **(Fig 20E)**.

Using this modified cell line, it was shown that knock-down of LYPD3 increases sensitivity to the GPX4 inhibitor RSL3 **(Fig. 20D)**. Our group also acquired a monoclonal antibody against human LYPD3[203] and demonstrated that this antibody, as a single agent, reduces the growth of TamR xenograft tumors in mice **(Fig. 20F)**. These findings highlight the potential of LYPD3 as a therapeutic target and underscore the need to understand how best to employ such an antibody as a therapeutic intervention.

We next undertook experiments to (1) probe the functional ties between ferroptosis and tumor growth in LYPD3 knock-down models, and (2) define the mechanisms underlying LYPD3 expression in tumor cells. Elucidating the mechanism by which LYPD3 suppresses ferroptosis may inform the development of synergistic combination therapies involving anti-LYPD3 monoclonal antibodies. Anti-LYPD3 treatments are especially promising as few healthy tissues express this protein, allowing for highly targeted toxicity. I have been working in close collaboration with postdoc Debarati Mukherjee to complete this story, with a particular interest in incorporating anti-LYPD3 antibodies into immune-enhancing cancer therapies.

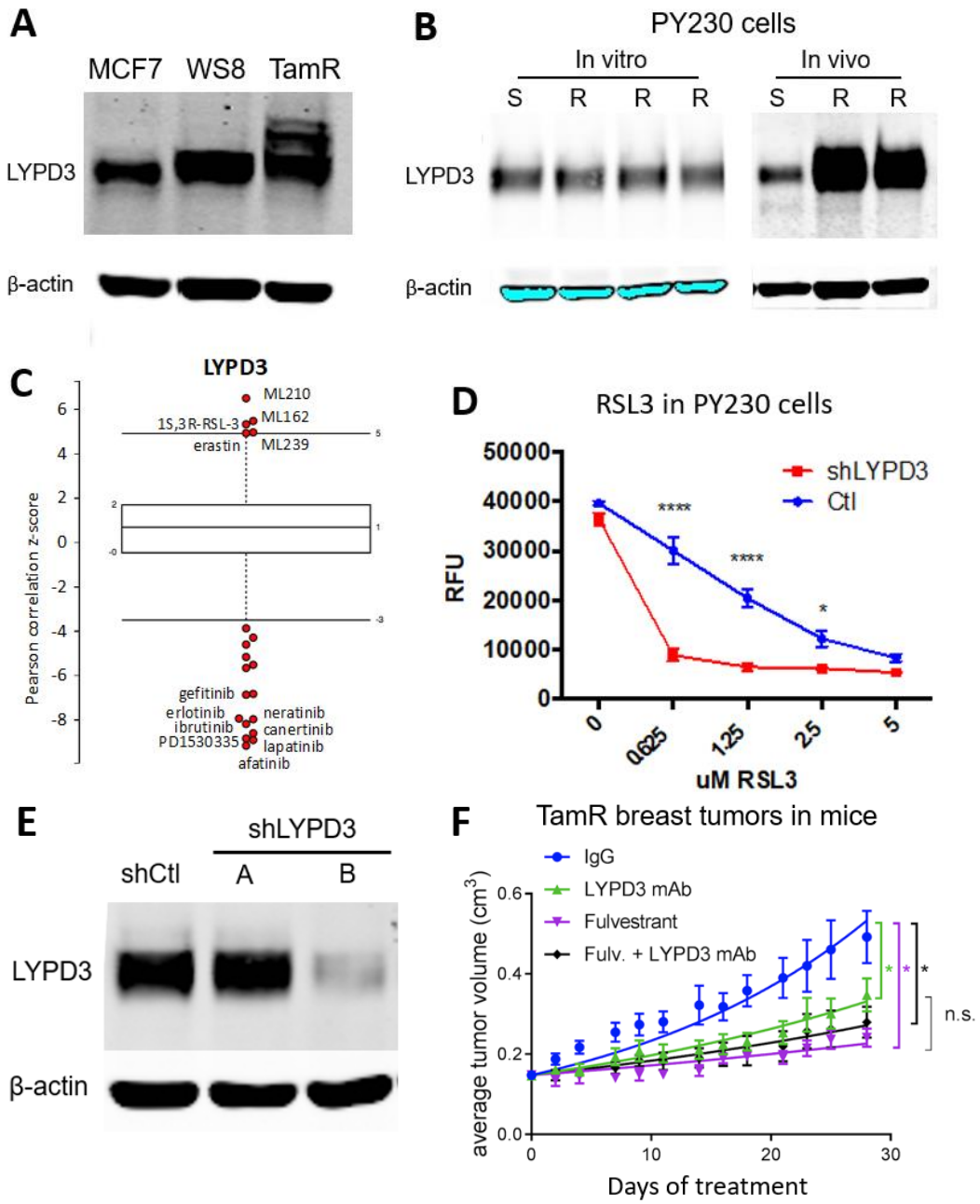


**Figure 20: Characterizing the role of LYPD3 in breast cancer.** (A) Various derivatives of the MCF7 cell line were analyzed for LYPD3 expression via Western immunoblot. (B) PY230 cells were cultured with 27-hydroxycholesterol (27HC) until the cells resumed proliferation. The parent PY230 cells were termed 27HC-sensitive (S), whereas the cells able to grow in 27HC were termed 27HC-resistant (R). S and R cells were passaged through mice and recovered from lung nodules. All these populations of PY230 cells were analyzed for LYPD3 expression via Western immunoblot. (C) The Cancer Therapeutics Response Portal, created by the Broad Institute, was used to correlate LYPD3 expression with sensitivity to ferroptosis inhibitors and tyrosine kinase inhibitors across many tumor lines. (D) PY230 cells were treated for 48 hours with 15 μM arachidonic acid and the GPX4 inhibitor RSL3, and total DNA content was measured using the FluoReporter dsDNA kit. N=3, standard error shown. (E) PY230 cells were transfected with a control shRNA knock-

down construct (shCtl) or one of two shLYPD3 knock-down constructs (A and B) and assayed for LYPD3 expression via Western immunoblot. (F) Nu/nu female mice bearing TamR xenograft tumors were injected twice weekly with 45 mg/kg anti-LYPD3 or IgG control (intraperitoneal) and with 25 mg/kg fulvestrant or corn oil vehicle (subcutaneous). N=10, standard error shown. Two-way ANOVA analysis showed significant differences between the IgG control and all treatment groups between days 14 and 28. All data presented in this figure were generated by Kim Cocce, Taylor Krebs, and Wen Liu, and included with permission.

## *3.2 Results*

### 3.2.1 LYPD3 ablation sensitizes metastatic tumors to ferroptosis

To definitively establish the role of LYPD3 in tumor ferroptosis resistance, we conducted metastasis studies using mouse breast tumor lines. We adopted a lung metastasis model because cells in this environment are subject to elevated oxidative stress compared to subcutaneous primary tumors[204,205]. Our initial study used 27HC-resistant PY230 cells recovered from mouse lungs, which display enhanced levels of LYPD3 expression **(Fig. 20B)**. These cells were modified to express luciferase and a constitutive shRNA construct that targets either LYPD3 or a non-specific control sequence. These tumor lines were injected via tail vein into nu/nu female mice, and the animals were treated with daily injections of ferrostatin-1 or a vehicle control. Ferrostatin-1 inhibits ferroptosis by directly scavenging the alkoxy radicals that cause lipid peroxidation, a mechanism independent of all the established anti-ferroptosis pathways[206]. Minimal metastasis was observed in mice injected with shLYPD3 tumor cells in the absence of ferrostatin, whereas mice injected with shControl cells exhibited a significant metastatic burden by day 45 regardless of ferrostatin administration **(Fig. 21A)**. Indeed, by day 61, all but two mice in the shControl groups presented detectable metastases, compared to only one mouse in the ferrostatin-free shLYPD3 group **(Fig. 21B)**. Importantly, ferrostatin administration in the shLYPD3 mice restored metastatic tumor progression to the same level as the shControl groups **(Fig. 21A-B)**. These results demonstrate that LYPD3 expression plays an essential role in promoting the growth of

PY230 metastatic tumor cells, but this role is only important when cells are vulnerable to ferroptosis.

To repeat these findings with a second tumor line, we modified the 4T1 mouse breast cancer line in the same manner described above. When propagated in nu/nu mice, the shLYPD3 4T1 and shControl 4T1 cells showed rapid rates of metastatic growth, but no significant difference was observed in metastatic burden by the humane endpoint on day 14 **(Fig. 21C)**. Concerned that the rapid growth rate could mask underlying differences in ferroptosis vulnerability, we repeated the 4T1 metastasis study using syngeneic Balb/c mice rather than the immune compromised nu/nu strain. While the rate of metastatic progression decreased modestly in the Balb/c background, no differences were observed between the shLYPD3 and shControl groups by day 20 **(Fig. 21D)**. Thus, not all tumor lines that express LYPD3 are highly reliant on this protein for *in vivo* ferroptosis protection.

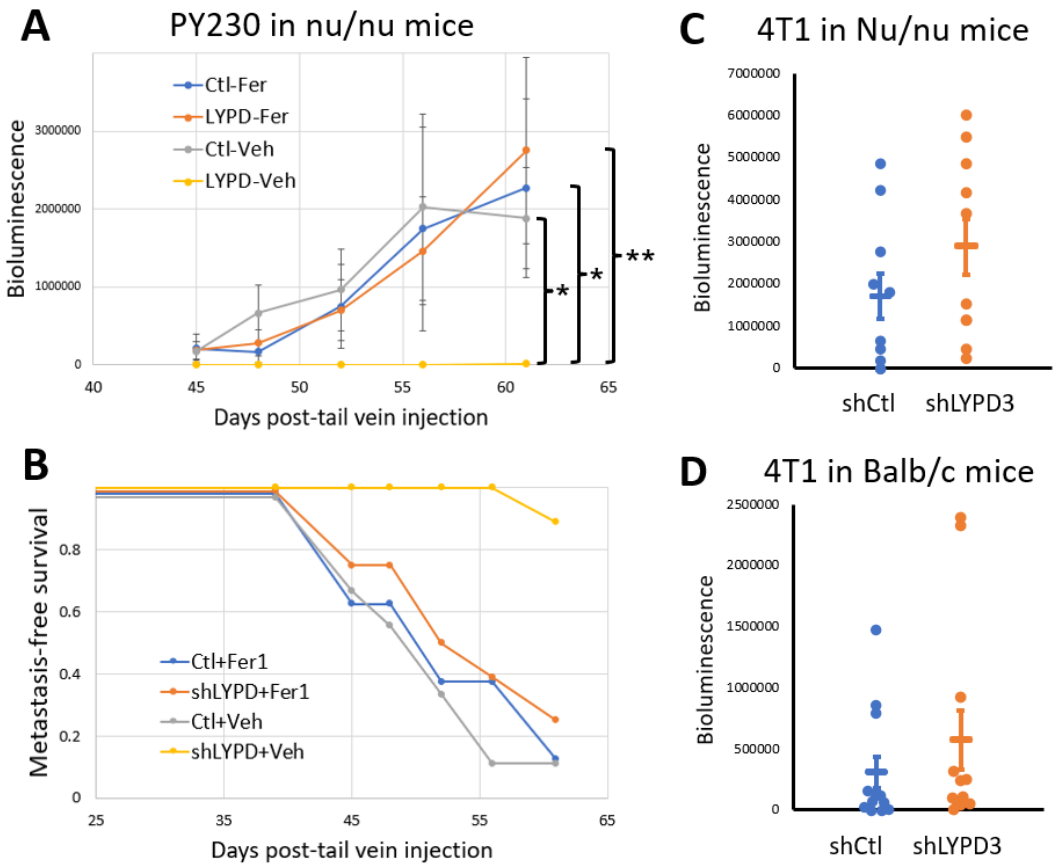


**Figure 21: LYPD3 protects PY230 tumors, but not 4T1 tumors, from ferroptosis in vivo.** (A-B) 500k luciferase-expressing shCtl or shLYPD3 PY230 tumor cells were injected via lateral tail vein into nu/nu mice. Mice then received daily intraperitoneal injections of 1 mg/kg Ferrostatin-1 or the normal saline vehicle control. (A) Luciferin bioluminescence imaging was used to measure whole-body tumor burden over time, and (B) metastasis-free survival was tracked. An IVIS signal of < 20,000 lumens/cm$^2$/sec was counted as "metastasis-free". N=9, standard error shown. (C) 500k luciferase-expressing shCtl or shLYPD3 4T1 tumor cells were injected via lateral tail vein into nu/nu mice. Luciferin bioluminescence imaging was used to measure whole-body tumor burden 14 days post-injection. N=9, standard error shown. (D) 500k luciferase-expressing shCtl or shLYPD3 4T1 tumor cells were injected via lateral tail vein into syngeneic balb/c mice. Luciferin bioluminescence imaging was used to measure whole-body tumor burden 20 days post-injection. N=10, standard error shown.

There are several important differences between the PY230 and 4T1 cell lines that could explain these inconsistent results. LYPD3 levels on 4T1 cells are significantly lower than on PY230, and the 4T1 cell line grows very quickly regardless of mouse model, perhaps causing the tumor studies to end before cells have accumulated critical levels of peroxidated lipids. Moreover, the 4T1 cells were not previously passaged through mice

like the PY230 cells, a process that caused LYPD3 upregulation in PY230 and potentially selected for a state of LYPD3 dependence. These factors are being closely considered in the selection and development of additional cell lines for this project. We used the CellMinerCDB database (NCI) to identify human tumor cell lines with high baseline levels of LYPD3 expression, relatively slow growth rates, and a published history of tail vein metastasis use. Using these criteria, we identified the KYSE-30 esophageal squamous cell carcinoma line and the PC-9 non-small cell lung carcinoma line. We are focusing on human cell lines for translational applicability, and these two cell lines are particularly relevant given the high prevalence of LYPD3 expression in esophageal and lung cancers. We transfected both cell lines with luciferase and are passaging them through nu/nu mice to select for increased expression of LYPD3 in the same manner observed in PY230 cells. Once recovered from these mice, the KYSE-30 and PC-9 cells will be transfected with a Tet-inducible shLYPD3 knock-down construct and used for metastasis studies similar to those conducted with the PY230 and 4T1 models.

### 3.2.2 IFNγ exposure downregulates LYPD3 expression

Lymphocyte-derived IFNγ has been shown to downregulate expression of the xCT complex, priming tumor cells for ferroptotic cell death. Since LYPD3 has also been shown to suppress ferroptosis, we investigated whether IFNγ affects LYPD3 levels in a manner similar to xCT. Specifically, we treated three LYPD3-expressing breast tumor lines with 10 or 100 ng/mL IFNγ for 48 hours and assayed LYPD3 expression levels using a Western immunoblot. Interestingly, IFNγ stimulation significantly reduces LYPD3 expression across all three cell lines **(Fig. 22)**. These data suggest that either (1) the same IFNγ-driven transcriptional mechanism suppressing xCT expression also suppresses LYPD3, or (2) there is a causative mechanism by which reduced LYPD3 leads to reduced xCT. As a GPI-anchored protein, LYPD3 lacks a cytoplasmic domain and cannot directly mediate

intracellular signaling. Thus, LYPD3 may regulates ferroptosis by directly interacting with, and possibly stabilizing, other cell-surface proteins such as xCT.

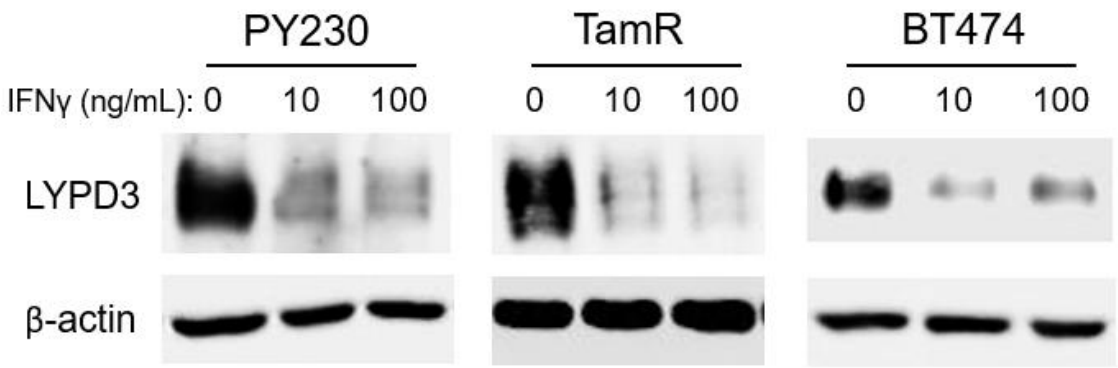


**Figure 22: IFNγ exposure downregulates LYPD3 expression**. PY230 cells were treated with 10-100 ng/mL murine IFNγ or a BSA control (0 ng/mL) for 48 hours, and LYPD3 expression was assayed using a Western immunoblot. TamR and BT474 cells were treated with 10-100 ng/mL human IFNγ or a BSA control (0 ng/mL) for 48 hours, and LYPD3 expression was assayed using a Western immunoblot. Proteins were resolved on a 7.5% acrylamide gel.

### 3.2.3 LYPD3 does not influence expression of cell-surface proteins previously linked to ferroptosis

Given the concomitant decrease in xCT and LYPD3 expression upon IFNγ stimulation, we hypothesized that LYPD3 might suppress ferroptosis by stabilizing cell-surface anti-ferroptosis proteins. The only known ligand of LYPD3 is AGR2, an ER-localized chaperone that becomes dysregulated in many cancers and whose expression correlates with tumor growth and metastasis[207]. However, AGR2 is not known to have any signal-transducing functions, lending support to the protein stabilization hypothesis. Besides xCT, there are several additional cell-surface anti-ferroptosis proteins, including ferroptosis suppressor protein 1 (FSP1) and ferroportin (FPN). The xCT complex imports cystine, which is converted to glutathione and used by GPX4 to neutralize lipophilic free radicals. Similarly, FSP1 neutralizes free radicals by regenerating $CoQH_2$, and FPN selectively exports reduced iron, which is required for the Fenton chemistry that drives lipid peroxidation[208]**(Fig. 23A)**. We conducted Western immunoblots to determine whether

LYPD3 knock-down affects xCT, FSP1, and FPN expression on PY230 and 4T1 tumor cells. All three proteins were detected, but expression of these proteins was not correlated with LYPD3 levels **(Fig. 23B-C)**. Thus, LYPD3 is unlikely to suppress ferroptosis by directly stabilizing cell-surface anti-ferroptosis proteins, though we have not ruled out a role for LYPD3 in activating these proteins through direct binding. With the most direct mechanism of action ruled out, we may need to investigate indirect mechanisms of action such as signaling through an unknown ligand.

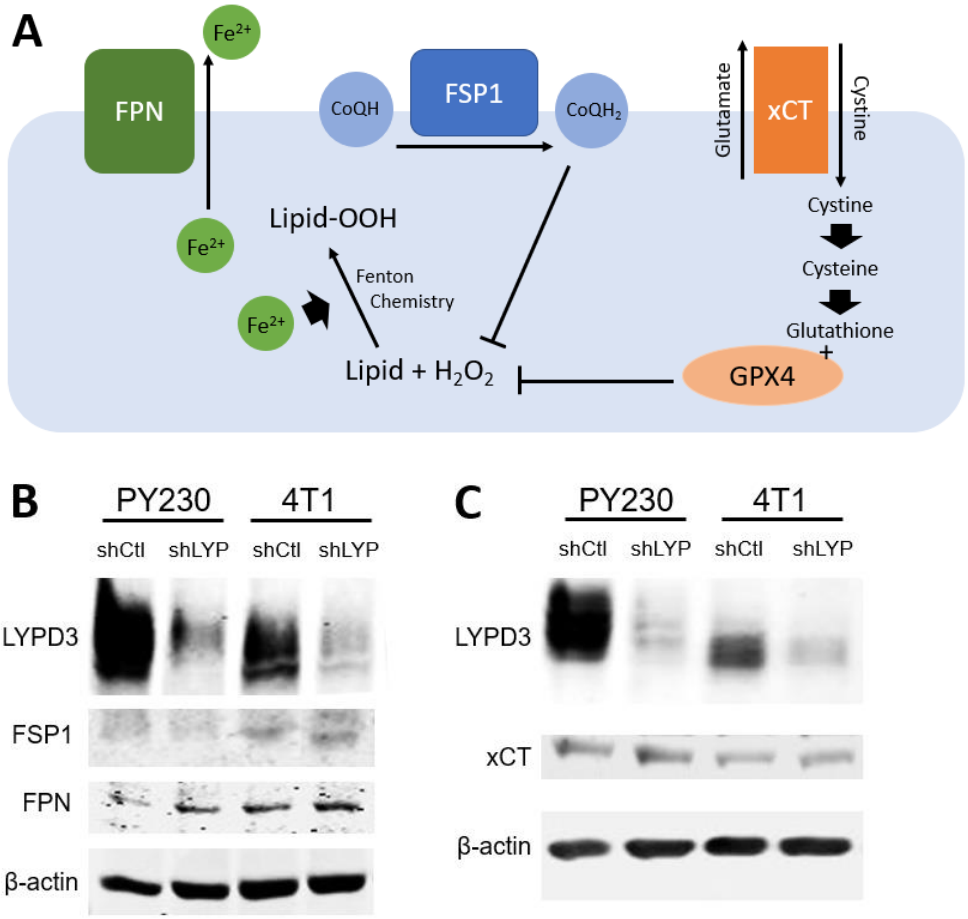


**Figure 23: LYPD3 ablation does not affect expression of cell-surface anti-ferroptosis proteins**. (A) The roles of ferroportin (FPN), ferroptosis suppressor protein 1 (FSP1), and GPX4/xCT in counteracting lipid peroxidation are depicted. (B-C) PY230 and 4T1 cell lines expressing constitutive shLYPD3 or shControl knock-down constructs were analyzed via Western immunoblot for expression of LYPD3, FSP1, FPN, and xCT (SLC7A11 subunit). 40 µg of protein was resolved on a 7.5% acrylamide gel (LYPD3, FPN) or on a 10% acrylamide gel (FSP1, xCT).

### 3.2.4 De novo LYPD3 expression is not seen in cell lines passaged *in vivo*

Considering how PY230 cells dramatically upregulate LYPD3 when passaged through mice, we postulated that LYPD3-negative cell lines might spontaneously acquire expression of this protein or select for rare cells which express high levels of LYPD3 when passaged *in vivo*. It is possible that LYPD3 expression serves as a generalizable ferroptosis protection mechanism necessary to upregulate or activate canonical anti-ferroptosis pathways. To test this idea, we used four LYPD3-negative cell lines that are well-validated tail vein metastasis models: the A7C11 mouse breast cancer line, the MDA-231 human breast cancer line, and the YUMM1.7 and B16-F10 mouse melanoma lines. These cell lines were injected into nu/nu mice via tail vein, lung nodules were harvested, recovered cells were propagated *in vitro*, and Western immunoblotting was used to detect LYPD3 expression. In total, we recovered cells from five A7C11 lung nodules, three MDA-231 lung nodules, four YUMM1.7 lung nodules, and two B16-F10 lung nodules, but none of the samples showed any level of de novo LYPD3 expression **(Fig. 24A-C)**. Despite being propagated in an *in vivo* environment with high oxidative stress for 31-37 days, these cells did not gain LYPD3 expression. Thus, LYPD3 is not a generalizable mechanism necessary for ferroptosis protection; rather, LYPD3 plays a critical role only in a subset of tumor types.

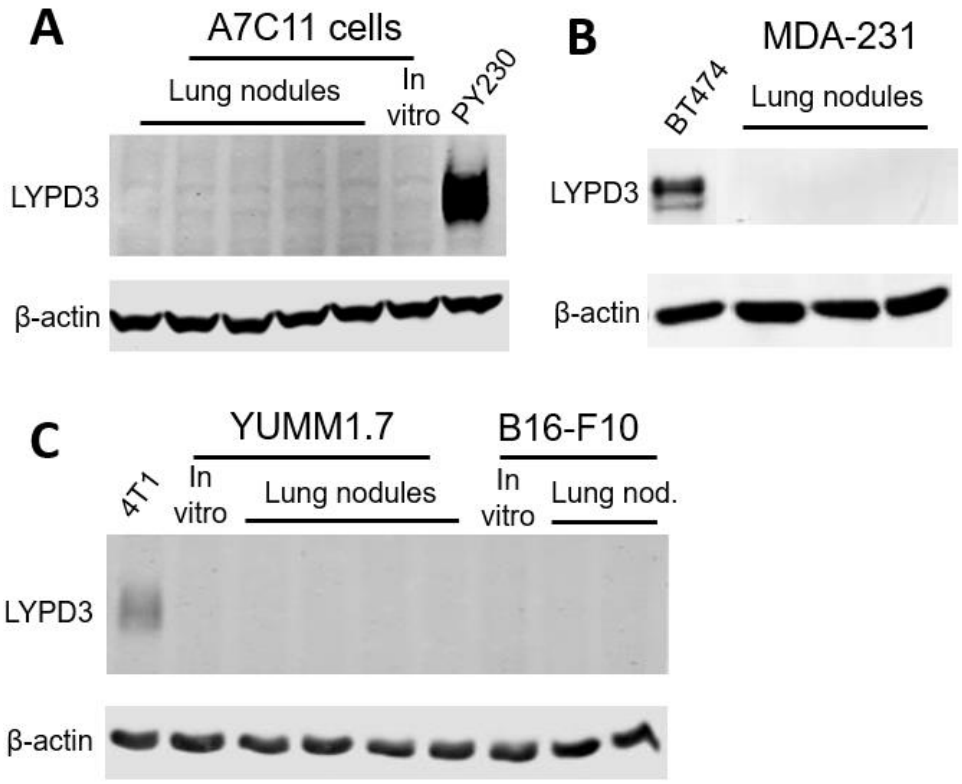


**Figure 24: Do novo LYPD3 expression was not observed in any LYPD3-negative cell lines passaged through mice**. (A) 500k neomycin-resistant A7C11 tumor cells were injected into the lateral tail vein of three WT BL/6 mice, and 37 days later, tumor cells were recovered from five metastatic lung nodules and propagated *in vitro* under neomycin selection. These recovered cells were analyzed for LYPD3 expression using a Western immunoblot and compared to the parent A7C11 cell line (in vitro) and the PY230 positive control. (B-C) 500k neomycin-resistant MDA-231, YUMM1.7, or B16-F10 tumor cells were injected into the lateral tail vein of four nu/nu mice each, and 31 days later, tumor cells were recovered from lung nodules and propagated *in vitro* under neomycin selection. These recovered cells were analyzed for LYPD3 expression using a Western immunoblot and compared to the proper parent cell line (in vitro) or the BT474 or 4T1 positive controls. In all panels, proteins were resolved on a 7.5% acrylamide gel.

## *3.3 Discussion*

### 3.3.1 Interpretation of results

Our work has demonstrated a novel function for LYPD3 in suppressing ferroptosis in tumor cells. We have shown that LYPD3 expression correlates with tumor aggressiveness and resistance to ferroptosis inhibitors in cancer cell lines. Moreover, we have demonstrated experimentally that ablation of LYPD3 sensitizes PY230 cells to ferroptosis both *in vitro* and in animal models of metastasis. Indeed, inhibiting ferroptosis through an independent mechanism (ferrostatin-1), completely restores the growth of LYPD3 knock-down metastases. IFNγ exposure is known to reduce xCT expression in tumor cells, priming tumors for ferroptotic cell death. Interestingly, we have shown that IFNγ also downregulates LYPD3 across at least three cell lines, suggesting a link between LYPD3 and xCT expression. However, an shRNA-mediated LYPD3 knock-down in two cell lines failed to produce a concomitant reduction in xCT, undercutting any causative link between LYPD3 and xCT expression levels. In a similar manner, LYPD3 expression showed no correlation with FPN or FSP1, two additional cell-surface anti-ferroptosis proteins. Thus, LYPD3 likely mediates ferroptosis protection through a hitherto unidentified signaling mechanism.

Moreover, we have yet to identify a driver for ectopic LYPD3 expression in tumor cells. Only a fraction of tumor cell lines express LYPD3, and these lines tend to increase LYPD3 expression as they adopt more aggressive features or when exposed to protracted oxidative stress (i.e. when passaged through mouse lungs), suggesting a critical anti-ferroptosis function. This critical importance is illustrated by the metastasis study we performed in which LYPD3 knock-down PY230 tumors completely fail to grow in most mice. However, we found no evidence that LYPD3-negative cell lines gain expression of this protein when exposed to intense oxidative stress. Together, these results suggest that

LYPD3 is critically important for some tumors to survive ferroptosis but entirely irrelevant to others, perhaps because redundant anti-ferroptosis pathways render LYPD3 unnecessary. Elucidating the mechanism by which LYPD3 regulates ferroptosis may shed light on this dichotomy between $LYPD3^{+}$ and $LYPD3^{-}$ tumor lines.

### 3.3.2 Future directions and applications

Our current priority is to replicate the robust phenotypes observed in PY230 cells using the KYSE-30 and PC-9 tumor lines. We will first demonstrate *in vitro* that shLYPD3 knock-down increases lipid peroxidation while decreasing cell survival, and we will then proceed with metastasis studies to establish a ferrostatin-reversible reduction in tumor growth upon shLYPD3 ablation. However, our ultimate goal is to elucidate the mechanism(s) linking LYPD3 expression to ferroptosis and translate these insights into novel therapeutic strategies. We have been unable to establish a link between LYPD3 and the expression or stabilization of cell-surface proteins like xCT, but perhaps LYPD3 binding improves the activity of one of these proteins. Using small molecule inhibitors of xCT, such as sorafenib or erastin, we can test whether the anti-ferroptosis effects of LYPD3 are mediated through xCT activity. If LYPD3 indirectly activates intracellular signaling pathways to modulate ferroptosis, then these effects should be observable in a phospho-proteomics screen or an mRNA sequencing screen of shLYPD3 knock-down tumor lines. Identifying the specific cell-surface LYPD3 ligand that transduces this signal would be more challenging, but a mass spectrometry immunoprecipitation assay could generate several candidates for further investigation.

Our work suggests several possible applications for anti-LYPD3 antibodies in combination with other cancer therapies. Direct GPX4 inhibitors such as RSL3 and ML210 are associated with significant systemic toxicity[209,210], but combining these compounds with anti-LYPD3 may enable a lower effective dose and reduced toxicity. Alternatively, if LYPD3 is shown to support the GPX4/xCT pathway, then combining GPX4 inhibitors with

anti-LYPD3 antibodies may produce a level of pathway inhibition not achievable with a single agent. Moreover, spontaneous tumors tend to be highly heterogenous, and subpopulations of tumor cells that express high levels of LYPD3 may be able to evade our current slate of ferroptosis-inducing therapies, which includes GPX4 and xCT inhibitors. Combining these therapies with anti-LYPD3 could prevent tumors from using the LYPD3 mechanism to escape ferroptosis-inducing compounds. Given the interplay between anti-tumor immunity and ferroptosis, we are especially interested in combining anti-LYPD3 with immune-activating treatments such as checkpoint inhibitors. Increased T cell and NK cell activity in the tumor would translate to higher IFNγ production, which could, in combination with anti-LYPD3, produce a synergistic vulnerability to ferroptosis. Overall, this project offers many exciting translational opportunities once we further establish the phenotype and mechanism linking LYPD3 to ferroptosis.

# 4 Conclusion

Our group has a longstanding interest in the role of CaMKK2 in cancer. In recent years, we have elucidated a variety of pro-tumor roles for this enzyme when expressed in tumor cells and myeloid immune cells, and we have worked with industry and academic collaborators to develop CaMKK2-modulating compounds. My thesis project began as a screen to identify CaMKK2 expression in non-myeloid immune cells in the tumor environment, enabling a more complete understanding of how CaMKK2 inhibition impacts tumor progression. This screen identified NK cells as a population of interest, and subsequent studies revealed an important role for CaMKK2 in preserving the fitness of tumor-infiltrating NK cells. These findings were highly intriguing for several reasons. First, CaMKK2 expression is greatly enhanced by exposure to lactic acid in the tumor environment, establishing a novel mechanism by which NK cells mitigate the effects of this suppressive metabolite. This robust, built-in adaptive response suggests a specific evolutionary advantage for preserving NK cell activity in lactate-rich environments. Second, CaMKK2 exhibits a unique mechanism of action in NK cells, improving NK fitness through a scaffold function independent of the AMPK pathway and mitochondrial regulation. This finding expands our understanding of CaMKK2's highly flexible and multifaceted role in different cell types. Third, our findings underscore the need to carefully dissect the mechanism of action not just for CaMKK2 inhibitors, but for novel cancer treatments in general. CaMKK2 LDDs confer beneficial effects when acting in certain cell types (i.e. macrophages and tumor cells) yet confer detrimental effects when acting in another cell type (i.e. NK cells), and the overall effect of such a treatment will depend on the relative abundance of each cell type and the importance of this pathway within each population. Thus, therapies must be selected carefully based on the characteristics of individual tumors.

Our group originally became interested in LYPD3 as a vulnerability in endocrine-therapy resistant breast cancer, but the project evolved into a broader study of LYPD3 as a regulator of ferroptosis. We have established a causative link between LYPD3 expression and ferroptosis resistance, suggesting that LYPD3 antagonism would be a novel mechanism to reduce tumor cell growth and enhance anti-tumor immunity. Together, the LYPD3 project and the NK cell CaMKK2 project demonstrate the broad range of pathways, both in immune cells and cancer cells, that can be modulated to enhance anti-tumor immunity. Ongoing work on both projects will continue to yield important insights in tumor biology and immunity, with many possible translational implications.

# Appendix: Methods and Materials

## A.1 Isolation and culture of primary NK cells

Spleens from WT or CaMKK2 KO BL/6 female mice aged 10-12 weeks were harvested and crushed through a 40 μm cell strainer into PBS+ 2% FBS. The EasySep Mouse NK Cell Isolation Kit (StemCell Technologies, cat no. 19855) was used to isolate NK cells through negative selection. NK cell purity was measured using an Accuri C6 flow cytometer (BD Biosciences) to determine the percentage of purified cells expressing CD49b. The following antibodies were used: CD49b-PE (BioLegend, cat no. 103506) and isotype control (Invitrogen, cat no. 12-4888-81). NK cells were cultured in either a 50/50 mixture of EO771 TCM and normal growth media, or normal growth media alone. Normal growth media consists of RMPI 1640 containing 10% fetal bovine serum (FBS), 1 mM sodium pyruvate, 0.1 mM non-essential amino acids, 10 mM HEPES, 2 mM L-glutamine, 55 μM 2-mercaptoethanol, and 100 units/mL Penicillin+ 100 μg/mL Streptomycin. Experiments requiring pH stabilization used 25 mM HEPES and 25 mM PIPES in place of 10 mM HEPES. All reagents were purchased from Gibco. 100 ng/mL IL2 (PeproTech, cat no. 212-12) and/or 100 ng/mL IL15 (PeproTech, cat no. 210-15) were added to the culture media depending on the experiment. All cells were incubated in a humidified chamber at 37°C in a 5% CO2 atmosphere.

## A.2 Cancer cell lines and growth media

EO771 is a murine breast tumor line acquired from the lab of Mark Dewhirst (Duke University). A7C11 is a murine breast tumor line acquired from the lab of Jose Conejo-Garcia (Moffitt Cancer Center). 4T1 is a murine breast tumor line purchase from ATCC. BT-474 is a human breast tumor line also purchased from ATCC. EO771, A7C11, 4T1, and BT474 were cultured in RPMI 1640 containing 10% FBS, 1 mM sodium pyruvate (NaPy), and 0.1 mM non-essential amino acids (NEAA). B16-F10 is a lung-tropic murine

melanoma line purchased from the Duke Cell Culture Facility. YUMM1.7 is a mouse melanoma line purchased from ATCC. MDA-231 is a human breast cancer line also purchased from ATCC. B16-F10, YUMM1.7, and MDA-231 were cultured in DMEM containing 10% FBS, 1 mM NaPy, and 0.1 mM NEAAs. PY230 is a murine breast tumor line purchased from ATCC and cultured in F-12K Nutrient Mixture, Kaighn's Modification (Gibco, cat no. 21127-022) containing 5% FBS and 0.1% of MITO serum extender. TamR is a human breast tumor line derived from MCF7 cells (ATCC) through prolonged exposure to tamoxifen. TamR cells were cultured in DMEM/F12 (1:1) Ham media (Gibco, cat no. 11330-032) containing 10% FBS, 1 mM NaPy, 0.1 mM NEAAs, and 100 nM 4-OH-tamoxifen. NK-92 is a human NK cell lymphoma line purchased from the Duke Cell Culture Facility. These cells were grown in suspension in Minimum Essential Medium (Sigma, cat no. M4526) containing 12.5% FBS, 12.5% horse Serum, 0.2 mM myo-inositol, 0.02 mM folic acid, 2 mM L-glutamine, 0.1 mM β-Mercaptoethanol, and 5,000 units/mL human IL2 (BD Bioscience, cat no. 40043B). All cells were incubated in a humidified chamber at 37°C in a 5% CO2 atmosphere.

### A.3 Generation of tumor-conditioned media

One million EO771 or A7C11 tumor cells were plated on a 10-cm cell culture dish in their standard RMPI growth media and incubated at 37°C. After exactly 72 hours, the growth media was recovered from each plate, centrifuged at 2000 x g for 5 minutes to remove debris, and the supernatant was frozen at -80°C.

### A.4 Mouse strains

The CaMKK2-/- (KO) mouse strain was originally generated in the lab of Anthony Means (Baylor College of Medicine)[108]. These mice were backcrossed for five generations to WT C57BL/6 mice (Jackson Labs) and have a genetic background that is at least 95% C57BL/6. The [Tg(CaMKK2-eGFP)BL/6] reporter mouse line originates from the Mutant

Mouse Regional Resource Center[166]. This strain features the sequence of enhanced green fluorescent protein (eGFP), followed by a polyadenylation sequence, inserted into the mouse genomic bacterial artificial chromosome RP23-31J24 at the initiation codon of the CaMKK2 gene. The Racioppi lab had backcrossed the original strain to Jackson Lab's WT BL/6 mice for 10 generations, generating the mice used in our studies.

NKp46-iCre mice were acquired from the lab of Joseph Sun (Memorial Sloan Kettering Cancer Center) and were originally created by Eric Vivier (Centre d'Immunologie de Marseille-Luminy). This strain features the Cre coding sequence preceded by an IRES inserted into the 3'UTR of the NKp46 (Ncr1) sequence. These mice were bred with CaMKK2 flox/flox mice to generate Ncr1-cre+/- CaMKK2 flox/flox experimental mice and Ncr1-cre+/- CaMKK2 wt/wt controls. The CaMKK2 flox mice were originally generated by the lab of Anthony Means (Baylor College of Medicine)[108].

Tamoxifen-inducible ERT2-cre+/- CaMKK2 flox/flox mice (including ERT2-negative controls) were generated by breeding CaMKK2 flox/flox mice (described above) with UBC-Cre-ERT2 mice acquired from Jackson Labs (strain #007001). ERT2+ mice and ERT2- controls were dosed with 2 mg tamoxifen citrate (Sigma-Aldrich, cat no. T9262) in corn oil via oral gavage daily for one week, and splenic NK cells were harvested 5 days after dosing ended.

The following mice were purchased from Jackson Labs as needed: WT C57BL/6 females (strain # 000664), NSG females (strain # 005557), and athymic nude females, or nu/nu (strain # 002019).

### A.5 CFSE proliferation assay

NK cell proliferation was measured via dilution of the anime-reactive CFSE dye. Splenic NK cells were treated with 5 μM CellTrace CFSE (Invitrogen, cat no. C34554A) in RMPI media+ 5% FBS for 5 minutes, washed twice with the same media, and cultured under various conditions for 72 hours. CFSE fluorescence decreases by half with each

round of cell division, enabling us to identify the proliferating fraction of NK cells via flow cytometry. NK cells were gated as live CD45+/CD3-/NK1.1+/CD49b+ cells.

### A.6 In vitro migration assay

NK cell migration was measured using a transwell migration assay. Splenic NK cells that had been cultured under various conditions for 72 hours were counted, and 500,000 live NK cells were suspended in 100 µL of normal growth media and added to the upper insert of a transwell migration chamber with 5 µm pores (Corning, cat no. 3421). 600 µL of normal growth media containing 0 or 250 ng/mL CCL4 (BioLegend, cat no. 554602) was added to the lower chamber, and the migration plate was incubated at 37°C for 3 hours. The Accuri C6 flow cytometer (BD Biosciences) was used to count the total number of CD49b+ cells present in the lower chamber.

### A.7 In vitro NK cytotoxicity assay

NK cell cytotoxic activity was measured via a co-culture with YAC1 tumor cells. YAC1 cells, a canonical MHC I-negative target for NK cells, were cultured in RMPI 1640 containing 10% FBS, 1 mM sodium pyruvate, 10 mM HEPES, and 3.5 g/L D-(+)-glucose (Sigma). The YAC1 cells were stained with CellTrace CFSE (Invitrogen, cat no. C34554A) for quick identification on flow cytometry. YAC1 cells were counted using a microscope hemocytometer chamber (Hausser Scientific), and 25,000 cells were added to each internal well of a flat-bottom 96 well plate (Corning) in 75 µL of their growth media. Splenic NK cells that had been cultured for 72 hours under various conditions were counted, and live NK cells were added to the YAC-1 cells at a ratio of 1:25, 1:5, 1:1, and 5:1 (NK:YAC1). The volume of each co-culture well was topped up to 150 µL with NK growth media. Three biological replicates were carried out at each co-culture ratio. The NK cells and YAC1 cells were incubated at 37°C for 4 hours, and cells were then stained with Live/dead stain and anti-CD45-BV605 for flow cytometry analysis. YAC1 cells were identified as CD45-

/CFSE+. The dead fraction of YAC1 cells (positive live/dead staining) were represented as a fraction of total YAC1 cells.

## A.8 Flow cytometry

The following reagents were used to prepare NK cells for flow cytometry. Anti-CD16/32 (Invitrogen, cat no. 14-0161-85) and anti-CD16.2 (BioLegend, cat no. 149502) were used for Fc receptor blocking, and LIVE/DEAD Fixable Violet Dead Cell Stain (Invitrogen, cat no. L34964) was used as a viability stain. NK cells were then stained with a combination of cell-surface fluorophore-antibody conjugates in BD Horizon Brilliant Stain, as listed in Table 2. NK cells were then permeabilized using eBioscience Fixation/Perm solution (Invitrogen, cat no. 00-5123-43 and 00-5223-56) and stained with some combination of intracellular fluorophore-antibody conjugates in Permeabilization Buffer (Invitrogen, cat no. 00-8333-56). Cells were then fixed in BD Cytofix fixation buffer diluted 1:4 (BD Bioscience, cat no. 554655). Flow cytometry data was collected on an LSRFortessa X-20 (BD Biosciences) and analyzed using FlowJo software version 10.7.1.

**Table 2: Flow cytometry antibodies**

| Target | Fluorochrome | Supplier | Cat no. |
|---|---|---|---|
| AnnexinV | AF488 | Invitrogen | A13201 |
| CD45 | BV605 | Invitrogen | 103139 |
| CD49b | BV650 | BD Biosciences | 740496 |
| NK1.1 | AF700 | Invitrogen | 56-5941-82 |
| CD3 | PerCP/Cy5.5 | BD Pharmigen | 560527 |
| NKp46 | BV711 | BioLegend | 137621 |
| NKG2D | FITC | BioLegend | 115711 |
| Ly49c | PE/Cy7 | BioLegend | 108210 |
| CD11b | PE | BioLegend | 101208 |
| CD27 | BV786 | BioLegend | 124241 |
| CCR5 | PE | Invitrogen | 12-1951-81 |
| CD24 | BUV496 | BD Horizon | 612953 |
| CD64 | PerCP/Cy5.5 | BioLegend | 139308 |
| IA/IE | BV711 | BD Horizon | 563414 |
| CD11c | APC/Cy7 | BD Pharmigen | 561241 |
| CD11b | AF700 | BioLegend | 101222 |
| Ly6G | BV785 | BioLegend | 127645 |
| Ly6C | BV711 | BioLegend | 128037 |
| Granzyme B | AF647 | BioLegend | 515406 |
| Ki67 | BUV395 | BD Horizon | 564071 |
| CD206 | FITC | BioLegend | 141710 |

## A.9 Western immunoblotting

The primary antibodies listed in Table 3 were used to detect the indicated proteins through Western immunoblotting. Fluorescent secondary antibodies purchase from Biotium were used for LI-COR imaging. Western blots were scanned using a LI-COR Odyssey Classic fluorescence scanner and processed using LI-COR Image Studio software, version 4.0.

**Table 3: Primary antibodies for Western immunoblotting**

| Target | Clone | Supplier | Cat no. | Dilution |
|---|---|---|---|---|
| CaM Kinase Kinase | 6/CaM Kinase | BD Transduction Labs | 610544 | 1:1,000 |
| β-actin | AC-15 | Sigma-Aldrich | A1978 | 1:10,000 |
| AMPKα | Polyclonal | Cell Signaling Technologies | 2532 | 1:1,000 |
| phospho-AMPKα (Thr172) | Polyclonal | Cell Signaling Technologies | 2531 | 1:1,000 |
| LYPD3 (human) | ERP9107 | Abcam | ab151709 | 1:1,000 |
| LYPD3 (mouse) | Polyclonal | R&D Systems | AF5567 | 1:500 |
| xCT (SLC7a11) | D2M7A | Cell Signaling Technologies | 12691 | 1:1,000 |
| Ferroprotin | Polyclonal | Novus Biologicals | NBP1-21502 | 1:500 |
| FSP1 | Polyclonal | Cell Signaling Technologies | 24972 | 1:1,000 |

## A.10 Creation of plasmid vector to knock-out MHC class I

The EO771 cell line was engineered using CRISPR to knock-out both alleles of the β2m locus, eliminating expression of the major histocompatibility complex class I. The Lenti-Cas9-gRNA-GFP plasmid vector (Addgene plasmid #124770) was first modified to contain two specific guide RNA (gRNA) sequences targeting the mouse β2m locus. This plasmid was linearized via digestion with the BsmBI restriction enzyme, separated on a 1% agarose gel, and recovered using the QIAquick gel extraction kit (Qiagen, cat no. 28706X4). The following forward and reverse primer sets were annealed together through gradual cooling from 95 degrees and then incubated with the linearized plasmid at room temperature for 30 minutes in the presence of the T4 ligase:

B2M-1F: 5’-CACCGAGTATACTCACGCCACCCAC-3’

B2M-1R: 5’-AAACGTGGGTGGCGTGAGTATACTC-3’

B2M-2F: 5’-CACCGAGTCGTCAGCATGGCTCGCT-3’

B2M-2R: 5’-AAACAGCGAGCCATGCTGACGACTC-3’

5 ug of each ligated plasmid was incubated with 50 uL of Stbl3 homologous recombination-deficient bacteria (ThermoFisher, cat no. 737303) on ice for 30 minutes. The bacteria were then heat shocked at 42 degrees for 40 seconds, added to 300 uL of SOC media, shaken at 37 degrees for 1 hour, and plated onto LB-Amp plates (100 ug/mL ampicillin). The two plates were incubated for 24 hours at 37 degrees, and 5 colonies from each plate were picked for a 24-hour expansion in 3 mL liquid LB-Amp media. The QIAprep mini prep kit (Qiagen, cat no. 27106X4) was used to isolated plasmid DNA from the 10 expanded bacteria colonies, and the samples were submitted to Eton Bio for sequencing with the “hU6” universal primer set. Using the procedure described in A.11, EO771 cells were transfected with the plasmid-cas9-gRNA constructs described above, and EO771 cells with homozygous ablation of β2m were isolated using flow cytometry-based cell sorting to select for GFP+, MHC I-negative cells.

### A.11 Transfection of cell lines

Various cell lines were modified to express a Tet-inducible shRNA knock-down construct or the luciferase enzyme, which enables bioluminescence imaging of tumor burden. To generate lentivirus transfection vectors, HEK293T cells (ATCC) were grown to 40% confluency in DMEM containing 10% FBS, 1 mM sodium pyruvate, 0.1 mM non-essential amino acids, and 2 mM L-glutamine. The following transfection mixture was prepared for one 10 cm culture plate: 263 Opti-Mem, 17 µL FuGENE-6 (Promega, cat no. E2692), 280 ng VSVG envelope vector (Addgene plasmid #8454), 2.8 µg PsPAX2 Lentivirus packaging vector (Addgene plasmid #12260), and 2.8 ug of the transfection vector (e.g. luciferase, Tet-inducible shRNA, or Cas9/ β2mg-RNA). The transfection mixture was incubated at room temperature for 30 minutes, added dropwise to the HEK293 cells, and the plate was incubated at 37°C. 24 hours later, the media was aspirated and replaced with the standard DMEM growth media containing 30% FBS. 24

hours later, the lentivirus-containing media was recovered, filtered through a 45 μm filter, and frozen at -80°C. New DMEM growth media containing 30% FBS was added to the plates, and this media was recovered and filtered in the same manner 24 hours later.

B16-F10 or EO771 cells were grown to 70% confluency in their standard growth media. The lentivirus-containing media was diluted in an equal volume of tumor growth media and added to the B16-F10 or EO771 cells. 24 hours later, the first round of lentivirus-containing media was aspirated, and a second round of diluted lentivirus-containing media was added. 24 hours later, the virus-containing media was replaced with standard tumor growth media, and the cells were incubated for 48 hours. Transfected cells were split across a six-well plate and cultured with various concentrations of neomycin (Geniticin brand, Gibco, cat no. 3480) ranging from 50 μg/mL to 2000 μg/mL for 10 days. The highest neomycin concentration that failed to kill all tumor cells was chose as the optimal selection dose and expanded.

### A.12 Tail vein metastasis studies

For NK cell studies, 6-7 week-old female NSG mice were purchased from Jackson Labs and used as models of metastatic tumor growth. The NSG mice were randomized, ear-punched for identification, and their chests shaved to improve bioluminescence signal. Splenic NK cells were isolated from 10-12 week-old WT and CaMKK2 KO female mice and cultured for 24 hours in NK cell growth media containing 100 ng/mL murine IL15. 250,000 live WT or KO NK cells were then injected into the lateral tail vein of NSG mice in a volume of 100 μL Hank's Balanced Salt Solution (HBSS, Gibco, cat no. 14025-092). When using the B16-F10 model, 500,000 tumor cells were injected concurrently with the NK adoptive transfer: NK cells and tumor cells were mixed immediately before injection in a total volume of 100 uL HBSS per mouse. "No NK" control mice were injected with tumor cells alone. Mice were discarded if the intravenous injection was not successful on the first attempt. 200 units of murine IL2 suspended in 100 uL PBS was injected into the peritoneal

cavity of every mouse (including controls) immediately after adoptive transfer of the NK cells and every third day thereafter. When using the β2m-/- EO771 model, 300,000 tumor cells were injected into the lateral tail vein 48 hours prior to adoptive transfer of NK cells to prevent immediate clearance of blood-borne tumor cells.

Starting at day 10 and repeating every 3-4 days thereafter, all mice were anesthetized with isoflurane and administered 100 uL luciferin substrate (Regis Technologies, cat no. 1-360243-200) via retroorbital injection immediately prior to imaging. Luciferase bioluminescence was measured using an IVIS Lumina XR optical imaging system with an exposure time of 2-3 minutes. The signal intensity range was standardized for all images collected in a particular session, and gates were drawn around any signal visualized above the minimum threshold. The total signal intensity from each mouse measured in lumens/sec/$cm^2$ was reported as “metastatic burden”. Signals emanating from the tail were treated as primary injection-site tumors and excluded from the “metastatic burden” summation. Studies were not blinded as this would require prohibitive amounts of effort from colleagues otherwise uninvolved in the project.

Mice were euthanized and lungs were extracted for flow cytometry profiling of the cellular populations. The lung tissue was mechanically pulverized in 5 mL DMEM+5% FBS and then enzymatically digested by adding 1 mg/mL Collagenase A (Roche, cat no. 10103586001) and 200 units/mL DNAse I (Sigma, D5025-150KU) and incubated for 30 minutes in a 37°C shaker. Each sample was then passed through a 40 μm cell strainer, centrifuged down, and resuspended in 1-2 mL ACK lysis buffer (Gibco, cat no. A10492-01) for 2 minutes to eliminate red blood cells. ACK lysis buffer was diluted in 10 volumes of PBS, and cells were stained with a variety of fluorophore-conjugated antibodies for flow cytometry analysis.

## A.13 Primary tumor studies

11-12 week-old CaMKK2-eGFP reporter mice were injected subcutaneously with 200,000 E0771 tumor cells in 100 µL HBSS. Tumor size was measured every 3-4 days using calipers, and upon reaching a volume of 1 $cm^3$, mice were euthanized, and tumors and spleens were extracted. Spleens were crushed through a 40 µm cell strainer, RBCs were lysed with ACK buffer, and splenocytes were stained for flow cytometry profiling. Tumor cells were mechanically pulverized and digested with Collagenase A and DNAse I, as described in the previous section, and stained for flow cytometry profiling.

## A.14 Statistical analysis

Standard error of the mean is shown based on 2-3 biological replicates per experiment. Microsoft Excel was used for statistical analysis. P-value was determined using an unpaired Student's t-test with a significance threshold of $P<0.05$ (*$P<0.05$, **$P<0.01$, ***$P<0.005$).

# References


1 Siegel, R. L., Miller, K. D. & Jemal, A. Cancer statistics, 2019. *CA Cancer J Clin* **69**, 7-34, doi:10.3322/caac.21551 (2019).

2 Wyld, L., Audisio, R. A. & Poston, G. J. The evolution of cancer surgery and future perspectives. *Nat Rev Clin Oncol* **12**, 115-124, doi:10.1038/nrclinonc.2014.191 (2015).

3 Baumann, M. *et al.* Radiation oncology in the era of precision medicine. *Nat Rev Cancer* **16**, 234-249, doi:10.1038/nrc.2016.18 (2016).

4 Huang, C. *et al.* Management of Non-small Cell Lung Cancer Patients with MET Exon 14 Skipping Mutations. *Curr Treat Options Oncol* **21**, 33, doi:10.1007/s11864-020-0723-5 (2020).

5 Cortesi, L., Rugo, H. S. & Jackisch, C. An Overview of PARP Inhibitors for the Treatment of Breast Cancer. *Target Oncol* **16**, 255-282, doi:10.1007/s11523-021-00796-4 (2021).

6 Di Cosimo, S. *et al.* Targeted-Gene Sequencing to Catch Triple Negative Breast Cancer Heterogeneity before and after Neoadjuvant Chemotherapy. *Cancers (Basel)* **11**, doi:10.3390/cancers11111753 (2019).

7 Weiner, G. J. Monoclonal antibody mechanisms of action in cancer. *Immunol Res* **39**, 271-278, doi:10.1007/s12026-007-0073-4 (2007).

8 Pescovitz, M. D. Rituximab, an anti-cd20 monoclonal antibody: history and mechanism of action. *Am J Transplant* **6**, 859-866, doi:10.1111/j.1600-6143.2006.01288.x (2006).

9 Hudis, C. A. Trastuzumab--mechanism of action and use in clinical practice. *N Engl J Med* **357**, 39-51, doi:10.1056/NEJMra043186 (2007).

10 Finkelmeier, F., Waidmann, O. & Trojan, J. Nivolumab for the treatment of hepatocellular carcinoma. *Expert Rev Anticancer Ther* **18**, 1169-1175, doi:10.1080/14737140.2018.1535315 (2018).

11 June, C. H., O'Connor, R. S., Kawalekar, O. U., Ghassemi, S. & Milone, M. C. CAR T cell immunotherapy for human cancer. *Science* **359**, 1361-1365, doi:10.1126/science.aar6711 (2018).

12 Santos Apolonio, J. *et al.* Oncolytic virus therapy in cancer: A current review. *World J Virol* **10**, 229-255, doi:10.5501/wjv.v10.i5.229 (2021).

13 Howard, F. M. & Olopade, O. I. Epidemiology of Triple-Negative Breast Cancer: A Review. *Cancer J* **27**, 8-16, doi:10.1097/PPO.0000000000000500 (2021).

14 Kleeff, J. *et al.* Pancreatic cancer. *Nat Rev Dis Primers* **2**, 16022, doi:10.1038/nrdp.2016.22 (2016).

15 Islami, F. *et al.* Disparities in liver cancer occurrence in the United States by race/ethnicity and state. *CA Cancer J Clin* **67**, 273-289, doi:10.3322/caac.21402 (2017).

16 Sarmento-Ribeiro, A. B., Scorilas, A., Goncalves, A. C., Efferth, T. & Trougakos, I. P. The emergence of drug resistance to targeted cancer therapies: Clinical evidence. *Drug Resist Updat* **47**, 100646, doi:10.1016/j.drup.2019.100646 (2019).

17 Abel, A. M., Yang, C., Thakar, M. S. & Malarkannan, S. Natural Killer Cells: Development, Maturation, and Clinical Utilization. *Front Immunol* **9**, 1869, doi:10.3389/fimmu.2018.01869 (2018).

18 Narni-Mancinelli, E. *et al.* Complement factor P is a ligand for the natural killer cell-activating receptor NKp46. *Sci Immunol* **2**, doi:10.1126/sciimmunol.aam9628 (2017).

19 Lanier, L. L. On guard--activating NK cell receptors. *Nat Immunol* **2**, 23-27, doi:10.1038/83130 (2001).

20 Debska-Zielkowska, J. *et al.* KIR Receptors as Key Regulators of NK Cells Activity in Health and Disease. *Cells* **10**, doi:10.3390/cells10071777 (2021).

21 Trapani, J. A. & Smyth, M. J. Functional significance of the perforin/granzyme cell death pathway. *Nat Rev Immunol* **2**, 735-747, doi:10.1038/nri911 (2002).

22 Karre, K., Ljunggren, H. G., Piontek, G. & Kiessling, R. Selective rejection of H-2-deficient lymphoma variants suggests alternative immune defence strategy. *Nature* **319**, 675-678, doi:10.1038/319675a0 (1986).

23 Croft, N. P. *et al.* Stage-specific inhibition of MHC class I presentation by the Epstein-Barr virus BNLF2a protein during virus lytic cycle. *PLoS Pathog* **5**, e1000490, doi:10.1371/journal.ppat.1000490 (2009).

24 Hengel, H. *et al.* Cytomegaloviral control of MHC class I function in the mouse. *Immunol Rev* **168**, 167-176, doi:10.1111/j.1600-065x.1999.tb01291.x (1999).

25 Huntington, N. D., Nutt, S. L. & Carotta, S. Regulation of murine natural killer cell commitment. *Front Immunol* **4**, 14, doi:10.3389/fimmu.2013.00014 (2013).

26 Fu, B., Tian, Z. & Wei, H. Subsets of human natural killer cells and their regulatory effects. *Immunology* **141**, 483-489, doi:10.1111/imm.12224 (2014).

27 Huntington, N. D. *et al.* IL-15 trans-presentation promotes human NK cell development and differentiation in vivo. *J Exp Med* **206**, 25-34, doi:10.1084/jem.20082013 (2009).

28 Tu, M. M., Mahmoud, A. B. & Makrigiannis, A. P. Licensed and Unlicensed NK Cells: Differential Roles in Cancer and Viral Control. *Front Immunol* **7**, 166, doi:10.3389/fimmu.2016.00166 (2016).

29 Fu, B. *et al.* CD11b and CD27 reflect distinct population and functional specialization in human natural killer cells. *Immunology* **133**, 350-359, doi:10.1111/j.1365-2567.2011.03446.x (2011).

30 Montaldo, E. *et al.* Human NK cell receptors/markers: a tool to analyze NK cell development, subsets and function. *Cytometry A* **83**, 702-713, doi:10.1002/cyto.a.22302 (2013).

31 Fehniger, T. A. *et al.* Differential cytokine and chemokine gene expression by human NK cells following activation with IL-18 or IL-15 in combination with IL-12: implications for the innate immune response. *J Immunol* **162**, 4511-4520 (1999).

32 Hanna, J. *et al.* Decidual NK cells regulate key developmental processes at the human fetal-maternal interface. *Nat Med* **12**, 1065-1074, doi:10.1038/nm1452 (2006).

33 Kuylenstierna, C. *et al.* NKG2D performs two functions in invariant NKT cells: direct TCR-independent activation of NK-like cytolysis and co-stimulation of activation by CD1d. *Eur J Immunol* **41**, 1913-1923, doi:10.1002/eji.200940278 (2011).

34 Krijgsman, D. *et al.* Characterization of circulating T-, NK-, and NKT cell subsets in patients with colorectal cancer: the peripheral blood immune cell profile. *Cancer Immunol Immunother* **68**, 1011-1024, doi:10.1007/s00262-019-02343-7 (2019).

35 Mocchegiani, E. & Malavolta, M. NK and NKT cell functions in immunosenescence. *Aging Cell* **3**, 177-184, doi:10.1111/j.1474-9728.2004.00107.x (2004).

36 Jongsma, M. L. M., Neefjes, J. & Spaapen, R. M. Playing hide and seek: Tumor cells in control of MHC class I antigen presentation. *Mol Immunol* **136**, 36-44, doi:10.1016/j.molimm.2021.05.009 (2021).

37 Sanchez-Correa, B. *et al.* Human NK cells in acute myeloid leukaemia patients: analysis of NK cell-activating receptors and their ligands. *Cancer Immunol Immunother* **60**, 1195-1205, doi:10.1007/s00262-011-1050-2 (2011).

38 Melaiu, O., Lucarini, V., Cifaldi, L. & Fruci, D. Influence of the Tumor Microenvironment on NK Cell Function in Solid Tumors. *Front Immunol* **10**, 3038, doi:10.3389/fimmu.2019.03038 (2019).

39 Lopez-Soto, A., Gonzalez, S., Smyth, M. J. & Galluzzi, L. Control of Metastasis by NK Cells. *Cancer Cell* **32**, 135-154, doi:10.1016/j.ccell.2017.06.009 (2017).

40 Lo, H. C. *et al.* Resistance to natural killer cell immunosurveillance confers a selective advantage to polyclonal metastasis. *Nat Cancer* **1**, 709-722, doi:10.1038/s43018-020-0068-9 (2020).

41 Lopez-Soto, A. *et al.* Epithelial-mesenchymal transition induces an antitumor immune response mediated by NKG2D receptor. *J Immunol* **190**, 4408-4419, doi:10.4049/jimmunol.1202950 (2013).

42 Lopez-Soto, A., Zapico, L. H., Acebes-Huerta, A., Rodrigo, L. & Gonzalez, S. Regulation of NKG2D signaling during the epithelial-to-mesenchymal transition. *Oncoimmunology* **2**, e25820, doi:10.4161/onci.25820 (2013).

43 Chen, X. H. *et al.* TGF-beta and EGF induced HLA-I downregulation is associated with epithelial-mesenchymal transition (EMT) through upregulation of snail in prostate cancer cells. *Mol Immunol* **65**, 34-42, doi:10.1016/j.molimm.2014.12.017 (2015).

44 Xing, S. & Ferrari de Andrade, L. NKG2D and MICA/B shedding: a 'tag game' between NK cells and malignant cells. *Clin Transl Immunology* **9**, e1230, doi:10.1002/cti2.1230 (2020).

45 Perussia, B. Fc receptors on natural killer cells. *Curr Top Microbiol Immunol* **230**, 63-88, doi:10.1007/978-3-642-46859-9_6 (1998).

46 Wu, L. *et al.* lenalidomide enhances natural killer cell and monocyte-mediated antibody-dependent cellular cytotoxicity of rituximab-treated CD20+ tumor cells. *Clin Cancer Res* **14**, 4650-4657, doi:10.1158/1078-0432.CCR-07-4405 (2008).

47 Roda, J. M. *et al.* The activation of natural killer cell effector functions by cetuximab-coated, epidermal growth factor receptor positive tumor cells is enhanced by cytokines. *Clin Cancer Res* **13**, 6419-6428, doi:10.1158/1078-0432.CCR-07-0865 (2007).

48 Collins, S. M. *et al.* Elotuzumab directly enhances NK cell cytotoxicity against myeloma via CS1 ligation: evidence for augmented NK cell function complementing ADCC. *Cancer Immunol Immunother* **62**, 1841-1849, doi:10.1007/s00262-013-1493-8 (2013).

49 Spiridon, C. I., Guinn, S. & Vitetta, E. S. A comparison of the in vitro and in vivo activities of IgG and F(ab')2 fragments of a mixture of three monoclonal anti-Her-2 antibodies. *Clin Cancer Res* **10**, 3542-3551, doi:10.1158/1078-0432.CCR-03-0549 (2004).

50 Arnould, L. *et al.* Trastuzumab-based treatment of HER2-positive breast cancer: an antibody-dependent cellular cytotoxicity mechanism? *Br J Cancer* **94**, 259-267, doi:10.1038/sj.bjc.6602930 (2006).

51 Michel, T. *et al.* Human CD56bright NK Cells: An Update. *J Immunol* **196**, 2923-2931, doi:10.4049/jimmunol.1502570 (2016).

52 Yu, J. *et al.* Pro- and antiinflammatory cytokine signaling: reciprocal antagonism regulates interferon-gamma production by human natural killer cells. *Immunity* **24**, 575-590, doi:10.1016/j.immuni.2006.03.016 (2006).

53 Castro, F., Cardoso, A. P., Goncalves, R. M., Serre, K. & Oliveira, M. J. Interferon-Gamma at the Crossroads of Tumor Immune Surveillance or Evasion. *Front Immunol* **9**, 847, doi:10.3389/fimmu.2018.00847 (2018).

54 Rock, K. L., York, I. A., Saric, T. & Goldberg, A. L. Protein degradation and the generation of MHC class I-presented peptides. *Adv Immunol* **80**, 1-70, doi:10.1016/s0065-2776(02)80012-8 (2002).

55 Barry, K. C. *et al.* A natural killer-dendritic cell axis defines checkpoint therapy-responsive tumor microenvironments. *Nat Med* **24**, 1178-1191, doi:10.1038/s41591-018-0085-8 (2018).

56 Bruno, A. *et al.* Angiogenin and the MMP9-TIMP2 axis are up-regulated in proangiogenic, decidual NK-like cells from patients with colorectal cancer. *FASEB J* **32**, 5365-5377, doi:10.1096/fj.201701103R (2018).

57 Neo, S. Y. *et al.* CD73 immune checkpoint defines regulatory NK cells within the tumor microenvironment. *J Clin Invest* **130**, 1185-1198, doi:10.1172/JCI128895 (2020).

58 Donnelly, R. P. *et al.* mTORC1-dependent metabolic reprogramming is a prerequisite for NK cell effector function. *J Immunol* **193**, 4477-4484, doi:10.4049/jimmunol.1401558 (2014).

59 Wang, Z. *et al.* IL-10 Enhances Human Natural Killer Cell Effector Functions via Metabolic Reprogramming Regulated by mTORC1 Signaling. *Front Immunol* **12**, 619195, doi:10.3389/fimmu.2021.619195 (2021).

60 Viel, S. *et al.* TGF-beta inhibits the activation and functions of NK cells by repressing the mTOR pathway. *Sci Signal* **9**, ra19, doi:10.1126/scisignal.aad1884 (2016).

61 Poggi, A., Boero, S., Musso, A. & Zocchi, M. R. Selective role of mevalonate pathway in regulating perforin but not FasL and TNFalpha release in human Natural Killer cells. *PLoS One* **8**, e62932, doi:10.1371/journal.pone.0062932 (2013).

62 Eckelhart, E. *et al.* A novel Ncr1-Cre mouse reveals the essential role of STAT5 for NK-cell survival and development. *Blood* **117**, 1565-1573, doi:10.1182/blood-2010-06-291633 (2011).

63 Marcais, A. *et al.* The metabolic checkpoint kinase mTOR is essential for IL-15 signaling during the development and activation of NK cells. *Nat Immunol* **15**, 749-757, doi:10.1038/ni.2936 (2014).

64 Marcais, A. *et al.* High mTOR activity is a hallmark of reactive natural killer cells and amplifies early signaling through activating receptors. *Elife* **6**, doi:10.7554/eLife.26423 (2017).

65 Poggi, A. *et al.* Differential survival of gammadeltaT cells, alphabetaT cells and NK cells upon engagement of NKG2D by NKG2DL-expressing leukemic cells. *Int J Cancer* **129**, 387-396, doi:10.1002/ijc.25682 (2011).

66 Nandagopal, N., Ali, A. K., Komal, A. K. & Lee, S. H. The Critical Role of IL-15-PI3K-mTOR Pathway in Natural Killer Cell Effector Functions. *Front Immunol* **5**, 187, doi:10.3389/fimmu.2014.00187 (2014).

67 Yoo, J. K., Cho, J. H., Lee, S. W. & Sung, Y. C. IL-12 provides proliferation and survival signals to murine CD4+ T cells through phosphatidylinositol 3-kinase/Akt signaling pathway. *J Immunol* **169**, 3637-3643, doi:10.4049/jimmunol.169.7.3637 (2002).

68 Yamanaka, Y. *et al.* Aberrant overexpression of microRNAs activate AKT signaling via down-regulation of tumor suppressors in natural killer-cell lymphoma/leukemia. *Blood* **114**, 3265-3275, doi:10.1182/blood-2009-06-222794 (2009).

69 Wang, X., Liu, W., Zhuang, D., Hong, S. & Chen, J. Sestrin2 and sestrin3 suppress NK-92 cell-mediated cytotoxic activity on ovarian cancer cells through AMPK and mTORC1 signaling. *Oncotarget* **8**, 90132-90143, doi:10.18632/oncotarget.21487 (2017).

70 Muller-Durovic, B. *et al.* Killer Cell Lectin-like Receptor G1 Inhibits NK Cell Function through Activation of Adenosine 5'-Monophosphate-Activated Protein Kinase. *J Immunol* **197**, 2891-2899, doi:10.4049/jimmunol.1600590 (2016).

71 Kim, K. Y. *et al.* Adiponectin is a negative regulator of NK cell cytotoxicity. *J Immunol* **176**, 5958-5964, doi:10.4049/jimmunol.176.10.5958 (2006).

72 Andris, F. & Leo, O. AMPK in lymphocyte metabolism and function. *Int Rev Immunol* **34**, 67-81, doi:10.3109/08830185.2014.969422 (2015).

73 Motoshima, H., Goldstein, B. J., Igata, M. & Araki, E. AMPK and cell proliferation--AMPK as a therapeutic target for atherosclerosis and cancer. *J Physiol* **574**, 63-71, doi:10.1113/jphysiol.2006.108324 (2006).

74 Inoki, K., Zhu, T. & Guan, K. L. TSC2 mediates cellular energy response to control cell growth and survival. *Cell* **115**, 577-590, doi:10.1016/s0092-8674(03)00929-2 (2003).

75 Naume, B., Gately, M. & Espevik, T. A comparative study of IL-12 (cytotoxic lymphocyte maturation factor)-, IL-2-, and IL-7-induced effects on immunomagnetically purified CD56+ NK cells. *J Immunol* **148**, 2429-2436 (1992).

76 Parkhurst, M. R., Riley, J. P., Dudley, M. E. & Rosenberg, S. A. Adoptive transfer of autologous natural killer cells leads to high levels of circulating natural killer cells but does not mediate tumor regression. *Clin Cancer Res* **17**, 6287-6297, doi:10.1158/1078-0432.CCR-11-1347 (2011).

77 Fujisaki, H. *et al.* Expansion of highly cytotoxic human natural killer cells for cancer cell therapy. *Cancer Res* **69**, 4010-4017, doi:10.1158/0008-5472.CAN-08-3712 (2009).

78 Sakamoto, N. *et al.* Phase I clinical trial of autologous NK cell therapy using novel expansion method in patients with advanced digestive cancer. *J Transl Med* **13**, 277, doi:10.1186/s12967-015-0632-8 (2015).

79 Murray, S. & Lundqvist, A. Targeting the tumor microenvironment to improve natural killer cell-based immunotherapies: On being in the right place at the right time, with resilience. *Hum Vaccin Immunother* **12**, 607-611, doi:10.1080/21645515.2015.1096458 (2016).

80 Streltsova, M. A., Barsov, E., Erokhina, S. A. & Kovalenko, E. I. Retroviral gene transfer into primary human NK cells activated by IL-2 and K562 feeder cells expressing membrane-bound IL-21. *J Immunol Methods* **450**, 90-94, doi:10.1016/j.jim.2017.08.003 (2017).

81 Kamiya, T., Seow, S. V., Wong, D., Robinson, M. & Campana, D. Blocking expression of inhibitory receptor NKG2A overcomes tumor resistance to NK cells. *J Clin Invest* **129**, 2094-2106, doi:10.1172/JCI123955 (2019).

82 Chang, Y. H. *et al.* A chimeric receptor with NKG2D specificity enhances natural killer cell activation and killing of tumor cells. *Cancer Res* **73**, 1777-1786, doi:10.1158/0008-5472.CAN-12-3558 (2013).

83 Biederstadt, A. & Rezvani, K. Engineering the next generation of CAR-NK immunotherapies. *Int J Hematol* **114**, 554-571, doi:10.1007/s12185-021-03209-4 (2021).

84 Xie, G. *et al.* CAR-NK cells: A promising cellular immunotherapy for cancer. *EBioMedicine* **59**, 102975, doi:10.1016/j.ebiom.2020.102975 (2020).

85 Wu, L., Zhang, C., Tian, Z. & Zhang, J. NK cell-based approach for screening novel functional immune genes. *Int Immunopharmacol* **11**, 274-279, doi:10.1016/j.intimp.2010.12.003 (2011).

86 Suck, G. *et al.* NK-92: an 'off-the-shelf therapeutic' for adoptive natural killer cell-based cancer immunotherapy. *Cancer Immunol Immunother* **65**, 485-492, doi:10.1007/s00262-015-1761-x (2016).

87 Hoerster, K. *et al.* HLA Class I Knockout Converts Allogeneic Primary NK Cells Into Suitable Effectors for "Off-the-Shelf" Immunotherapy. *Front Immunol* **11**, 586168, doi:10.3389/fimmu.2020.586168 (2020).

88 Sayitoglu, E. C. *et al.* Boosting Natural Killer Cell-Mediated Targeting of Sarcoma Through DNAM-1 and NKG2D. *Front Immunol* **11**, 40, doi:10.3389/fimmu.2020.00040 (2020).

89 Yang, B. *et al.* Blocking transforming growth factor-beta signaling pathway augments antitumor effect of adoptive NK-92 cell therapy. *Int Immunopharmacol* **17**, 198-204, doi:10.1016/j.intimp.2013.06.003 (2013).

90 Marcelo, K. L., Means, A. R. & York, B. The Ca(2+)/Calmodulin/CaMKK2 Axis: Nature's Metabolic CaMshaft. *Trends Endocrinol Metab* **27**, 706-718, doi:10.1016/j.tem.2016.06.001 (2016).

91 Chin, D. & Means, A. R. Calmodulin: a prototypical calcium sensor. *Trends Cell Biol* **10**, 322-328, doi:10.1016/s0962-8924(00)01800-6 (2000).

92 Racioppi, L. & Means, A. R. Calcium/calmodulin-dependent protein kinase kinase 2: roles in signaling and pathophysiology. *J Biol Chem* **287**, 31658-31665, doi:10.1074/jbc.R112.356485 (2012).

93 Gocher, A. M. *et al.* Akt activation by Ca(2+)/calmodulin-dependent protein kinase kinase 2 (CaMKK2) in ovarian cancer cells. *J Biol Chem* **292**, 14188-14204, doi:10.1074/jbc.M117.778464 (2017).

94 Fogarty, S. *et al.* AMPK Causes Cell Cycle Arrest in LKB1-Deficient Cells via Activation of CAMKK2. *Mol Cancer Res* **14**, 683-695, doi:10.1158/1541-7786.MCR-15-0479 (2016).

95 Anderson, K. A. *et al.* Components of a calmodulin-dependent protein kinase cascade. Molecular cloning, functional characterization and cellular localization of Ca2+/calmodulin-dependent protein kinase kinase beta. *J Biol Chem* **273**, 31880-31889, doi:10.1074/jbc.273.48.31880 (1998).

96 Langendorf, C. G. *et al.* CaMKK2 is inactivated by cAMP-PKA signaling and 14-3-3 adaptor proteins. *J Biol Chem* **295**, 16239-16250, doi:10.1074/jbc.RA120.013756 (2020).

97 Lentini Santo, D., Petrvalska, O., Obsilova, V., Ottmann, C. & Obsil, T. Stabilization of Protein-Protein Interactions between CaMKK2 and 14-3-3 by Fusicoccins. *ACS Chem Biol* **15**, 3060-3071, doi:10.1021/acschembio.0c00821 (2020).

98 Wayman, G. A. *et al.* Regulation of axonal extension and growth cone motility by calmodulin-dependent protein kinase I. *J Neurosci* **24**, 3786-3794, doi:10.1523/JNEUROSCI.3294-03.2004 (2004).

99 Cao, W. *et al.* Differential effects of PKA-controlled CaMKK2 variants on neuronal differentiation. *RNA Biol* **8**, 1061-1072, doi:10.4161/rna.8.6.16691 (2011).

100 Kokubo, M. *et al.* BDNF-mediated cerebellar granule cell development is impaired in mice null for CaMKK2 or CaMKIV. *J Neurosci* **29**, 8901-8913, doi:10.1523/JNEUROSCI.0040-09.2009 (2009).

101 Peters, M. *et al.* Loss of Ca2+/calmodulin kinase kinase beta affects the formation of some, but not all, types of hippocampus-dependent long-term memory. *J Neurosci* **23**, 9752-9760 (2003).

102 Scott, J. W. *et al.* Autophosphorylation of CaMKK2 generates autonomous activity that is disrupted by a T85S mutation linked to anxiety and bipolar disorder. *Sci Rep* **5**, 14436, doi:10.1038/srep14436 (2015).

103 Erhardt, A. *et al.* Association of polymorphisms in P2RX7 and CaMKKb with anxiety disorders. *J Affect Disord* **101**, 159-168, doi:10.1016/j.jad.2006.11.016 (2007).

104 Luo, X. J. *et al.* Convergent lines of evidence support CAMKK2 as a schizophrenia susceptibility gene. *Mol Psychiatry* **19**, 774-783, doi:10.1038/mp.2013.103 (2014).

105 Atakhorrami, M. *et al.* A genetic variant in CAMKK2 gene is possibly associated with increased risk of bipolar disorder. *J Neural Transm (Vienna)* **123**, 323-328, doi:10.1007/s00702-015-1456-7 (2016).

106 McCullough, L. D. *et al.* Inhibition of calcium/calmodulin-dependent protein kinase kinase beta and calcium/calmodulin-dependent protein kinase IV is detrimental in cerebral ischemia. *Stroke* **44**, 2559-2566, doi:10.1161/STROKEAHA.113.001030 (2013).

107 Liu, L., McCullough, L. & Li, J. Genetic deletion of calcium/calmodulin-dependent protein kinase kinase beta (CaMKK beta) or CaMK IV exacerbates stroke outcomes in ovariectomized (OVXed) female mice. *BMC Neurosci* **15**, 118, doi:10.1186/s12868-014-0118-2 (2014).

108 Anderson, K. A. *et al.* Hypothalamic CaMKK2 contributes to the regulation of energy balance. *Cell Metab* **7**, 377-388, doi:10.1016/j.cmet.2008.02.011 (2008).

109 Marcelo, K. L. *et al.* Research Resource: Roles for Calcium/Calmodulin-Dependent Protein Kinase Kinase 2 (CaMKK2) in Systems Metabolism. *Mol Endocrinol* **30**, 557-572, doi:10.1210/me.2016-1021 (2016).

110 Anderson, K. A. *et al.* Deletion of CaMKK2 from the liver lowers blood glucose and improves whole-body glucose tolerance in the mouse. *Mol Endocrinol* **26**, 281-291, doi:10.1210/me.2011-1299 (2012).

111 Oury, F. *et al.* CREB mediates brain serotonin regulation of bone mass through its expression in ventromedial hypothalamic neurons. *Genes Dev* **24**, 2330-2342, doi:10.1101/gad.1977210 (2010).

112 Cary, R. L. *et al.* Inhibition of Ca(2)(+)/calmodulin-dependent protein kinase kinase 2 stimulates osteoblast formation and inhibits osteoclast differentiation. *J Bone Miner Res* **28**, 1599-1610, doi:10.1002/jbmr.1890 (2013).

113 Ye, L., Robertson, M. A., Mastracci, T. L. & Anderson, R. M. An insulin signaling feedback loop regulates pancreas progenitor cell differentiation during islet

development and regeneration. *Dev Biol* **409**, 354-369, doi:10.1016/j.ydbio.2015.12.003 (2016).

114 Lin, F., Ribar, T. J. & Means, A. R. The Ca2+/calmodulin-dependent protein kinase kinase, CaMKK2, inhibits preadipocyte differentiation. *Endocrinology* **152**, 3668-3679, doi:10.1210/en.2011-1107 (2011).

115 York, B. *et al.* Pharmacological inhibition of CaMKK2 with the selective antagonist STO-609 regresses NAFLD. *Sci Rep* **7**, 11793, doi:10.1038/s41598-017-12139-3 (2017).

116 Schmitt, J. M., Smith, S., Hart, B. & Fletcher, L. CaM kinase control of AKT and LNCaP cell survival. *J Cell Biochem* **113**, 1514-1526, doi:10.1002/jcb.24020 (2012).

117 Chen, Z. *et al.* CaMKK2 Promotes the Progression of Ovarian Carcinoma through the PI3K/PDK1/Akt Axis. *Comput Math Methods Med* **2022**, 7187940, doi:10.1155/2022/7187940 (2022).

118 Jin, L. *et al.* The PLAG1-GDH1 Axis Promotes Anoikis Resistance and Tumor Metastasis through CamKK2-AMPK Signaling in LKB1-Deficient Lung Cancer. *Mol Cell* **69**, 87-99 e87, doi:10.1016/j.molcel.2017.11.025 (2018).

119 Frigo, D. E. *et al.* CaM kinase kinase beta-mediated activation of the growth regulatory kinase AMPK is required for androgen-dependent migration of prostate cancer cells. *Cancer Res* **71**, 528-537, doi:10.1158/0008-5472.CAN-10-2581 (2011).

120 Stewart, L. M. *et al.* CaMKK2 facilitates Golgi-associated vesicle trafficking to sustain cancer cell proliferation. *Cell Death Dis* **12**, 1040, doi:10.1038/s41419-021-04335-x (2021).

121 Lin, F. *et al.* The camKK2/camKIV relay is an essential regulator of hepatic cancer. *Hepatology* **62**, 505-520, doi:10.1002/hep.27832 (2015).

122 Wang, S. *et al.* CAMKK2 Defines Ferroptosis Sensitivity of Melanoma Cells by Regulating AMPKNRF2 Pathway. *J Invest Dermatol* **142**, 189-200 e188, doi:10.1016/j.jid.2021.05.025 (2022).

123 Racioppi, L. *et al.* Calcium/calmodulin-dependent kinase kinase 2 regulates hematopoietic stem and progenitor cell regeneration. *Cell Death Dis* **8**, e3076, doi:10.1038/cddis.2017.474 (2017).

124 Broxmeyer, H. E. *et al.* CaMKK2 Knockout Bone Marrow Cells Collected/Processed in Low Oxygen (Physioxia) Suggests CaMKK2 as a Hematopoietic Stem to Progenitor Differentiation Fate Determinant. *Stem Cell Rev Rep*, doi:10.1007/s12015-021-10306-8 (2022).

125 Merhi, F. *et al.* Targeting CAMKK2 and SOC Channels as a Novel Therapeutic Approach for Sensitizing Acute Promyelocytic Leukemia Cells to All-Trans Retinoic Acid. *Cells* **10**, doi:10.3390/cells10123364 (2021).

126 Teng, E. C., Racioppi, L. & Means, A. R. A cell-intrinsic role for CaMKK2 in granulocyte lineage commitment and differentiation. *J Leukoc Biol* **90**, 897-909, doi:10.1189/jlb.0311152 (2011).

127 Racioppi, L., Noeldner, P. K., Lin, F., Arvai, S. & Means, A. R. Calcium/calmodulin-dependent protein kinase kinase 2 regulates macrophage-mediated inflammatory responses. *J Biol Chem* **287**, 11579-11591, doi:10.1074/jbc.M111.336032 (2012).

128 Huang, W. *et al.* Calcium/Calmodulin Dependent Protein Kinase Kinase 2 Regulates the Expansion of Tumor-induced Myeloid-Derived Suppressor Cells. *Frontiers in Immunology*, 4286 (2021).

129 Racioppi, L. *et al.* CaMKK2 in myeloid cells is a key regulator of the immune-suppressive microenvironment in breast cancer. *Nat Commun* **10**, 2450, doi:10.1038/s41467-019-10424-5 (2019).

130 Hawley, S. A. *et al.* Calmodulin-dependent protein kinase kinase-beta is an alternative upstream kinase for AMP-activated protein kinase. *Cell Metab* **2**, 9-19, doi:10.1016/j.cmet.2005.05.009 (2005).

131 Eduful, B. J. *et al.* Hinge Binder Scaffold Hopping Identifies Potent Calcium/Calmodulin-Dependent Protein Kinase Kinase 2 (CAMKK2) Inhibitor Chemotypes. *J Med Chem* **64**, 10849-10877, doi:10.1021/acs.jmedchem.0c02274 (2021).

132 Price, D. J. *et al.* An orally available, brain-penetrant CAMKK2 inhibitor reduces food intake in rodent model. *Bioorg Med Chem Lett* **28**, 1958-1963, doi:10.1016/j.bmcl.2018.03.034 (2018).

133 An, S. & Fu, L. Small-molecule PROTACs: An emerging and promising approach for the development of targeted therapy drugs. *EBioMedicine* **36**, 553-562, doi:10.1016/j.ebiom.2018.09.005 (2018).

134 Martin-Acosta, P. & Xiao, X. PROTACs to address the challenges facing small molecule inhibitors. *Eur J Med Chem* **210**, 112993, doi:10.1016/j.ejmech.2020.112993 (2021).

135 Tovell, H. *et al.* Design and Characterization of SGK3-PROTAC1, an Isoform Specific SGK3 Kinase PROTAC Degrader. *ACS Chem Biol* **14**, 2024-2034, doi:10.1021/acschembio.9b00505 (2019).

136 Jiang, B. *et al.* Development of Dual and Selective Degraders of Cyclin-Dependent Kinases 4 and 6. *Angew Chem Int Ed Engl* **58**, 6321-6326, doi:10.1002/anie.201901336 (2019).

137 Buhimschi, A. D. *et al.* Targeting the C481S Ibrutinib-Resistance Mutation in Bruton's Tyrosine Kinase Using PROTAC-Mediated Degradation. *Biochemistry* **57**, 3564-3575, doi:10.1021/acs.biochem.8b00391 (2018).

138 Burslem, G. M. *et al.* Targeting BCR-ABL1 in Chronic Myeloid Leukemia by PROTAC-Mediated Targeted Protein Degradation. *Cancer Res* **79**, 4744-4753, doi:10.1158/0008-5472.CAN-19-1236 (2019).

139 Faubert, B. *et al.* Lactate Metabolism in Human Lung Tumors. *Cell* **171**, 358-371 e359, doi:10.1016/j.cell.2017.09.019 (2017).

140 Wang, J. X. *et al.* Lactic Acid and an Acidic Tumor Microenvironment suppress Anticancer Immunity. *Int J Mol Sci* **21**, doi:10.3390/ijms21218363 (2020).

141 Sanderson, S. M. & Locasale, J. W. Revisiting the Warburg Effect: Some Tumors Hold Their Breath. *Cell Metab* **28**, 669-670, doi:10.1016/j.cmet.2018.10.011 (2018).

142 Payen, V. L., Mina, E., Van Hee, V. F., Porporato, P. E. & Sonveaux, P. Monocarboxylate transporters in cancer. *Mol Metab* **33**, 48-66, doi:10.1016/j.molmet.2019.07.006 (2020).

143 Niu, D. *et al.* Lactic acid, a driver of tumor-stroma interactions. *Int Immunopharmacol* **106**, 108597, doi:10.1016/j.intimp.2022.108597 (2022).

144 Huang, X. *et al.* High expressions of LDHA and AMPK as prognostic biomarkers for breast cancer. *Breast* **30**, 39-46, doi:10.1016/j.breast.2016.08.014 (2016).

145 Guan, X., Rodriguez-Cruz, V. & Morris, M. E. Cellular Uptake of MCT1 Inhibitors AR-C155858 and AZD3965 and Their Effects on MCT-Mediated Transport of L-Lactate in Murine 4T1 Breast Tumor Cancer Cells. *AAPS J* **21**, 13, doi:10.1208/s12248-018-0279-5 (2019).

146 Park, S. *et al.* ERRalpha-Regulated Lactate Metabolism Contributes to Resistance to Targeted Therapies in Breast Cancer. *Cell Rep* **15**, 323-335, doi:10.1016/j.celrep.2016.03.026 (2016).

147 Altinok, O. *et al.* Malate-aspartate shuttle promotes l-lactate oxidation in mitochondria. *J Cell Physiol* **235**, 2569-2581, doi:10.1002/jcp.29160 (2020).

148 Walters, D. K., Arendt, B. K. & Jelinek, D. F. CD147 regulates the expression of MCT1 and lactate export in multiple myeloma cells. *Cell Cycle* **12**, 3175-3183, doi:10.4161/cc.26193 (2013).

149 Kozlov, A. M., Lone, A., Betts, D. H. & Cumming, R. C. Lactate preconditioning promotes a HIF-1alpha-mediated metabolic shift from OXPHOS to glycolysis in normal human diploid fibroblasts. *Sci Rep* **10**, 8388, doi:10.1038/s41598-020-65193-9 (2020).

150 Seliger, C. *et al.* Lactate-modulated induction of THBS-1 activates transforming growth factor (TGF)-beta2 and migration of glioma cells in vitro. *PLoS One* **8**, e78935, doi:10.1371/journal.pone.0078935 (2013).

151 Vegran, F., Boidot, R., Michiels, C., Sonveaux, P. & Feron, O. Lactate influx through the endothelial cell monocarboxylate transporter MCT1 supports an NF-

kappaB/IL-8 pathway that drives tumor angiogenesis. *Cancer Res* **71**, 2550-2560, doi:10.1158/0008-5472.CAN-10-2828 (2011).

152 Colegio, O. R. *et al.* Functional polarization of tumour-associated macrophages by tumour-derived lactic acid. *Nature* **513**, 559-563, doi:10.1038/nature13490 (2014).

153 Husain, Z., Huang, Y., Seth, P. & Sukhatme, V. P. Tumor-derived lactate modifies antitumor immune response: effect on myeloid-derived suppressor cells and NK cells. *J Immunol* **191**, 1486-1495, doi:10.4049/jimmunol.1202702 (2013).

154 Shime, H. *et al.* Tumor-secreted lactic acid promotes IL-23/IL-17 proinflammatory pathway. *J Immunol* **180**, 7175-7183, doi:10.4049/jimmunol.180.11.7175 (2008).

155 Brand, A. *et al.* LDHA-Associated Lactic Acid Production Blunts Tumor Immunosurveillance by T and NK Cells. *Cell Metab* **24**, 657-671, doi:10.1016/j.cmet.2016.08.011 (2016).

156 Dietl, K. *et al.* Lactic acid and acidification inhibit TNF secretion and glycolysis of human monocytes. *J Immunol* **184**, 1200-1209, doi:10.4049/jimmunol.0902584 (2010).

157 Harmon, C. *et al.* Lactate-Mediated Acidification of Tumor Microenvironment Induces Apoptosis of Liver-Resident NK Cells in Colorectal Liver Metastasis. *Cancer Immunol Res* **7**, 335-346, doi:10.1158/2326-6066.CIR-18-0481 (2019).

158 Dodard, G. *et al.* Inflammation-Induced Lactate Leads to Rapid Loss of Hepatic Tissue-Resident NK Cells. *Cell Rep* **32**, 107855, doi:10.1016/j.celrep.2020.107855 (2020).

159 Xie, D., Zhu, S. & Bai, L. Lactic acid in tumor microenvironments causes dysfunction of NKT cells by interfering with mTOR signaling. *Sci China Life Sci* **59**, 1290-1296, doi:10.1007/s11427-016-0348-7 (2016).

160 Potzl, J. *et al.* Reversal of tumor acidosis by systemic buffering reactivates NK cells to express IFN-gamma and induces NK cell-dependent lymphoma control without other immunotherapies. *Int J Cancer* **140**, 2125-2133, doi:10.1002/ijc.30646 (2017).

161 Zhang, D. *et al.* Metabolic regulation of gene expression by histone lactylation. *Nature* **574**, 575-580, doi:10.1038/s41586-019-1678-1 (2019).

162 Dai, X., Lv, X., Thompson, E. W. & Ostrikov, K. K. Histone lactylation: epigenetic mark of glycolytic switch. *Trends Genet* **38**, 124-127, doi:10.1016/j.tig.2021.09.009 (2022).

163 Latham, T. *et al.* Lactate, a product of glycolytic metabolism, inhibits histone deacetylase activity and promotes changes in gene expression. *Nucleic Acids Res* **40**, 4794-4803, doi:10.1093/nar/gks066 (2012).

164 Feng, J. *et al.* Tumor cell-derived lactate induces TAZ-dependent upregulation of PD-L1 through GPR81 in human lung cancer cells. *Oncogene* **36**, 5829-5839, doi:10.1038/onc.2017.188 (2017).

165 Sisignano, M., Fischer, M. J. M. & Geisslinger, G. Proton-Sensing GPCRs in Health and Disease. *Cells* **10**, doi:10.3390/cells10082050 (2021).

166 Gong, S. *et al.* A gene expression atlas of the central nervous system based on bacterial artificial chromosomes. *Nature* **425**, 917-925, doi:10.1038/nature02033 (2003).

167 Yu, Y. R. *et al.* A Protocol for the Comprehensive Flow Cytometric Analysis of Immune Cells in Normal and Inflamed Murine Non-Lymphoid Tissues. *PLoS One* **11**, e0150606, doi:10.1371/journal.pone.0150606 (2016).

168 Ceredig, R. & Rolink, T. A positive look at double-negative thymocytes. *Nat Rev Immunol* **2**, 888-897, doi:10.1038/nri937 (2002).

169 Busse, C. E., Krotkova, A. & Eichmann, K. The TCRbeta enhancer is dispensable for the expression of rearranged TCRbeta genes in thymic DN2/DN3 populations but not at later stages. *J Immunol* **175**, 3067-3074, doi:10.4049/jimmunol.175.5.3067 (2005).

170 Fink, P. J. The biology of recent thymic emigrants. *Annu Rev Immunol* **31**, 31-50, doi:10.1146/annurev-immunol-032712-100010 (2013).

171 Tario, J. D., Jr., Muirhead, K. A., Pan, D., Munson, M. E. & Wallace, P. K. Tracking immune cell proliferation and cytotoxic potential using flow cytometry. *Methods Mol Biol* **699**, 119-164, doi:10.1007/978-1-61737-950-5_7 (2011).

172 Zhu, J., Wang, K. Z. & Chu, C. T. After the banquet: mitochondrial biogenesis, mitophagy, and cell survival. *Autophagy* **9**, 1663-1676, doi:10.4161/auto.24135 (2013).

173 Sabbir, M. G., Taylor, C. G. & Zahradka, P. CAMKK2 regulates mitochondrial function by controlling succinate dehydrogenase expression, post-translational modification, megacomplex assembly, and activity in a cell-type-specific manner. *Cell Commun Signal* **19**, 98, doi:10.1186/s12964-021-00778-z (2021).

174 Senovilla, L. *et al.* Trial watch: Prognostic and predictive value of the immune infiltrate in cancer. *Oncoimmunology* **1**, 1323-1343, doi:10.4161/onci.22009 (2012).

175 Sconocchia, G. *et al.* Defective infiltration of natural killer cells in MICA/B-positive renal cell carcinoma involves beta(2)-integrin-mediated interaction. *Neoplasia* **11**, 662-671, doi:10.1593/neo.09296 (2009).

176 Stojanovic, A. & Cerwenka, A. Natural killer cells and solid tumors. *J Innate Immun* **3**, 355-364, doi:10.1159/000325465 (2011).

177 Guillerey, C. *et al.* Toll-like receptor 3 regulates NK cell responses to cytokines and controls experimental metastasis. *Oncoimmunology* **4**, e1027468, doi:10.1080/2162402X.2015.1027468 (2015).

178 Dillekas, H., Rogers, M. S. & Straume, O. Are 90% of deaths from cancer caused by metastases? *Cancer Med* **8**, 5574-5576, doi:10.1002/cam4.2474 (2019).

179 Rashid, O. M. *et al.* Is tail vein injection a relevant breast cancer lung metastasis model? *J Thorac Dis* **5**, 385-392, doi:10.3978/j.issn.2072-1439.2013.06.17 (2013).

180 Brownlie, D. *et al.* Metastasis-associated macrophages constrain antitumor capability of natural killer cells in the metastatic site at least partially by membrane bound transforming growth factor beta. *J Immunother Cancer* **9**, doi:10.1136/jitc-2020-001740 (2021).

181 Qin, J. *et al.* The UDP/P2y6 axis promotes lung metastasis of melanoma by remodeling the premetastatic niche. *Cell Mol Immunol* **17**, 1269-1271, doi:10.1038/s41423-020-0392-0 (2020).

182 Sade-Feldman, M. *et al.* Resistance to checkpoint blockade therapy through inactivation of antigen presentation. *Nat Commun* **8**, 1136, doi:10.1038/s41467-017-01062-w (2017).

183 Michel, T., Hentges, F. & Zimmer, J. Consequences of the crosstalk between monocytes/macrophages and natural killer cells. *Front Immunol* **3**, 403, doi:10.3389/fimmu.2012.00403 (2012).

184 Castriconi, R. *et al.* Transforming growth factor beta 1 inhibits expression of NKp30 and NKG2D receptors: consequences for the NK-mediated killing of dendritic cells. *Proc Natl Acad Sci U S A* **100**, 4120-4125, doi:10.1073/pnas.0730640100 (2003).

185 Wang, X. & Zhao, X. Y. Transcription Factors Associated With IL-15 Cytokine Signaling During NK Cell Development. *Front Immunol* **12**, 610789, doi:10.3389/fimmu.2021.610789 (2021).

186 Frumento, G. *et al.* Tryptophan-derived catabolites are responsible for inhibition of T and natural killer cell proliferation induced by indoleamine 2,3-dioxygenase. *J Exp Med* **196**, 459-468, doi:10.1084/jem.20020121 (2002).

187 Kilgour, M. K. *et al.* 1-Methylnicotinamide is an immune regulatory metabolite in human ovarian cancer. *Sci Adv* **7**, doi:10.1126/sciadv.abe1174 (2021).

188 Stolwijk, J. A. *et al.* pH sensing in skin tumors: Methods to study the involvement of GPCRs, acid-sensing ion channels and transient receptor potential vanilloid channels. *Exp Dermatol* **29**, 1055-1061, doi:10.1111/exd.14150 (2020).

189 Halestrap, A. P. & Price, N. T. The proton-linked monocarboxylate transporter (MCT) family: structure, function and regulation. *Biochem J* **343 Pt 2**, 281-299 (1999).

190 Beloueche-Babari, M. *et al.* Monocarboxylate transporter 1 blockade with AZD3965 inhibits lipid biosynthesis and increases tumour immune cell infiltration. *Br J Cancer* **122**, 895-903, doi:10.1038/s41416-019-0717-x (2020).

191 Rezvani, K., Rouce, R., Liu, E. & Shpall, E. Engineering Natural Killer Cells for Cancer Immunotherapy. *Mol Ther* **25**, 1769-1781, doi:10.1016/j.ymthe.2017.06.012 (2017).

192 Wang, W. *et al.* CD8(+) T cells regulate tumour ferroptosis during cancer immunotherapy. *Nature* **569**, 270-274, doi:10.1038/s41586-019-1170-y (2019).

193 Wen, Q., Liu, J., Kang, R., Zhou, B. & Tang, D. The release and activity of HMGB1 in ferroptosis. *Biochem Biophys Res Commun* **510**, 278-283, doi:10.1016/j.bbrc.2019.01.090 (2019).

194 Yamazaki, T. *et al.* Defective immunogenic cell death of HMGB1-deficient tumors: compensatory therapy with TLR4 agonists. *Cell Death Differ* **21**, 69-78, doi:10.1038/cdd.2013.72 (2014).

195 Luo, X. *et al.* Oxygenated phosphatidylethanolamine navigates phagocytosis of ferroptotic cells by interacting with TLR2. *Cell Death Differ* **28**, 1971-1989, doi:10.1038/s41418-020-00719-2 (2021).

196 Tang, R. *et al.* Ferroptosis, necroptosis, and pyroptosis in anticancer immunity. *J Hematol Oncol* **13**, 110, doi:10.1186/s13045-020-00946-7 (2020).

197 Kriegbaum, M. C., Jacobsen, B., Hald, A. & Ploug, M. Expression of C4.4A, a structural uPAR homolog, reflects squamous epithelial differentiation in the adult mouse and during embryogenesis. *J Histochem Cytochem* **59**, 188-201, doi:10.1369/0022155410394859 (2011).

198 Smith, H. W. & Marshall, C. J. Regulation of cell signalling by uPAR. *Nat Rev Mol Cell Biol* **11**, 23-36, doi:10.1038/nrm2821 (2010).

199 Liu, J. F. *et al.* C4.4A as a biomarker of head and neck squamous cell carcinoma and correlated with epithelial mesenchymal transition. *Am J Cancer Res* **5**, 3505-3515 (2015).

200 Hu, P. *et al.* Elevated Expression of LYPD3 Is Associated with Lung Adenocarcinoma Carcinogenesis and Poor Prognosis. *DNA Cell Biol* **39**, 522-532, doi:10.1089/dna.2019.5116 (2020).

201 Willuda, J. *et al.* Preclinical Antitumor Efficacy of BAY 1129980-a Novel Auristatin-Based Anti-C4.4A (LYPD3) Antibody-Drug Conjugate for the Treatment of Non-Small Cell Lung Cancer. *Mol Cancer Ther* **16**, 893-904, doi:10.1158/1535-7163.MCT-16-0474 (2017).

202 Cocce, K. J. *et al.* The Lineage Determining Factor GRHL2 Collaborates with FOXA1 to Establish a Targetable Pathway in Endocrine Therapy-Resistant Breast Cancer. *Cell Rep* **29**, 889-903 e810, doi:10.1016/j.celrep.2019.09.032 (2019).

203 Arumugam, T. *et al.* New Blocking Antibodies against Novel AGR2-C4.4A Pathway Reduce Growth and Metastasis of Pancreatic Tumors and Increase Survival in Mice. *Mol Cancer Ther* **14**, 941-951, doi:10.1158/1535-7163.MCT-14-0470 (2015).

204 Alvarez, S. W. *et al.* NFS1 undergoes positive selection in lung tumours and protects cells from ferroptosis. *Nature* **551**, 639-643, doi:10.1038/nature24637 (2017).

205 Ubellacker, J. M. *et al.* Lymph protects metastasizing melanoma cells from ferroptosis. *Nature* **585**, 113-118, doi:10.1038/s41586-020-2623-z (2020).

206 Miotto, G. *et al.* Insight into the mechanism of ferroptosis inhibition by ferrostatin-1. *Redox Biol* **28**, 101328, doi:10.1016/j.redox.2019.101328 (2020).

207 Jach, D., Cheng, Y., Prica, F., Dumartin, L. & Crnogorac-Jurcevic, T. From development to cancer - an ever-increasing role of AGR2. *Am J Cancer Res* **11**, 5249-5262 (2021).

208 Yan, H. F. *et al.* Ferroptosis: mechanisms and links with diseases. *Signal Transduct Target Ther* **6**, 49, doi:10.1038/s41392-020-00428-9 (2021).

209 Yoo, S. E. *et al.* Gpx4 ablation in adult mice results in a lethal phenotype accompanied by neuronal loss in brain. *Free Radic Biol Med* **52**, 1820-1827, doi:10.1016/j.freeradbiomed.2012.02.043 (2012).

210 Seiler, A. *et al.* Glutathione peroxidase 4 senses and translates oxidative stress into 12/15-lipoxygenase dependent- and AIF-mediated cell death. *Cell Metab* **8**, 237-248, doi:10.1016/j.cmet.2008.07.005 (2008).

# Biography

Patrick Juras is the son of Barry and Laura Juras and was raised in the town of Lake Zurich, Illinois. As an undergraduate, he attended the Massachusetts Institute of Technology, graduating in 2016 with a major in Biology and a minor in Business. He moved to North Carolina to join the Duke Medical Scientist Program and completed two years of medical training prior to joining the McDonnell lab in 2018. In January 2022, he married Hannah Miele. He plans to graduate from Duke University School of Medicine in 2023 and pursue a residency in internal medicine, with an intention to practice oncology. Patrick is an author on one currently published paper and two papers that are in review.

Published:

Rashidian, M., Keliher, E.J., Dougan, M., **Juras, P.K.**, Cavallari, M., *et al.* The use of (18)F-2-fluorodeoxyglucose (FDG) to label antibody fragments for immuno-PET of pancreatic cancer. *ACS Cent Sci* **1**, 142-147, doi:10.1021/acscentsci.5b00121 (2015).

In review:

**Juras, P.K.**, Racioppi, L., Mukherjee, D., Artham, S., Gao, X., *et al*. Increased CaMKK2 expression is an adaptive response that maintains the fitness of tumor-infiltrating natural killer cells. *Cancer Immunology Research*. Submitted May 16, 2022.

Mukherjee, D., Previs, R., **Juras, P.K**., Al Abo, M., Strickland, K., *et al*. Ca2+/Calmodulin Dependent Protein Kinase Kinase-2 (CaMKK2) promotes Protein Kinase G (PKG)-dependent actin cytoskeletal assembly to increase tumor metastasis. *Cancer Research.* Submitted May 17, 2022.